Ecological and environmental consequences of Oceanic Anoxic Events and the Cretaceous-Paleogene mass extinction event: a molecular-isotopic approach

Dissertation
zur Erlangung des Doktorgrades
der Naturwissenschaften
- Dr. rer. Nat. –

Am Fachbereich Geowissenschaften
der Universität Bremen

vorgelegt von

Julio C. Sepúlveda Arellano

Bremen
September 2008

Thesis committee

1. Supervisor: Prof. Kai-Uwe Hinrichs, University of Bremen, Germany
2. Co-Supervisor: Prof. Roger E. Summons, Massachusetts Institute of Technology, USA
3. Member: Prof. Jörn Peckmann, University of Bremen, Germany
4. Member: Prof. Wolfgang Bach, University of Bremen, Germany

Thesis defense

Monday, 17th November 2008

Faculty of Geosciences, University of Bremen

Mira niñita, te voy a llevar a ver la luna brillando en el mar…

Para Annette y Amaya

TABLE OF CONTENTS

THESIS ABSTRACT

The main aim of this thesis was to study the biotic and abiotic consequences of extreme environmental conditions during Cretaceous Oceanic Anoxic Events (OAE), and the recovery of primary production at the Cretaceous-Paleogene (K-Pg) mass extinction event through the use of lipid biomarkers, compound-specific stable isotopes, and bulk geochemistry. This multiproxy approach contributes new evidence for understanding the intricate environmental and biological interactions occurring during these important events in Earth's history, which were responsible for rapid biological turnover that greatly impacted biogeochemical cycles.

Two OAEs covering the Late Cretaceous were studied - the Coniacian-Turonian Boundary OAE2 (~ 93.5 million years ago, Ma) in an intra-shelf basin of the Levant Platform in Central Jordan, and the Coniacian OAE3 (~ 88-89 Ma) at the western equatorial Atlantic off the coast of Surinam (ODP Site 1259, Demerara Rise). OAE2 at Jordan was characterized by sea-level changes that resulted in water column stratification with a fluctuating chemocline, hypersalinity, and oxygen depletion, whereas evidence of photic zone euxinia (PZE) was only found after the termination of this event. Abundant steranes and hopanoids, including 2-methyl hopanes (2-MeH), and ^{13}C enriched aryl isoprenoids suggest that the observed environmental changes were accompanied by ecological successions of planktonic assemblages dominated by algae, including dinoflagellates, cyanobacteria and green-sulfur bacteria. The synchronous occurrence of 2-MeH and $\delta^{15}N$ values around 0‰ provides evidence for the importance of cyanobacteria and N_2-fixation fueling primary production at this stratified/anoxic continental platform. OAE3 at Demerara Rise was characterized by apparently cyclic, concomitant variations of stable isotopic composition of carbon and hydrogen ($\delta^{13}C$ and δD, respectively) of marine- and terrestrial-derived *n*-alkanes. This pattern suggested a tight coupling between marine and terrestrial systems. Intervals of enhanced marine productivity were evidenced by positive $\delta^{13}C$ excursions of the algal marker *n*-C_{17}, likely related to increased growth rates and primary productivity. Parallel ^{13}C enrichments in C_{29} and C_{31} *n*-alkanes of higher land plant waxes suggest simultaneous changes of

terrestrial ecosystems. Lowered concentrations of atmospheric CO_2 resulting in increased importance of C_4 plants was one possible scenario explaining the observed molecular-isotopic patterns. These intervals were also accompanied by δD enrichments in *n*-C_{17} suggestive of changes in δD_{water}, likely due to variations in the evaporation/precipitation balance and continental runoff. Overall, these results revealed a complex interplay of the climatic and oceanographic regime and a potential coupling of marine and terrestrial environmental changes.

In addition, the mass extinction event at the K-Pg (~ 65.5 Ma) was studied in an exceptionally expanded section of the renowned "Fish Clay" layer at Stevns Klint, Denmark. At this location, decreased photosynthesis resulting from the low solar transmission after the meteorite impact may have lasted less than 50 years. A highly diminished contribution of algal biomarkers and increased heterotrophic bacterial activity was characteristic of the 2-mm-thick organic-rich layer deposited immediately after the boundary. This period preceded the onset of recovery in algal production. This result strongly supported models suggesting a rapid resurgence of carbon fixation and ecological reorganization after this major impact event, and provided a more comprehensive view of the biotic recovery compared to more traditional microfossil studies.

KURZFASSUNG

Diese Dissertation untersucht einerseits die biotischen und abiotischen Reaktionen auf extreme Umweltbedingungen während der kreidezeitlichen „Oceanic Anoxic Events“ (OAE) und andererseits die Erholungphase der Primärproduzenten im Anschluss an das Aussterbeereignis der Kreide-Paläogen (K-Pg) Grenze. Zu diesem Zweck wurden organisch-geochemische Biomarker, komponenten-spezifische stabile Isotope und geochemische Gesamtparameter analysiert. Diese Multiproxy-Studie beleuchtet die komplexe Wechselbeziehung zwischen Umwelt und Biologie, während dieser wichtigen Ereignisse der Erdgeschichte, die für einen schnellen biologischen „Turnover“ verantwortlich waren und weitreichende Auswirkungen auf biogeochemische Kreisläufe hatten.

Zwei OAEs der Oberkreide wurden untersucht – das OAE2 der Coniacium-Turonium Grenze (~ 93.5 Millionen Jahre, Ma) im Intraschelf-Becken der Levant-Plattform in Zentraljordanien, und das OAE3 des Coniacium (~ 88-89 Ma) im westlichen äquatorialen Atlantik nahe der Küste Surinams (ODP Site 1259, Demerara Rise). Zu den prägnanten Merkmalen des OAE2 in Jordanien gehörten Meeresspiegelschwankungen, einhergehend mit einer Stratifizierung der Wassersäule, variierender Position der Chemokline, Hypersalinität und Sauerstoff Mangel; während nach Beendigung des OAE2 Hinweise für eine euxinische, photische Zone (PZE) vorlagen. Erhöhte Konzentrationen an Steranen und Hopanoiden, einschließlich 2-Methyl Hopanen (2-MeH) und ^{13}C angereicherten Aryl-Isoprenoiden, weisen darauf hin, dass die beobachteten Umweltveränderungen von einer ökologischen Sukzession, der von Algen (inkl. Dinoflagellaten, Cyanobakterien, Grün-Schwefel Bakterien) dominierten Plankton-Vergesellschaftungen begleitet wurden. Des Weiteren lässt das synchrone Auftreten von 2-MeH und $\delta^{15}N$-Werten um 0‰ auf die Bedeutung von Cyanobakterien und N_2-Fixierung als die treibende Kraft der Primärproduktion unter den bestehenden stratifizierten/anoxischen Bedingungen schließen.

Die enge Kopplung zwischen marinem und terrestrischem System war charakteristisch für das OAE3 am Demerara Rise und ging einher mit einer zyklischen Variation der stabilen Kohlenstoff- und Wasserstoff-Isotopenzusammensetzung ($\delta^{13}C$

und δD) in marinen sowie terrestrischen *n*-Alkanen. Episoden mit gesteigerter mariner Produktivität waren gekennzeichnet durch positive $\delta^{13}C$-Anomalien des Algenbiomarkers C_{17} *n*-Alkan, welche voraussichtlich durch einen Anstieg in der Wachstumsrate sowie der Primärproduktion hervorgerufen wurden. Die parallele ^{13}C Anreicherung in C_{29} und C_{31} *n*-Alkanen (Biomarker für Wachse höherer Landplanzen) lässt auf eine simultane Veränderung des terrestrischen Ökosystems schließen. Eine mögliche Erklärung für dieses Phänomen könnte eine Verringerung der atmosphärischen CO_2-Konzentration und dadurch zunehmender Bedeutung von C_4-Pflanzen sein. Zusätzlich wurden diese Intervalle mit δD-Anreicherungen in *n*-C_{17} begleitet, welche auf Variationen in der Balance zwischen Evaporation/Niederschlag und kontinentalem Abfluss hinweisen. Diese Ergebnisse verdeutlichen das komplexe Zusammenspiel von klimatischen und ozeanographischen Faktoren und legen eine Kopplung zwischen marinen und terrestrischen Umweltveränderungen nahe.

Das Aussterbeereignis der K-Pg Grenze (~ 65.5 Ma) wurde an einem außergewöhnlich mächtigem Profil des „Fish Clay“ bei Stevns Klint (Dänemark) untersucht. An dieser Lokation führte, die von einem Meteoriten Impakt verursachte, geringere solare Einstrahlung zu einer Reduzierung der Photosyntheserate, die einen Zeitraum von weniger als 50 Jahre umspannte. Biomarkeranalysen in der daran anschließenden 2-mm mächtigen, organikreichen Lage ergaben eine Dominanz von heterotrophen, bakteriellen Prozessen, die dem erneuten Aufblühen der Algen-Vergesellschaftungen vorausgingen. Die Ergebnisse dieser Studie unterstützen Modelle die ein schnelles Wiedereinsetzen der Kohlenstoff-Fixierung und ökologischen Restrukturierung nach diesem Impakt-Ereignis befürworten. Somit bieten sie einen umfassenderen Einblick in die biotische Entwicklung im Vergleich zu traditionellen Studien basierend auf Mikrofossilien.

ACKNOWLEDGEMENTS

Formerly trained as a marine biologist and oceanographer, I had never seen or worked with Cretaceous rocks before coming to Bremen. It was here and during the realization of my PhD that I was fortunate to meet people who introduced me to the fascinating worlds of organic geochemistry, geobiology, and geology. Here I would like to express my immense gratefulness to those who contributed to my work and life in Bremen during these three and half years. I would like to start thanking my supervisor, Prof. Kai-Uwe Hinrichs, for giving me the opportunity to join his group and for guiding my way through my PhD with such a great enthusiasm. Thanks Kai, for trusting me so much, for giving me your support, and for opening my eyes and letting me develop my own ideas with complete freedom. I would also like to thank my co-supervisor, Prof. Roger E. Summons, for receiving me at his lab at MIT, and for expressing so much interest on my research, always providing encouraging suggestions that greatly contributed to my understanding of the K/Pg event. I look forward to continuing our work at Cambridge. I am also indebted to Profs. Jörn Peckmann and Wolfgang Bach, for accepting being members of my thesis committee. The EUROPROX Program and the Deutsche Forschungsgemeinschaft are thanked for funding my studies.

A great part of the work included in this thesis would not have been possible without the help from many people. Many thanks to my friend Jens Wendler, for making the discussions about the Cretaceous' world such an enjoyable experience, and for the inspiring moments of music together with Egon. To Arne Leider, who supported important parts of my project during his undergraduate and master thesis, and to Jeff Salacup, for helping me with the K/Pg project as a summer student. Very special thanks goes to Xavi Prieto, who besides being a great friend kept the lab running wonderfully well, and to Pamela Rossel for being like my sister during these years (gracias chiquitita). I'm highly thankful to Steffi Tille, Ulrike Beckert, Jenny Wendt, Patrick Simundic, Tim Kahs, Monika Segl, and Hella Buschhoff for their support in the lab. To Markus Elvert and Daniel Birgel, for guiding my first steps into lipid analysis and mass spectrometry. To Birgit Schmincke, for her immense support, and for making my life easier when I had to deal with administrative stuff (which I still don't fully understand), as well as Marion

Milling-Goldbach, Maria Petrogiannis, and Anja Stöckl. To the Organic Geochemistry and Geobiology groups: Julius, Flo, Frauke, Simone, Arne, Xavi, Pame, Kai, Verena, Marcus, Daniel, Birgit, Marcos, Tobi E., Solveig, Nadine, Benni, Tobi H., Ester, Yu-Shih, Marlene, Matthias K., Matthias S., Xiaolei, Sebastien, Jörn, Florian, Jan, Boonraksa, Monika, Steffi T., Steffi L., and Henning, for providing this place with the best working atmosphere, and for their constant support and friendship. To Beth! Orcutt, for proof reading several parts of this thesis even when being on a cruise in the middle of the Pacific Ocean, and for her great friendship and discussions about politics. To my best friend Sergio Contreras, for making this world a better place to live - always keep that great smile on your face, buddy. To my German teacher, Ursula Meyers, for giving me the hope that some day I will finally learn the language, Vielen dank liebe Ula!

To the EUROPROX group, including my fellow students, postdocs, proponents and speakers. To the Geobiology Group at MIT, for receiving me for half a year; special thanks go to Laura Sherman, Carolyn Colonero, and Alla Skorokhod for their generous help. To my friends at WHOI, Ricardo, Cristina & Margarita, Chanda & Tim, YingTsong, Grace & Robert, Sébastien, Konrad, Carlos & Jessica. To many good friends with whom I shared great moments in Bremen, especially at the Lagerhaus and Heartbreak Hotel: Petra, Cécile & Rick, Elvan & Jerome, Barbara & Marius, Gulnaz & Xavier, Catalina, Igaratza, Ilham, Christian, Luisa, Jean, Isabelle, Jeroen, Ed, Ines, Uli, Markus, Eva, Magaly, Daniel & Gina, Lars H., Elsabe J., Sybille, and Frank. To Mahyar "Adrian Smith" Mohtadi and his brother Mehran, for the best Iron Maiden gigs of my life. To my former supervisors in Chile, Silvio "Maestro" Pantoja and Carina Lange, and my friends in Concepción for being always so close despite of the distance.

To my German family, Siegrun, Hans, Brigitte, Christoph & Diane, and Henny, for receiving me with so much love and for giving me the warm feeling of a family.

To my parents Julio and Patricia, and my siblings Constanza, Consuelo, and Felipe, for their unconditional love and support now and ever, and for believing in my dreams inspired by Jacques-Yves Cousteau since I was a child.

Finally, to the two persons that changed my life forever in the most wonderful way, filling my life with love and making me a proud partner and father, this work and all my efforts are dedicated to my two loves, Annette and Amaya.

LIST OF FIGURES

LIST OF TABLES

LIST OF ABBREVIATIONS

2-MeHI	2-Methyl hopane index
$CaCO_3$	Calcium carbonate
CPI	Carbon preference index
CTB	Cenomanian-Turonian Boundary
$\delta^{13}C$	Stable carbon isotopic composition (‰)
$\delta^{13}C_{carb}$	Stable carbon isotopic composition of bulk carbonates (‰)
$\delta^{13}C_{org}$	Stable carbon isotopic composition of organic matter (‰)
$\delta^{15}N$	Stable nitrogen isotopic composition of bulk sediment (‰)
δD	Stable hydrogen isotopic composition (‰)
DCM	Dichloromethane
DIC	Dissolved inorganic carbon
DSDP	Deep Sea Drilling Program
ε_p	Isotopic fractionation
FC	Fish Clay
GC-irMS	Gas chromatography-isotope ratio-mass spectrometry
GC-MS	Gas chromatography mass spectrometry
GI	Gammacerane index
Gt	Gigatons
HHI	Homohopane index
K-Pg	Cretaceous-Paleogene boundary
ky	Kilo years or thousand years
LCA	Long-chain *n*-alkane
Ly	Lycopane
Ma	Million years
mcd	Meters of composite depth
MeOH	Methanol
MRM-GG-MS	Metastable reaction monitoring gas chromatography mass spectrometry
OAE	Oceanic anoxic event

ODP	Ocean Drilling Program
OMZ	Oxygen minimum zone
ρCO_2	Partial pressure of CO_2
Ph	Phytane
Pr	Pristane
Pr/Ph	Pristane/phytane ratio
P-T	Permian-Triassic
PZE	Photic zone euxinia
SCA	Short-chain *n*-alkane
SSS	Sea surface salinity
SST	Sea surface temperature
TOC	Total organic carbon

CHAPTER I

INTRODUCTION

GENERAL INTRODUCTION

This introductory section provides an overview of the environmental, biogeochemical, and biological processes (and feedback mechanisms) controlling the global carbon cycle, and leading to the development and sustainment of anoxia/euxinia in marine environments over geological times, with special focus on the Late Cretaceous Period (~ 94-65.5 million years, Ma). Additionally, this section introduces the main theories explaining the mass extinction event at the Cretaceous-Paleogene Boundary, and its biotic and abiotic consequences including mechanisms controlling extinction and survival. Finally, the concept of lipid biomarkers and stable isotopes in the study of paleoenvironments is discussed.

I.1. BIOLOGICAL AND GEOLOGICAL PROCESSES INFLUENCING THE GOBAL CARBON AND NUTRIENT CYCLES

The evolution of the three dominant groups of modern eukaryotic phytoplankton (coccolithophores, dinoflagellates, and diatoms) reached ecological predominance during the Mesozoic and changed both ecosystem structure and biogeochemical cycles (Falkowski et al., 2004). Due to their capacity for rapid growth, marine microorganisms are major drivers of global nutrient cycles (Arrigo, 2005) and have shaped the geological carbon cycle and the redox state of ocean and atmosphere (Hayes et al., 1999). The latter can be exemplified by the evolutionary history of these three groups of primary producers since the Early Jurassic, the increase of organic carbon burial efficiency in marine sediments, and the long-term enrichment in $\delta^{13}C$ of the mobile carbon reservoir (Fig. I.1; Katz, 2005). These changes were tightly coupled to the continental rifting responsible for the ocean's configuration and coastline extension. Sea level changes, on the other hand, regulated nutrient influx from the continents and allowed the flourishing of phytoplanktonic groups along continental margins. Carbon burial over geological time scales has also influenced the partial pressure of atmospheric CO_2 (ρCO_2) and climate (Freeman and Hayes, 1992; Hayes et al., 1999), which is suggested to have favored, for

instance, the expansion of the C_4-type photosynthetic system in terrestrial plants (e.g., Kuypers et al., 1999; Pagani et al., 1999; 2005).

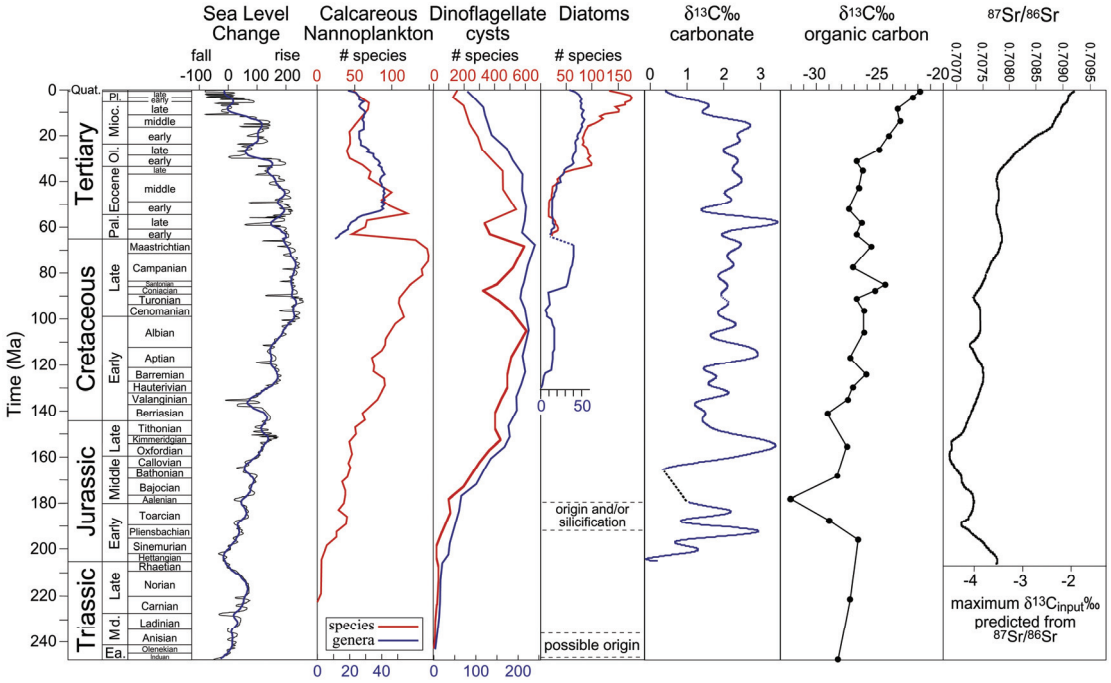

Figure I.1. Long-term relationship between sea level change, the evolutionary trajectories of major eukaryotic phytoplankton, and carbon cycle for the past 240 Ma (Katz, 2005). From left to right, sea level curve; number of calcareous nannoplankton species and genera; number of dinoflagellate cysts species and genera; number of diatom species and genera; $\delta^{13}C$ of bulk carbonate; $\delta^{13}C$ of organic carbon; $^{87}Sr/^{86}Sr$ as an indicator of $\delta^{13}C$ input from continental erosion. Modified from Katz (2005), see original reference for further details about data sources.

The long-term trend of biological and geochemical evolution was interrupted by periods of biotic crises and geochemical anomalies which occurred during discrete intervals of widespread ocean anoxia in the Cretaceous (Arthur et al., 1988; Leckie et al., 2002), and the mass extinction event that marks the end of the Cretaceous (Alvarez et al., 1980; D'Hondt, 2005). It is during some of these intervals of environmental stress during the Cretaceous that other marine planktonic groups, namely prokaryotes including photosynthetic cyanobacteria and chemoautotrophic archaea, played a key ecological and geochemical role globally (Kuypers et al., 2001; 2002a; 2004b). Nitrogen fixation by cyanobacteria is suggested to have controlled primary productivity and ρCO_2 variations

on geological timescales (Falkowski, 1997). However, the role of prokaryotic organisms during the mass extinction event at the end of the Cretaceous remains largely unknown.

I.2. OCEANIC ANOXIA DURING THE CRETACIOUS

Ocean anoxia and euxinia accompanied several events during the Phanerozoic (last 545 million year, Ma) including biotic crises during the Permian-Triassic boundary (e.g., Grice et al., 2005), and the Cretaceous (Leckie et al., 2002). The Cretaceous Period, extending from the end of the Jurassic (145.5 ± 4 Ma) to the beginning of the Paleogene (65.5 ± 0.5 Ma), witnessed some of the most extraordinary changes in climate, oceanography, biogeochemical cycles, and biotic turnover observed during the last 250 Ma of Earth's history (e.g., Leckie et al., 2002).

Oceanic anoxic events and forcing mechanisms. The realization that vast areas of the world oceans might have experienced oxygen-depleted conditions and euxinia during Cretaceous time arose from the observation that organic-carbon-rich sediments (black shales) formed in a variety of paleo-bathymetric settings, including coastal and open ocean areas, and epicontinental seas (Schlanger and Jenkyns, 1976; Jenkyns, 1980). These events have been named oceanic anoxic events (OAE; Schlanger and Jenkyns, 1976), and are thought to represent time intervals of widespread marine anoxia (in the water column and/or sediments) and burial of large amounts of organic carbon on the ocean floor (e.g., Schlanger and Jenkyns, 1976; Arthur et al., 1987; 1988). Black shales are mudrocks characterized by a high organic content (usually > 1%) with a color varying from medium gray to olive-brown to black. Black shales are usually devoid of benthonic fauna and contain distinct laminations (Arthur and Sageman, 1994); they can also be highly enriched in several redox-sensitive and sulfide-forming trace metals (Brumsack, 2006). Several OAEs varying in duration and geographical extension have been described between the Early Aptian and the Santonian (see summary Table I.1). The two most widespread OAEs are the early Aptian OAE1a and the Cenomanian-Turonian Boundary OAE2 (Arthur et al., 1987; Schlanger et al., 1987). On the other hand, the Coniacian-

Santonian OAE3 appears as the most extended in time (e.g., Meyers et al., 2006). However, it has received comparatively less attention than its counterparts, likely due to its regional restriction to the Atlantic basin (Wagner et al., 2004), in spite of the evidence of complex, and orbitally-driven climatic-oceanographic processes controlling the deposition of black shales during this interval (Nederbragt et al., 2007).

Table I.1. A summary of the mid-Cretaceous Oceanic Anoxic events (Meyers, 2006)

Event	Common name	Geological time	Absolute duration
OAE 3	"None"	Coniacian-Santonian	87.3–84.6 Ma (~ 2.7 My)
OAE 2	Bonarelli event	Latest Cenomanian	93.8–93.5 Ma (~ 300 ky)
OAE 1d	Breistroffer event	Late Albian	100.6–100.2 Ma (~ 400 ky)
OAE 1c	Tollebuc event	Late Albian	103.7–103.4 Ma (~ 300 ky)
OAE 1b (several)	Urbino event	Early Albian	110.9–110.6 Ma (~ 300 ky)
	Paquier event	Early Albian	112.0–111.6 Ma (~ 400 ky)
	Jacob event	Late Aptian	113.6–113.2 Ma (~ 400 ky)
OAE 1a	Selli event	Early Aptian	124.2–123.4 Ma (~ 800 ky)

Although an intense discussion about the main mechanisms controlling black shales formation has occurred during the last few decades, elevated levels of primary productivity in surface waters, as well as increased organic matter preservation under oxygen-deficient conditions, are considered as most plausible explanations (e.g., Sinninghe Damsté and Köster, 1998; Kuypers et al., 2002b; Mort et al., 2007). However, the actual trigger mechanism has not clearly been identified. The interaction of factors such as enhanced ocean crust production, volcanic activity, and massive magmatic episodes (Leckie et al., 2002; Turgeon and Creaser, 2008) are assumed to have caused the elevated concentrations of atmospheric CO_2 (Bice and Norris, 2002; Bice et al., 2006) and the associated greenhouse climate with exceptionally high sea surface temperatures at mid to low (Schouten et al., 2003; Bice et al., 2006; Forster et al., 2007) and high-latitudes (Jenkyns et al., 2004). The latter contributed to the presence of ice-free poles and a weaker than modern equator-to-pole surface-temperature gradient (Poulsen et al., 1999). Rising sea level has been also advocated as an important mechanism to the formation of black shales, responsible for the flooding of extended coastal areas, the transfer of continental nutrients into the ocean, and the formation of epicontinental seas

(cf., Arthur et al., 1987; Schlanger et al., 1987; Leckie et al., 2002). Finally, increased thermohaline stratification due to high sea surface temperatures and continental runoff might have affected deep-water formation and elevated carbon burial in restricted basins of the western Tethys and North Atlantic (e.g., Erbacher et al., 2001).

Recent model results suggest that reduced oxygen solubility during warm climates and nutrient-trapping controlled by continent configuration have a more important role in controlling oceanic euxinia than stagnant circulation (Meyer and Kump, 2008). A sequence of probable forcing mechanisms and feedback loops involved in the development of anoxia and euxinia is summarized in Figure I.2. Active volcanism during the Cretaceous was assumed to be the main trigger of elevated ρCO_2 levels and resulted in global warming, and an intensification of continental weathering and higher delivery rates of nutrients (phosphate) into the oceans. This led to increased marine productivity and export to the deep ocean promoting oxygen depletion and euxinia, due to both organic matter respiration through sulfate reduction and decreased oxygen solubility at relatively high ocean temperatures. Reducing conditions facilitated phosphate

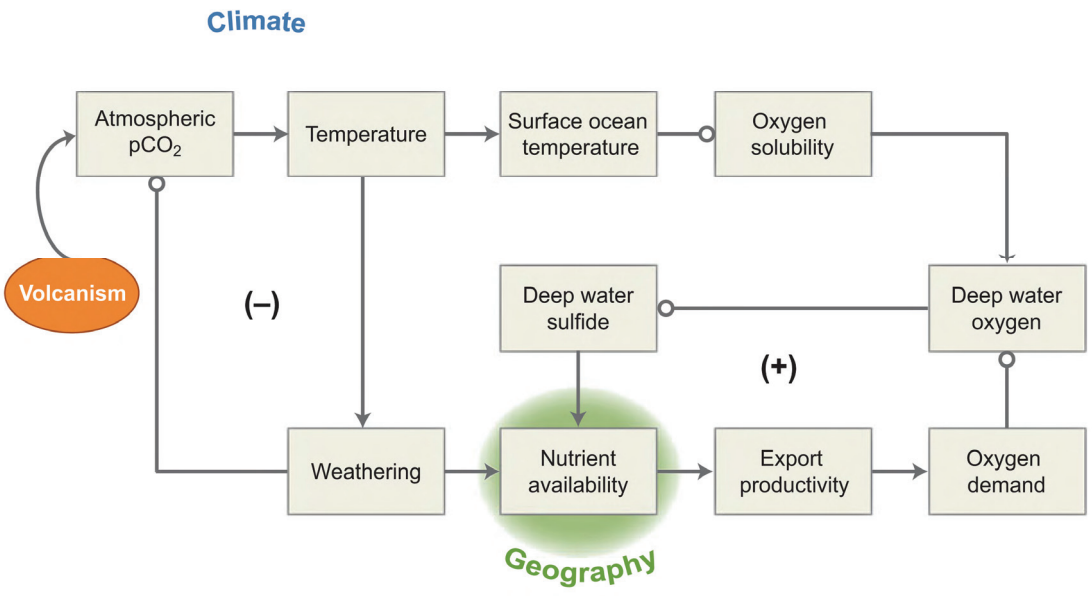

Figure I.2. Conceptual model displaying the main components involved in the establishment and maintenance of euxinia in the ocean, and feedback mechanisms (Meyer and Kump, 2008). Positives relationships are denoted by "normal arrows" and indicate the direction of the response; negative relationships are denoted by "circular arrow heads" and indicate that the response is in the opposite direction. (-) and (+) denotes negative and positive feedback loops, respectively.

mobilization from sediments, thus keeping a positive feedback loop on productivity and persistent euxinic conditions until volcanism ceased (Meyer and Kump, 2008).

Although the proxy record covering the Cretaceous provides evidence for the interaction of several of the mentioned mechanisms as responsible for oxygen depletion and the formation of black shales, it remains difficult to conceive how marine primary production could have been sustained for an extended period of time. Besides salinity stratification due to magnified runoff under an accelerated hydrological cycle, oceanographic models also include the role of sustained enhanced upwelling under favorable atmospheric circulation (Figure I.3; Meyers, 2006). As observed in modern coastal environments dominated by permanent or semi-permanent upwelling conditions such as the eastern Pacific, Indian, and western Atlantic oceans, high rates of primary production are fueled by the vertical transport of oxygen-poor and nutrient-rich subsurface waters, leading to a high oxygen demand, the development of oxygen minimum zones (OMZ), and to excellent preservation of organic matter in surface sediments (e.g., Helly and Levin, 2004; Cowie, 2005). Analogous oceanographic conditions have been invoked to explain the orbitally-driven deposition of black shales during the Cretaceous off the coast of northwest Africa (e.g., Kuypers et al., 2002b; Lüning et al., 2004; Kolonic et al., 2005) and northeast South America (Nederbragt et al., 2007; Friedrich et al., 2008).

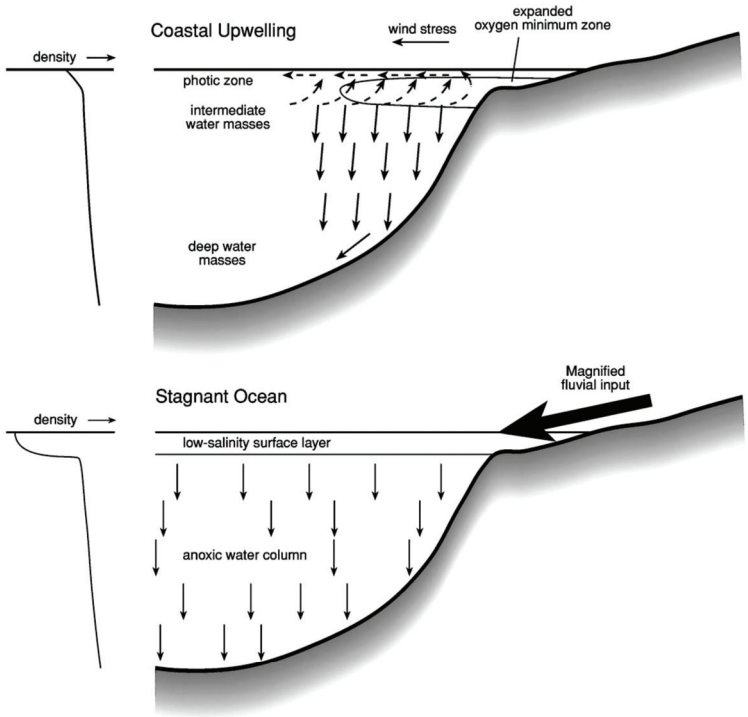

Figure I.3. Two conceptual models characterizing a highly productive and a strongly stratified environments favoring anoxia and euxinia in ocean margin settings (from Meyers, 2006; see original reference for further details). Upper panel represents coastal upwelling conditions characterized by high productivity and the development of a marked OMZ. Lower panel represent a strongly stratified and productive system with a marked pycnocline due to continental runoff. Downward arrows indicate organic matter fluxes to the sea floor.

Biological and geochemical consequences of OAEs. OAEs represent periods of a major perturbation of the global carbon and nutrient cycles, as evidenced by a marked positive carbon isotopic excursion in the geological record (Fig. I.4) attributed to a change in the isotopic composition of the total inorganic carbon pool that resulted from increased marine productivity and burial of ^{13}C-depleted organic matter (Arthur et al., 1988). During photosynthesis, phytoplankton discriminate against ^{13}C, which results in an isotopic depletion of the organic matter and an enrichment of the remaining inorganic carbon pool (e.g., Freeman and Hayes, 1992). The occurrence of carbon-isotope events coincide with episodes of biotic turnover in the marine fossil record, which has promoted the use of carbon-isotope curves and correlation as a global stratigraphic tool (Jarvis et al., 2006; Fig. I.4).

Environmental changes associated with OAEs are reported to have caused accelerated rates of speciation and extinction of planktonic calcareous organisms (e.g., Leckie et al., 2002). On the other hand, some OAEs have been related to the flourishing of planktonic archaea as important primary producers (Kuypers et al., 2001; 2004b). Marine archaeal lipids found in sediments of the North Atlantic Ocean deposited during

the early Albian OAE1b are suggested to dominate the bulk of organic matter present in black shales, indicating that planktonic chemoautotrophic archaea played an important ecological role and contributed to the formation of black shales (Kuypers et al., 2001; 2002a). Additionally, nitrogen deficiency due to denitrification and anaerobic ammonium oxidation in anoxic waters during OAEs might have given N_2-fixing cyanobacteria a competitive advantage over algae (Kuypers et al., 2004b). This group seemed to have comprised an important fraction of the planktonic assemblage over a vast array of coastal and open ocean environments during OAEs, and was likely responsible for the supply of fixed nitrogen for other members of the planktonic community (Kuypers et al., 2004b; Dumitrescu and Brassell, 2005; Ohkouchi et al., 2006; Kashiyama et al., 2008).

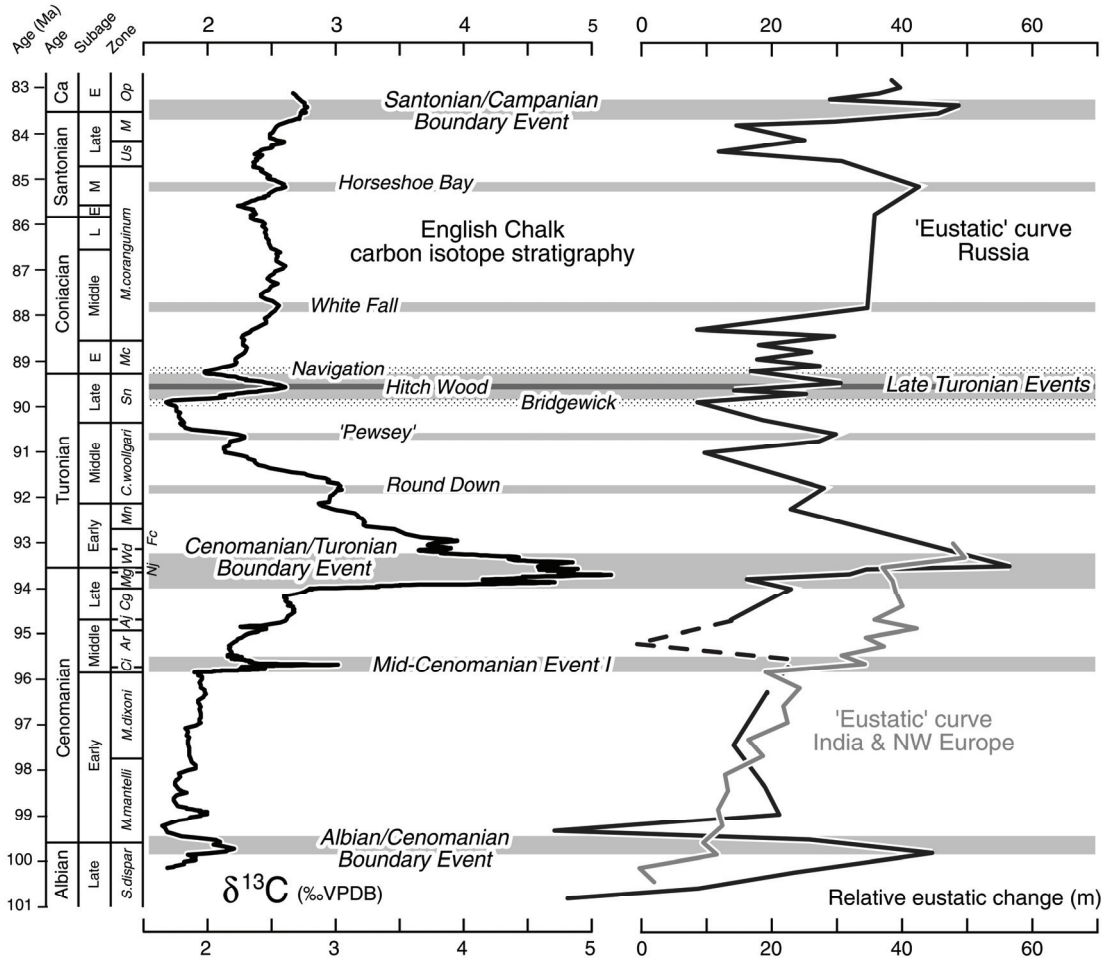

Figure I.4. For figure caption see next page

Figure I.4. Relationship between carbon-isotope record and sea level change for the Late Albian – Early Campanian (Jarvis et al., 2006). Left panel is a smoothed (5-point moving average) version of the English Chalk $\delta^{13}C$ composite age-calibrated curve compared with sea-level curves from the Russian Platform and Siberia, India, and NW Europe (see Jarvis et al., 2006). Gray areas represent isotopes events associated to perturbations of the carbon cycle. Note the positive relationship between isotopic anomalies (OAEs) and sea level, especially well developed during the Cenomanian-Turonian Boundary OAE2.

I.3. CRETACEOUS-PALEOGENE MASS EXTINCTION EVENT

The mass extinction event recorded at the Cretaceous-Paleogene Boundary (K/Pg; 65.5 million years ago) is the most recent of the so called "big five" Phanerozoic mass extinctions and marks the end of the Mesozoic era (Sepkoski Jr, 1996; Figure I.5). Two-thirds of all living species on Earth, including the dinosaurs, went into extinction, whereas the total diversity of fossilized marine genera declined by about 50% (Sepkoski Jr, 1996; Figure I.5).

Although several hypotheses have been suggested to explain the massive and abrupt nature of the K/Pg, it was not until the early eighties that a revolutionary theory changed its geological interpretation entirely. Based on anomalously high concentrations of iridium (a rare element in the earth' crust) found in deep-sea limestones deposited at several localities during the boundary, Alvarez et al., (1980) suggested that an asteroid 10 ± 4 kilometers in diameter must have impacted the Earth, resulting in the ejection of a dust cloud of pulverized rock into the stratosphere for several years, causing darkness and the disruption of photosynthesis that led to mass extinction. The theory stimulated considerable scientific and public interest during the following years; the subsequent discovery of the iridium anomaly in several other sections worldwide (e.g., Alvarez et al., 1980), as well as shocked quartz characteristic of impact cratering (Bohor et al., 1984) offered further evidence. But the discovery of a buried 180-km-diameter circular crater in the Yucatan Peninsula (Chicxulub crater) one decade later (Hildebrand et al., 1991; Pope et al., 1991), indicated that a meteorite impact occurred at the K/Pg. After almost three decades since its publication and the focus of intense scientific discussion, a compelling amount of geological evidence has supported the Alvarez's hypothesis and provided its wide acceptance (see Ryder, 1996; Kring, 2007).

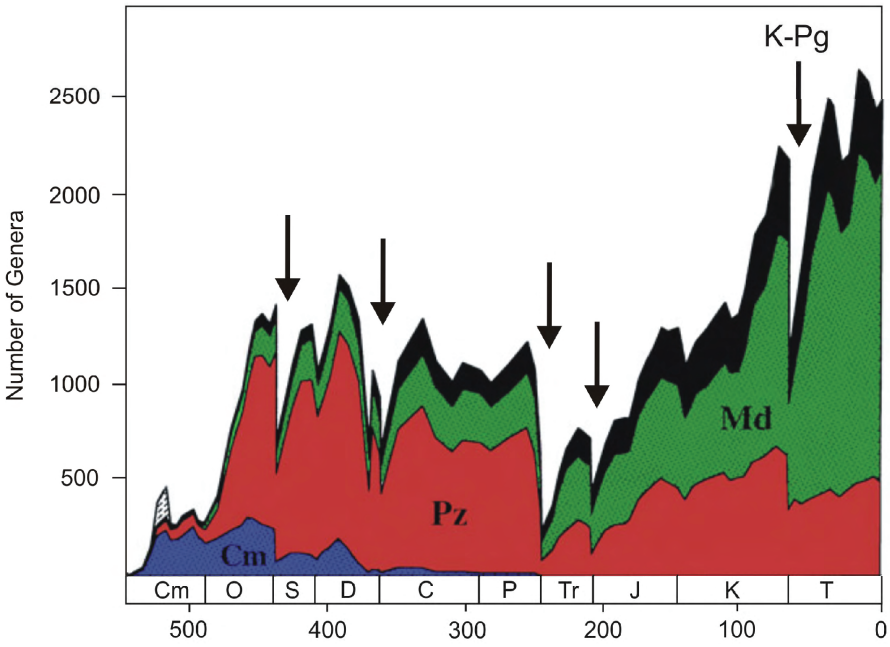

Figure I.5. Biodiversity by the number of genera during the Phanerozoic (Sepkoski Jr, 1996). Cm = Cambrian fauna, Pz = Paleozoic fauna, Md =modern fauna. Notice the abrupt decreases in diversity during the so called "big five" mass extinction events during the Phanerozoic (black arrows), such as the K-Pg.

An alternative and/or parallel mechanism described to have contributed to the mass extinction event at the K/Pg is the generation of a large igneous province on the Deccan Plateau of west-central India (Keller, 2003). This event is known as the Deccan Traps; it is dated within less than 1 Ma of the K/Pg boundary (Keller et al., 2008), and it may correspond to the greatest episode of continental flood basalt volcanism in the Phanerozoic. The Deccan Traps are responsible for flooding about 2.6 x 10^6 km^2 of India with basaltic lavas, releasing 5 x 10^{17} moles of mantle CO_2 into Earth's atmosphere over a duration 0.53-1.36 Ma (McLean, 1985). Environmental consequences of such a massive volcanic activity include a greenhouse warming affecting the global climate, a perturbation of the entire carbon cycle likely affecting ocean chemistry and promoting ocean acidification, and sea level and sedimentation changes, i.e., a combination of factors contributing to ecological instability and extinction (e.g., McLean, 1985). However, due to uncertainties about its precise duration and timing it has remained a rather speculative theory, although recent dating results placing the Deccan traps eruption

close to the K/Pg have strengthened its relationship with the mass extinction (Chenet et al., 2007; Keller et al., 2008).

The immediate causes of the extinction remain under discussion; however, several environmental and biological consequences of the meteor impact on a global scale have been proposed (c.f., Kring, 2007). Models have suggested that the nature of the impacted material (a submerged marine carbonate platform), and the energy released by the impact (0.7-3.4 x 10^{31} ergs), could have generated over 200 Gt of SO_2 and vapor water, and over 500 Gt of CO_2 (Pope et al., 1994; 1997; Kring, 2007). This probably produced an aerosol plume towards the stratosphere that caused more than a decade of reduced solar transmission, global cooling, acid rain, and disruption of ocean circulation (Pope et al., 1994; 1997). Recent constraints of the global cooling event suggest that its effects on ocean circulation (cooling of both surface and deeper waters) might have lasted for ~ 2 k.y. (Galeotti et al., 2004). Acid rain derived by the formation of sulfuric and nitric acids from sulfate aerosols, however, might have not been sufficient to acidify ocean basins (D'Hondt et al., 1994). Wildfires are thought to have occurred almost worldwide due to the widespread distribution of soot (Wolbach et al., 1988) and polycyclic aromatic hydrocarbons (Venkatesan and Dahl, 1989; Arinobu et al., 1999) in boundary samples coinciding with the iridium spike. Based on stable carbon isotope values of terrestrial biomarkers, and using a carbon mass balance between terrestrial above-ground biomass and atmosphere, it has been suggested that about 18-24% of the terrestrial above-ground biomass could have been instantaneously combusted at the K/Pg (Arinobu et al., 1999). Wildfires are estimated to have injected elevated concentrations of CO_2 into the atmosphere resulting in an interval of greenhouse warming (Crutzen, 1987; Wolbach et al., 1988). An alternative theory has recently challenged the global wildfire hypothesis though; based on the discovery of carbon cenospheres derived from the incomplete combustion of pulverized coal or fuel-oil droplets, it has been suggested that the impact combusted an organic-rich target crust (Harvey et al., 2008).

Biological and geochemical effects; biotic recovery. One of the most important biological consequences of the impact was the shutdown of photosynthesis and the collapse of the global food chain that resulted from the reduction of sunlight transmission due to a dust cover in the stratosphere (Alvarez et al., 1980). However, the disruption of photosynthesis appears to be related to the impact production of sulfate aerosols from the target rock (Pope et al., 1994; 1997; 1998), and to the soot produced by global wildfires (c.f., Kring, 2007), rather than to the impact dust theory (Pope, 2002). The reduced solar transmission has been estimated to have lasted for up to about a decade (Pope et al., 1994; 1997).

The disruption of photosynthesis in pelagic environments affected the global carbon cycle as observed by a pronounced negative carbon isotopic excursion in biogenic carbonates worldwide (Hsü et al., 1982; Zachos et al., 1989; D'Hondt et al., 1998). Carbon isotope records of planktic and benthic foraminifera obtained from deep-sea basins exhibit an abrupt disturbance of the "normal" isotopic gradient between surface and deep ocean waters at the K/Pg, assumed to represent the ceasing of organic matter export to the sea floor (Hsü et al., 1982; Zachos et al., 1989; D'Hondt et al., 1998). This isotopic anomaly has been interpreted to characterize two different scenarios; the first one includes the complete shutdown of primary production or an unusually low level of biological production in surface waters after the impact (Hsü et al., 1982). This theory has been described as the "Strangelove Ocean" model or an ocean "without life" (see review by D'Hondt, 2005). An alternative theory, also known as the "living ocean" model (Adams et al., 2004), involves a rapid recovery of primary production in surface waters after the impact but a sustained low export of organic matter to the deep ocean (D'Hondt et al., 1998). The latter assumes that the structure of the post-impact open-ocean ecosystems was completely altered (e.g., absence of large pelagic grazers or a decreased mean size of phytoplankton), resulting in a diminished packaging of organic matter into large particles and reduced export to the deep ocean (D'Hondt et al., 1998). Independent of the scenario, both fossil and geochemical records suggest that the evolutionary and biogeochemical recovery of the oceans occurred in two steps after about 3 Ma of the K/Pg, (Hsü et al., 1982; Zachos et al., 1989; D'Hondt et al., 1998; Adams et al., 2004; Coxall et al., 2006). The long observed recovery implies that the time required to

regenerate the pelagic ecosystem and to restore normal food webs was extremely long compared to the immediate physical effects of the impact.

Primary productivity following the K/Pg might not have diminished to the same extent and duration everywhere, though, especially at high-latitudes. Carbon isotope records from planktic and benthic foraminifera obtained in Antarctica indicates that the effects of the impact on productivity might have been smaller than at lower latitudes (Stott and Kennett, 1989). The recovery of the ecosystem in Antarctica and Denmark has been calculated to have occurred in ~ 500 ky (Barrera and Keller, 1994). Records of siliceous plankton (diatom and radiolarian) obtained from New Zealand indicate that bioproductivity might have been relatively high during the first 1 Ma following the K/Pg (Hollis et al., 1995; Hollis et al., 2003).

Survival across the boundary was governed by selective extinction; the shutdown of photosynthesis affected trophic webs that more strongly depended on living plant matter compared to those based on detritus (Sheehan and Hansen, 1986; Sheehan et al., 1996). Among marine microplankton, the groups more strongly forced to extinction included calcareous nannoplankton (coccoliths, nannoliths, and calcispheres) and planktonic foraminifera (MacLeod et al., 1997). Detritivorous organisms such as marine benthic scavengers and deposit feeders are thought to have buffered extinction at the boundary due to their ability to survive during the time that photosynthesis was halted (Sheehan and Hansen, 1986). Selective extinction appeared to have provided comparatively high survival rates to primary producers with benthic cysts or resting stages such as dinoflagellates (Brinkhuis and Zachariasse, 1988; Brinkhuis et al., 1998; Wendler et al., 2002), and to neritic and opportunistic species (Sheehan et al., 1996), notably at high latitude regions (Keller et al., 1993). Dinoflagellate cysts do not show accelerated rates of extinction across the K/Pg boundary (Brinkhuis and Zachariasse, 1988), and both organic-walled and calcareous-walled cyst-producing species dwelled during the earliest Paleocene (Brinkhuis et al., 1998; Wendler and Willems, 2002). Evidence for a rapid recovery of marine primary production has been found in neritic environments and close to continental margins, compared to relatively long recoveries of pelagic systems. Isotopic and geochemical evidence from Caravaca, Spain, suggests that a recovery of primary production occurred in about 7-13 ky (Kaiho et al., 1999). This

result is consistent with a biomarker record from Hokkaido, Japan, which revealed a recovery in algal production at about 9 ky after the K-Pg (Mita and Shimoyama, 1999). However, the resurgence of marine primary production in the globally distributed boundary clay layer separating the Late Maastrichtian from the Early Danian limestones remains poorly constrained. The latter is explained by the fact that the biotic recovery after the K/Pg has been classically addressed by the study of calcareous microfossils. Microfossil-based studies can be limited due to poor fossil preservation and reworking (Schmitz et al., 1992; Kaiho and Lamolda, 1999; Hart et al., 2004), and they disregard ubiquitous primary producers lacking hard-fossil structures such as eukaryotic microalgae and prokaryotic cyanobacteria. Moreover, alternative strategies of survival such as mixotrophy have received little or no attention when evaluating ecological recovery; e.g., small planktonic algae (<5 μm) can account for about 40-95% of bacterivory in the euphotic layer of stratified oceanic temperate waters (Zubkov and Tarran, 2008).

The boundary clay layer and the Fish Clay. The official K-Pg boundary Global Stratotype Section and Point (GSSP) at El Kef, Tunisia, contains all the internationally accepted criteria defining the K-Pg (Fig. I.6; Keller et al., 1995). One of the key features of the boundary layer marking the transition from the Late Maastrichtian to the earliest Danian is a clay layer that can be identified worldwide. At El Kef, the boundary is characterized by the presence of a 2-mm-thick red layer enriched in iridium, nickel-rich spinels, and clay spherules, and it is assumed to represent the "fallout" lamina resulting from the impact (sometimes also referred as "fire layer"). This layer is followed by a 50-cm-thick dark, organic-rich, and carbonate-poor clay which exhibits a 2-3‰ negative excursion in $\delta^{13}C$ interpreted to represent the global shutdown of marine productivity. The K/Pg boundary is defined at the base of the red layer, also characterized by fossil "biomarker" events such as the extinction of Cretaceous species and the first appearance of Paleogene species (Keller et al., 1995). However, large differences in the thickness of the clay layer are found among sections worldwide. The thickness varies from a few millimeters/centimeters in pelagic environments (e.g., deep sea cores), and up to several tens of centimeters.

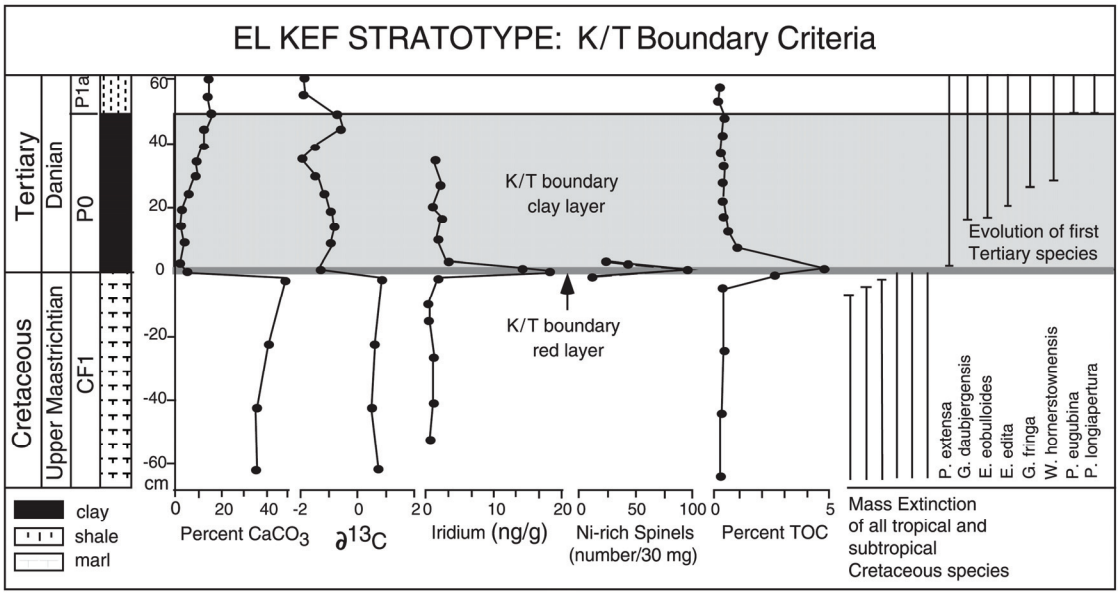

Figure I.6. Geochemical profiles and other criteria defining the K/Pg boundary at El Kef, Tunisia (Keller et al., 1995). From left to right, calcium carbonate content, $\delta^{13}C$ of bulk carbonate, iridium concentration, abundance of Ni-rich spinels, total organic carbon content, and planktonic foraminifera extinction and evolution. Dark gray area represents the position of the red layer, whereas the light gray area represents the organic-rich clay layer.

One of the classical sites for the study of the K/Pg is the so called "Fish Clay" boundary layer at Stevns Klint, Denmark, which has been intensively studied since the 19th century (see Christensen et al., 1973). The renowned section at Højerup (~ 7 cm thick) has been subdivided into six different beds according to lithology (Christensen et al., 1973), four of them lying within the fish clay (Fig. I.7). Bed-I corresponds to the Late Maastrichtian gray chalk, a calcareous silt with abundant bryozoans representing a typical Late Cretaceous fossil assemblage. Bed-II at the base of the fish clay (often considered as a transition into the red layer) is a 1-2 cm-thick gray and layered marl. Bed-III corresponds to the red layer (sometimes dark in color), a1-2 cm-thick silty marl with pyrite concretions and high concentrations of iridium and other rare elements. Bed-IV is a 3-5 cm-thick dark to light gray, laminated, organic-rich marl, which contains a high content of clays and a relatively low content of calcium carbonate. Bed-V is a light, streaked and veined marl up to 7-cm-thick, and contains white chalk fragments; bed-VI correspond to the so called "Cerithium-limestone", a white, sometimes slightly yellow indurated limestone which overlies the fish clay. The laminated nature of the fish clay

and the lack of bioturbation (e.g., Christensen et al., 1973; Hart et al., 2004), the presence of pyrite, and sulfur isotopes suggestive of intense microbial sulfate reduction (Schmitz, 1985), indicate deposition under oxygen-depleted conditions. Recently, Hart et al., (2004) described an extended (~ 40-cm-thick) counterpart of the section at Højerup. It is located at Kulstirenden (northern part of Stevns Klint) and shares the same features described for the fish clay at Højerup. Taking into account the relatively high organic content of the fish clay (Schmitz et al., 1988), this section offers an extraordinary opportunity to study biomarkers and other geochemical parameters at a high resolution. To date, lipid-based studies at the K/Pg have yielded contradictory results. Early studies of the fish clay suggested that preservation of organic material might have been compromised by high bacterial reworking and weathering (Simoneit and Beller, 1987; Meyers and Simoneit, 1990), whereas more recent studies from a section in Hokkaido, Japan, provided some of the first indications of a rapid recovery of primary production after the K/Pg (Mita and Shimoyama, 1999; Shimoyama et al., 2001), thus highlighting the potential of these studies. In combination with more sensitive techniques such as Metastable Reaction Monitoring Gas Chromatography Mass Spectrometry (MRM-GC-MS), biomarker studies in the fish clay at Kulstirenden might offer a completely new perspective for our understanding of the biotic recovery in the immediate aftermath of the K/Pg boundary.

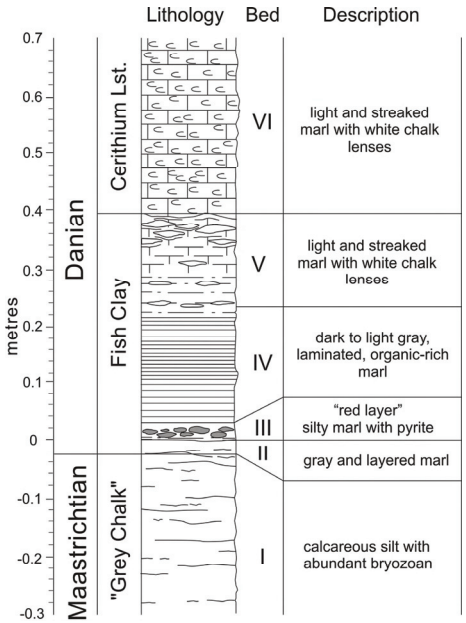

Figure I.7. Subdivision of the Cretaceous-Paleogene boundary layer at Kulstirenden, Stevns Klint, Denmark. Figure modified from Hart et al. (2004). Subdivision of different beds is based on the interpretation given to the fish clay at Højerup (Christensen et al., 1973). See text for the description of the different beds (I-VI)

I.4. BIOMARKER CONCEPT

"Biological markers or biomarkers can be defined as complex molecular fossils derived from biochemicals, particularly lipids, in once-living organisms" (Peters et al., 2005). The fundamental concept implies that the presence of a given lipid in an environmental sample (e.g., water column, sediments, rocks, fossil fuels, etc.) can be related to a particular organism or to a group of organisms inhabiting a distinctive environment. Thus, two important characteristics defining a biomarker are a limited number of known biological precursor(s), and a good preservation potential in sedimentary records. Biomarkers therefore can be used for constraining biotic/abiotic parameters of ancient environments, such as the ecology of marine primary producers, different sources of organic matter (e.g., marine versus terrestrial), and habitat of their precursors (e.g., water depth, oxygenation). Lipid biomarkers found in marine sedimentary records can originate from all three domains of life (i.e., archaea, bacteria, and eukaryotes); e.g., steroids occur generally in eukaryotes (e.g., algae and higher plants), hopanoids are exclusively synthesized by bacteria (e.g., some heterotrophic bacteria and cyanobacteria), and acyclic and cyclic isoprenoid glycerol ether lipids are restricted to the archaea (Fig. I.8; see Table I.2 for relationships between biomarkers, precursors, and characteristic environments; Peters et al., 2005). In living organisms, lipids serve a wide range of roles as membrane fluidity regulators, rigidifiers, barriers to proton exchange (e.g., steroids, hopanoids), energy sources (e.g., triacylglycerols of fatty acids), energy acquisition (e.g., pigments), metabolism (e.g., hormones, vitamins), and protective coating (e.g., leaf waxes).

In order to reconstruct a history of marine primary production from lipid biomarker proxies, one must understand the evolution of biomarkers from their genesis by marine phytoplankton to their preservation in marine sediments. First, organic matter produced by phytoplankton can be exported from surface waters to the sea floor either by the sinking of dense fecal pellets from zooplankton grazing or via the formation of marine aggregates. During transit through the water column, the organic matter can

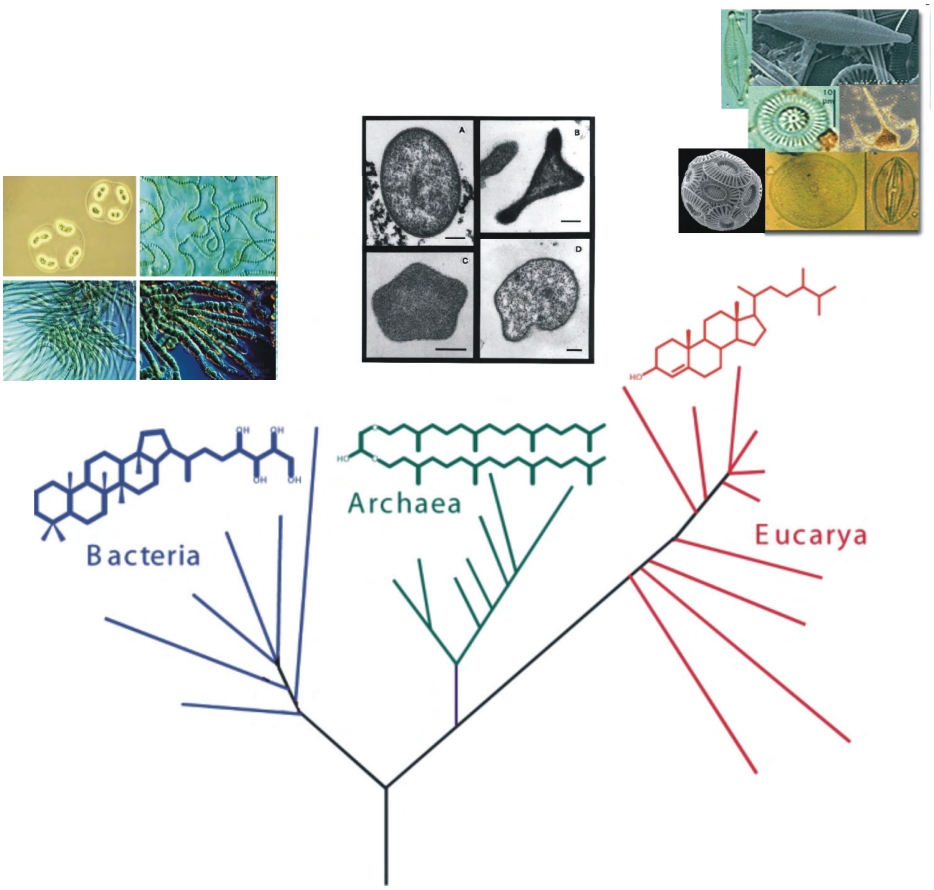

Figure I.8. Tree of life exhibiting the three main domains of life and their characteristic lipids. Bacteria and hopanoids; pictures depict heterotrophic bacteria and cyanobacteria (http://universe-review.ca). Archaea and archaeol; pictures depict archaeal cells (http://web.mit.edu). Eukarya and steroids; pictures depict different phytoplanktonic groups (http://www.learner.org).

undergo intense microbial degradation; usually only a small fraction (generally less than 0.1%) of the photosynthetically-produced organic matter in surface waters eventually accumulates in sediments (Wakeham and Lee, 1993). Of the organic matter that actually accumulates in the sediments, biomarkers can provide information regarding depositional conditions, diagenesis (biological, physical, and chemical alterations of organic matter at temperatures < 50°C during burial), thermal maturation during catagenesis (thermal alteration at temperatures ~50-150°C), biodegradation, lithology, and age (Peters et al., 2005). Diagenesis of biomarkers can result in a series of transformations such as oxidation/mineralization, defunctionalization, sulfurization, isomerisation, and aromatization (e.g., Peters et al., 2005). Defunctionalization of biolipids (loss of

functional groups) can occur due to dehydration, reduction, and decarboxylation, and leads to the formation of hydrocarbon skeletons, either saturated or aromatic, most commonly preserved in geological records. The incorporation of sulfur into biolipids during the early stages of diagenesis (sulfurization) occurs due to the reaction of inorganic sulfur species (sulfide, polysulfides) with functional groups (e.g., hydroxyl group, double bonds), and in the absence of iron which otherwise would lead to the formation of pyrite. This process can result in the formation of low- and high-molecular-weight organic sulfur compounds (intramolecular and intermolecular S incorporation, respectively), and plays an important role for the preservation of lipids and organic matter in organic-rich sediments from euxinic environments (e.g., Sinninghe Damsté and de Leeuw, 1990; Koopmans et al., 1996a). The interconversion of isomers (isomerization) such as the migration of double bonds in unsaturated biomarkers and configurational isomerization involving the intramolecular movement of hydrogen and methyl groups, can provide important information regarding thermal maturity (e.g., Farrimond et al., 1998). Molecular maturity parameters are based on the recognition of systematic changes in biomarker composition with increasing burial depth (and thus thermal maturation); they are based on the relative abundance of two stereoisomers, a thermally stable (non-biological) and a thermally unstable with the original biological configuration (e.g., Farrimond et al., 1998).

The stable isotopic composition of lipids (especially carbon and hydrogen) comprises an additional and important source of paleoenvironmental information. For carbon isotopes, for example, the isotopic composition of a naturally occurring biomarker depends on the carbon source utilized, the isotopic fractionation associated with carbon assimilation, metabolism and biosynthesis, and carbon budgets (Hayes, 1993). Thus, the stable carbon isotopic composition of a biomarker can provide important information about its parent organism(s), carbon source, position within an ancient ecosystem, and environmental conditions (Hayes, 1993; Hayes, 2001). Specific examples of the application of stable carbon and hydrogen isotopes in paleo-studies are given in following section.

Table I.2. Examples of selected biomarkers (including those used in this thesis) as indicators of biological sources and depositional environment (after Peters et al., 2005; see original citation for further references)

Compound	Biological precursor	Environment
nC$_{15}$, nC$_{17}$, nC$_{19}$	Algae	Lacustrine, marine
nC$_{27}$, nC$_{29}$, nC$_{31}$	Higher plants	Terrigenous
Mid-chain monomethylalkanes	Cyanobacteria	Hypersaline
Pristane/phytane (low)	Phototrophs, archaea	Anoxic, high salinity
C$_{20}$ HBI, C$_{25}$ HBI	Diatoms	Marine, lacustrine
C$_{31}$-C$_{40}$ head-to-head isoprenoids	Archaea	Unspecific
C$_{27-29}$ steranes	Algae and higher plants	Various
23,24-Dimethyl-cholestanes	Dinoflagellates, haptophytes	Marine
C$_{30}$ 24-*n*-propyl-cholestanes (4-desmethyl)	Chrysophyte algae	Marine
4-Methylsteranes	Some bacteria, dinoflagellates	Lacustrine or marine
Diasteranes	Algae/higher plants	Clay-rich rocks
Dinosteranes	Dinoflagellates	Marine, Triassic or younger
25,28,30-trisnorhopane	Bacteria	Anoxic marine, upwelling?
C$_{35}$ 17α,21β(H)-hopane	Bacteria	Reducing to anoxic
2-Methylhopanes	Cyanobacteria	Enclosed basin
3-Methylhopanes	Methanotrophic bacteria	Lacustrine?
Gammacerane	Tetrahymanol from ciliates	Stratified water, hypersaline
18α-Oleanane	Cretaceous or younger, terrestrial plants	Continent
^{13}C-rich 2,3,6-trimethyl-subtituted aryl isoprenoids, isorenieratene, isorenieratane	*Chlorobiaceae*, anaerobic green sulfur bacteria	Photic zone euxinia

I.5. PALEOENVIRONMENTAL RECONSTRUCTIONS BASED ON THE USE OF LIPID BIOMARKERS AND COMPOUND SPECIFIC ISOTOPE RATIOS

Molecular-isotopic signatures can comprise the only means to decipher past ecosystems and biological inputs for organisms that leave no morphological imprint in the geological record, and in sedimentary settings, where preservation of hard-fossils is precluded.

As an example, our understanding about the crucial role of photosynthetic cyanobacteria in the evolution of geochemical cycles over geological time scales, and their role as important photoautotrophs during some OAEs would have been difficult to assess without using biomarkers and stable isotopes. The combined presence of 2-methyl hopanes diagnostic of cyanobacteria (expressed as the 2-methyl hopane index (2-MeHI); Summons et al., 1999), and bulk nitrogen isotopes indicative of nitrogen fixation, has been used to infer that diazotrophy was the main source for nutrient N during Cretaceous OAEs (Kuypers et al., 2004b; Fig. I.9.). This interpretation has been recently supported by the stable nitrogen isotopic composition of geoporphyrins extracted from black shales deposited during OAE2, which led to the suggestion that diazotrophic cyanobacteria were major primary producers and contributed to the formation of black shales (Ohkouchi et al., 2006). Cyanobacteria also seemed to have played a key ecological role at the Permian-Triassic (P-T) mass extinction event. Biomarker evidence obtained from Meishan sections in Zhejiang, South China, indicates that maxima in the 2-MeHI occurred after two episodes of faunal mass extinction at the Permian-Triassic boundary (PTB), likely reflecting microbial responses to the catastrophic events that caused the extinction and ecosystem changes (Xie et al., 2005). New high-resolution data from the same locality shows even higher values of 2-MeHI and provides support for multiple episodes of paleoenvironmental change in the Early Triassic (Cao et al., in review), greatly highlighting the ecological role of cyanobacteria during this mass extinction event. This aspect, however, has not yet been addressed for the mass extinction

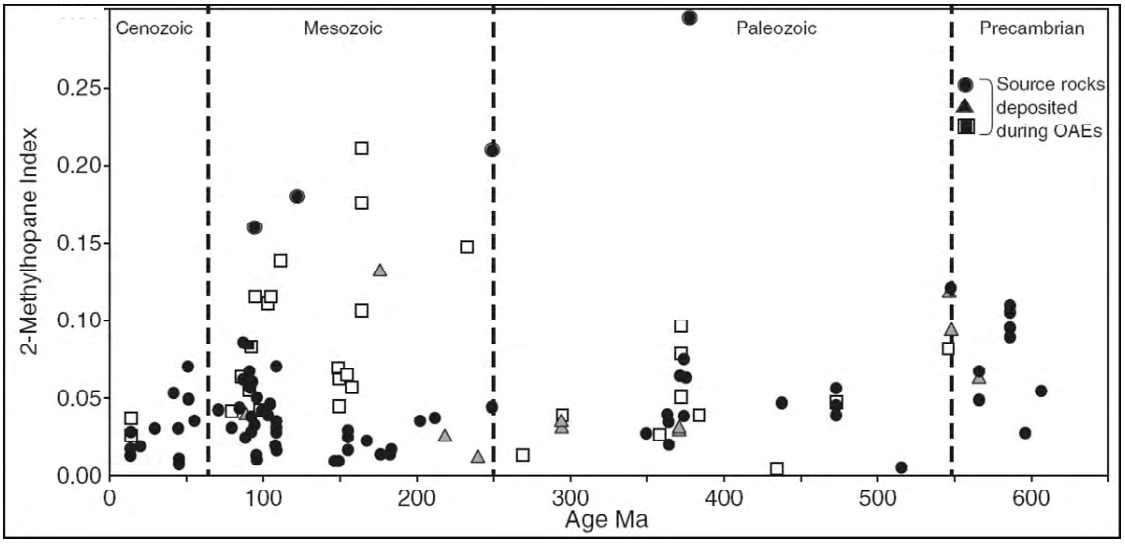

Figure I.9. 2-methylhopanoid index through geological time obtained from oils and organic-rich sediments (Knoll et al., 2007). Notice the increased values during Mesozoic OAEs and at the Permian-Triassic boundary.

event at the K-Pg, which could contribute to a better understanding of the associated ecological reorganization and recovery.

Biomarkers can also be used as paleoenvironmental "proxies". A given environmental variable of interest (e.g., temperature) can be reconstructed indirectly by using a single or multiple lipids, by combining different isomers, or from their stable isotopic composition. Some of the most pertinent properties accessible to molecular proxies for paleo-studies, including those frequently applied for Cretaceous OAEs, are sea surface temperature (SST), sea surface salinity (SSS), oxygenation, and ρCO2 (see Table I.3 for a summary).

For instance, the presence of isotopically enriched isorenieratane, derived from green sulfur bacteria in organic-rich sediments deposited during Cretaceous OAEs, has been used to suggest the widespread occurrence of photic zone euxinia (PZE) during these intervals (e.g., Sinninghe Damsté and Köster, 1998; Kuypers et al., 2004a; Wagner et al., 2004; Kolonic et al., 2005; Beckmann et al., 2008). Since *Chlorobiaceae* inhabit water depths deeper than most algae, where concentrations of CO_2 are high (chemocline), the combined carbon isotopic composition of isorenieratane and algal markers has been used to constrain the recycling of respired CO_2 during OAEs (van Breugel et al., 2006). Evidence for PZE is commonly accompanied by the presence of isotopically enriched

gammacerane, suggesting the presence of biomass derived from marine ciliates thriving at the chemocline and feeding on isotopically enriched *Chlorobiaceae*, which provides further evidence for water column stratification (e.g., Sinninghe Damsté et al., 1995). The lycopane/*n*-C_{31} ratio, based on the enhanced preservation of lycopane under anoxic conditions, is also suggested as an indicator for tracing changes in palaeoxicity (Sinninghe Damsté et al., 2003).

Table I.3. Selected paleoenvironmental proxies derived from lipid biomarkers

Parameter	Proxy	Rationale	Source	Reference
Sea surface temperature	Uk'$_{37}$ index	Unsaturation degree of long-chain ketones (alkenones)	Haptophyte algae	Brassell et al., 1986; Brassell, 1993
	TEX_{86} index	Distribution of glycerol dialkyl glycerol tetraethers (GDGTs) with different number of cyclopentane rings	Membrane lipids of planktonic archaea	Schouten et al., 2002
Oxygenation, water-column stratification	Isorenieratene, isorenieratane, aryl isoprenoids	Indicators of photic zone euxinia	Green sulfur bacteria	Summons and Powell, 1987; Koopmans et al., 1996b
	Gammacerane index	Present in stratified, anoxic, and/or hypersaline environments	Ciliates	ten Haven et al., 1989; Sinninghe Damsté et al., 1995
	Extended hopanes (homohopane index)	Present in euxinic and/or hypersaline environments	Bacteria	de Leeuw and Sinninghe Damsté, 1990; Peters and Moldowan, 1991
	Lycopane/*n*-C_{31} ratio	Preferential preservation of lycopane under anoxic conditions	Ly = marine photoautotroph? *n*-C_{31} = land-plants	Schulte et al., 2000; Sinninghe Damsté et al., 2003
	Phytane/pristane ratio	Degradation of phytol under anoxic and oxic conditions	marine photoautotroph	ten Haven et al., 1987
Partial pressure of CO_2 (ρCO_2)	$\delta^{13}C$ alkenone $\delta^{13}C$ phytane $\delta^{13}C$ sterols	Knowledge of isotopic fractionation factors are needed	Haptophyte Aquatic algae Aquatic algae	Freeman and Hayes, 1992; Pagani et al., 2005; Sinninghe Damsté et al., 2008
Sea surface salinity	δD alkenones	Salinity effect on fractionation	Haptophyte algae	Schouten et al., 2006
	δD n-C_{17}		Aquatic algae	Pagani et al., 2006

The carbon isotopic fractionation associated with the photosynthetic fixation of CO_2 is significantly correlated with the concentration of dissolved CO_2 in the environment. Thus, the isotopic composition of lipids found in sedimentary records, in combination with empirically-obtained isotopic fractionation factors of lipids in biological precursors, can be used to reconstruct changes in atmospheric ρCO2 in ancient environments (Freeman and Hayes, 1992). This approach has been used to calculate high ρCO_2 levels for the Cretaceous greenhouse climate (Freeman and Hayes, 1992; Kuypers et al., 1999; Bice et al., 2006; Sinninghe Damsté et al., 2008), which may be related to the elevated reconstructed SST of Cretaceous oceans (Schouten et al., 2003; Forster et al., 2007). ρCO2 reconstructions for the Cenomanian-Turonian OAE2 based on the compound-specific carbon isotopic composition of algal- and terrestrial-derived biomarkers, have been used to suggest the presence of a large and abrupt fall in atmospheric CO_2 concentrations which might have been responsible for the invoked expansion of C_4 plants on land during the Cretaceous (Kuypers et al., 1999; Sinninghe Damsté et al., 2008).

Culture experiments have demonstrated that the stable hydrogen isotopic fractionation associated with the synthesis of long chain alkenones in hapthophyte algae is linearly correlated with salinity, suggesting a potential use for salinity reconstructions in ancient environments (Schouten et al., 2006). This approach, in combination with other proxies, has reflected abrupt variations in SSS during the Late Holocene freshening of the Black Sea (van der Meer et al., 2008), and during the formation of Mediterranean sapropels (van der Meer et al., 2007). The same approach has been applied to biomarkers with a less specific source such as *n*-C_{17} alkane to reconstruct hydrological changes in the Arctic ocean during the Paleocene-Eocene thermal maximum (Pagani et al., 2006). However, its application for Cretaceous oceans remains less constrained.

I.6. RESEARCH FOCI AND OBJECTIVES

Through the combined use of molecular biomarkers, stable isotopes, and bulk geochemical parameters, the general scope of this thesis is to study the response of marine planktonic ecosystems to extreme environmental stress during the Cretaceous and at the K-Pg boundary.

This thesis can be divided into three main research topics with specific goals:

1. The Cenomanian-Turonian Boundary OAE-2 at the Levant carbonate platform of Central Jordan.
    - The main objective of this project is to assess the ecological and geochemical consequences of anoxia/euxinia during OAE2.
    - I asses whether episodes of anoxia/euxinia were accompanied by ecological changes in the community of marine primary producers, i.e, successions between algae and photosynthetic bacteria.
    - Additionally, it is aimed to construct a conceptual model illustrating the mechanisms leading to the development of oxygen depletion and the deposition of organic-rich sediments.

2. The Coniacian OAE-3 at the eastern equatorial Atlantic (ODP Site 1259, Demerara Rise off the coast of Surinam).
    - This project aims to unravel the oceanographic and climatic dynamics leading to variations in marine primary production through the use of compound-specific stable carbon and hydrogen isotopes in marine- and terrestrial-derived *n*-alkanes. An especial emphasis is giving to the role of upwelling and continental runoff on sustained high primary production.
    - Additionally, it is aimed to study the effects of varying primary production on the eccentricity-driven deposition of carbonate- and organic-rich sediments. To achieve this, a sedimentary sequence covering and entire cycle of alternated facies is studied.

3. The Cretaceous-Paleogene mass extinction event: The Fish Clay section at Stevns Klint, Denmark.
    - I test the hypothesis that marine photosynthesis recovered rapidly during the immediate aftermath of the K/Pg after incoming solar radiation levels returned to "normal". As yet, this topic has been addressed almost entirely by using microfossils and their stable carbon and oxygen isotopic composition, whereas no detailed recovery of photosynthetic organisms without hard-fossil structures exists. By studying phytoplanktonic biomarkers in a high-resolution record of an exceptionally thick section of the Fish Clay at Denmar, I expect to resolve short-term variations in primary production in order to provide a more comprehensive view of the biotic recovery at the K-Pg.

I.7. CONTRIBUTIONS TO PUBLICATIONS

This thesis includes the full version of three manuscripts in different stages for publication in international, peer-reviewed journals. Chapter II is accepted for publication pending moderate revisions; chapter III is the first draft of a manuscript in preparation; chapter IV is ready for submission.

CHAPTER II – full manuscript

Molecular-isotopic evidence of environmental and ecological changes across the Cenomanian-Turonian boundary in the Levant Platform of central Jordan

Julio Sepúlveda, Jens Wendler, Arne Leider, Hans-Joachim Kuss, Roger E. Summons, and Kai-Uwe Hinrichs

Julio Sepúlveda developed research strategy, performed laboratory work for the preparation and analysis of samples by GC-MS, MRM-GC-MS, and GC-irMS, processed and interpreted data, and produced figures. Jens Wendler developed research strategy, performed fieldtrip and sampling, and produced biostratigraphy and bulk geochemical data. Arne Leider assisted with laboratory work for the preparation and analysis of

samples for GC-MS and GC-irMS, and processed data as part of his undergraduate thesis. Hans-Joachim Kuss developed research strategy, and performed fieldtrip and sampling. Roger E. Summons facilitated his laboratory at MIT and contributed with data interpretation. Kai-Uwe Hinrichs developed research strategy and contributed with data interpretation. Julio Sepúlveda wrote the paper with contributions from Kai-Uwe Hinrichs, Roger E. Summons, and Jens Wendler. All co-authors provided editorial comments.

Accepted for publication with moderate comments (August 2008) in *Organic Geochemistry*

CHAPTER III – first draft of full manuscript

Oceanographic and climatic dynamics in the Late Cretaceous Equatorial Atlantic (ODP Site 1259): a compound-specific stable isotope approach into the formation of organic-rich sediments

Julio Sepúlveda, Arne Leider, and Kai-Uwe Hinrichs

Julio Sepúlveda developed research strategy, performed part of the laboratory work for the preparation and analysis of samples by GC-MS and GC-irMS, interpreted data and produced figures. Arne Leider conducted the laboratory work for the preparation and analysis of samples for GC-MS and GC-irMS, and contributed with data processing as part of his master thesis. Kai-Uwe Hinrichs developed research strategy and contributed to data interpretation. Julio Sepúlveda wrote the paper with contributions from Kai-Uwe Hinrichs.

First draft of manuscript in preparation for submission to *Earth and Planetary Science Letters*

CHAPTER IV – full manuscript

Rapid Resurgence of Marine Productivity after the Cretaceous-Paleogene Mass Extinction Event

Julio Sepúlveda, Jens Wendler, Roger E. Summons, and Kai-Uwe Hinrichs

Julio Sepúlveda developed research strategy, performed fieldtrip and sampling, performed laboratory work for the preparation and analysis of samples for GC-MS and MRM-GC-MS, processed and interpreted data, and produced figures. Jens Wendler guided fieldtrip and sampling, and provided geological background for data interpretation. Roger E. Summons developed research strategy, facilitated his laboratory at MIT, and contributed with data interpretation. Kai-Uwe Hinrichs developed research strategy, performed fieldtrip and sampling, and contributed with data interpretation. Julio Sepúlveda wrote the paper with contributions from all co-authors.

Manuscript ready for submission to *Nature*

I.8. REFERENCES

Adams, J.B., Mann, M.E., D'Hondt, S., 2004. The Cretaceous-Tertiary extinction: Modeling carbon flux and ecological response. Paleoceanography 19, PA1002, doi:10.1029/2002PA000849.

Alvarez, L.W., Alvarez, W., Asaro, F., Michel, H.V., 1980. Extraterrestrial cause for the Cretaceous-Tertiary extinction. Science 208, 1095-1108.

Arinobu, T., Ishiwatari, R., Kaiho, K., Lamolda, M.A., 1999. Spike of pyrosynthetic polycyclic aromatic hydrocarbons associated with an abrupt decrease in delta 13 C of a terrestrial biomarker at the Cretaceous-Tertiary boundary at Caravaca, Spain. Geology 27, 723-726.

Arrigo, K.R., 2005. Marine microorganisms and global nutrient cycles. Nature 437, 349-355.

Arthur, M.A., Schlanger, S.O., Jenkyns, H.C., 1987. The Cenomanian-Turonian Oceanic Anoxic Event, II. Palaeoceanographic controls on organic-matter production and preservation. Geological Society, London, Special Publications 26, 401-420.

Arthur, M.A., Dean, W.E., Pratt, L.M., 1988. Geochemical and climatic effects of increased marine organic carbon burial at the Cenomanian/Turonian boundary. Nature 335, 714-717.

Arthur, M.A., Sageman, B.B., 1994. Marine Black Shales: Depositional Mechanisms and Environments of Ancient Deposits. Annual Review of Earth and Planetary Sciences 22, 499-551.

Barrera, E., Keller, G., 1994. Productivity across the Cretaceous/Tertiary boundary in high latitudes. Geological Society of America Bulletin 106, 1254-1266.

Beckmann, B., Hofmann, P., März, C., Schouten, S., Sinninghe Damsté, J.S., Wagner, T., 2008. Coniacian-Santonian deep ocean anoxia/euxinia inferred from molecular and inorganic markers: Results from the Demerara Rise (ODP Leg 207). Organic Geochemistry In Press, Corrected Proof,

Bice, K.L., Norris, R.D., 2002. Possible atmospheric CO2 extremes of the Middle Cretaceous (late Albian–Turonian). Paleoceanography 17, 1070, doi:10.1029/2002PA000778.

Bice, K.L., Birgel, D., Meyers, P.A., Dahl, K.A., Hinrichs, K.-U., Norris, R.D., 2006. A multiple proxy and model study of Cretaceous upper ocean temperatures and atmospheric CO_2 concentrations. Paleoceanography 21, PA2002, doi:10.1029/2005PA001203.

Bohor, B.F., Foord, E.E., Modreski, P.J., Triplehorn, D.M., 1984. Mineralogic Evidence for an Impact Event at the Cretaceous-Tertiary Boundary. Science 224, 867-869.

Brassell, S.C., Eglinton, G., Marlowe, I.T., Pflaumann, U., Sarnthein, M., 1986. Molecular stratigraphy: a new tool for climatic assessment. Nature 320, 129-133.

Brassell, S.C., 1993. Applications of biomarkers for delineating marine paleoclimatic fluctuations during the Pleistocene. Organic Geochemistry: Principles and Applications 699-738.

Brinkhuis, H., Zachariasse, W.J., 1988. Dinoflagellate cysts, sea level changes and planktonic foraminifers across the Cretaceous-Tertiary boundary at El Haria, northwest Tunisia. Marine Micropaleontology 13, 153-191.

Brinkhuis, H., Bujak, J.P., Smit, J., Versteegh, G.J.M., Visscher, H., 1998. Dinoflagellate-based sea surface temperature reconstructions across the Cretaceous-Tertiary boundary. Palaeogeography, Palaeoclimatology, Palaeoecology 141, 67-83.

Brumsack, H.-J., 2006. The trace metal content of recent organic carbon-rich sediments: Implications for Cretaceous black shale formation. Palaeogeography, Palaeoclimatology, Palaeoecology 232, 344-361.

Cao, C., Love, G.D., Hays, L.E., Bowring, S.A., Wanga, W., Shena, S., Summons, R.E., in review. Biogeochemical evidence for euxinic oceans and ecological disturbance presaging the end-Permian Mass Extinction Event. Earth and Planetary Science Letters

Chenet, A.-L., Quidelleur, X., Fluteau, F., Courtillot, V., Bajpai, S., 2007. ^{40}K-^{40}Ar dating of the Main Deccan large igneous province: Further evidence of KTB age and short duration. Earth and Planetary Science Letters 263, 1-15.

Christensen, L., Fregerslev, S., Simonsen, A., Thiede, J., 1973. Sedimentology and depositional environment of Lower Danian Fish Clay from Stevns Klint, Denmark. Bulletin of the Geological Society of Denmark 22, 193-212.

Cowie, G., 2005. The biogeochemistry of Arabian Sea surficial sediments: A review of recent studies. Progress In Oceanography 65, 260-289.

Coxall, H.K., D'Hondt, S., Zachos, J.C., 2006. Pelagic evolution and environmental recovery after the Cretaceous-Paleogene mass extinction. Geology 34, 297-300.

Crutzen, P.J., 1987. Acid rain at the K/T boundary. Nature 330, 108-109.

D'Hondt, S., Pilson, M.E.Q., Sigurdsson, H., Hanson, J.A.K., Carey, S., 1994. Surface-water acidification and extinction at the Cretaceous-Tertiary boundary. Geology 22, 983-986.

D'Hondt, S., Donaghay, P., Zachos, J.C., Luttenberg, D., Lindinger, M., 1998. Organic Carbon Fluxes and Ecological Recovery from the Cretaceous-Tertiary Mass Extinction. Science 282, 276-279.

D'Hondt, S., 2005. Consequences of the Cretaceous/Paleogene mass extinction for marine ecosystems. Annual Review of Ecology, Evolution, and Systematics 36, 295-317.

de Leeuw, J.W., Sinninghe Damsté, J.S., 1990. Organic sulphur compounds and other biomarkers as indicators of palaeosalinity. In: W.L. Orr, C.M. White (Eds.), Geochemistry of Sulfur in Fossil Fuels, ACS Symposium Series 429, American Chemical Society, Washington DC, pp. 417-443.

Dumitrescu, M., Brassell, S.C., 2005. Biogeochemical assessment of sources of organic matter and paleoproductivity during the early Aptian Oceanic Anoxic Event at Shatsky Rise, ODP Leg 198. Organic Geochemistry 36, 1002-1022.

Erbacher, J., Huber, B.T., Norris, R.D., Markey, M., 2001. Increased thermohaline stratification as a possible cause for an ocean anoxic event in the Cretaceous period. Nature 409, 325-327.

Falkowski, P.G., 1997. Evolution of the nitrogen cycle and its influence on the biological sequestration of CO2 in the ocean. Nature 387, 272-275.

Falkowski, P.G., Katz, M.E., Knoll, A.H., Quigg, A., Raven, J.A., Schofield, O., Taylor, F.J.R., 2004. The Evolution of Modern Eukaryotic Phytoplankton. Science 305, 354-360.

Farrimond, P., Taylor, A., TelnAEs, N., 1998. Biomarker maturity parameters: the role of generation and thermal degradation. Organic Geochemistry 29, 1181-1197.

Forster, A., Schouten, S., Baas, M., Sinninghe Damsté, J.S., 2007. Mid-Cretaceous (Albian&-Santonian) sea surface temperature record of the tropical Atlantic Ocean. Geology 919-922.

Freeman, K.H., Hayes, J.M., 1992. Fractionation of Carbon Isotopes by Phytoplankton and Estimates of Ancient Co2 Levels. Global Biogeochemical Cycles 6, 185–198.

Friedrich, O., Norris, R.D., Bornemann, A., Beckmann, B., Pälike, H., Worstell, P., Hofmann, P., Wagner, T., 2008. Cyclic changes in Turonian to Coniacian planktic foraminiferal assemblages from the tropical Atlantic Ocean. Marine Micropaleontology 68, 299-313.

Galeotti, S., Brinkhuis, H., Huber, M., 2004. Records of post-Cretaceous-Tertiary boundary millennial-scale cooling from the western Tethys: A smoking gun for the impact-winter hypothesis? Geology 32, 529-532.

Grice, K., Cao, C., Love, G.D., Bottcher, M.E., Twitchett, R.J., Grosjean, E., Summons, R.E., Turgeon, S.C., Dunning, W., Jin, Y., 2005. Photic Zone Euxinia During the Permian-Triassic Superanoxic Event. Science 307, 706-709.

Hart, M.B., Feist, S.E., Price, G.D., Leng, M.J., 2004. Reappraisal of the KT boundary succession at Stevns Klint, Denmark. Journal of the Geological Society (London) 161, 885-892.

Harvey, M.C., Brassell, S.C., Belcher, C.M., Montanari, A., 2008. Combustion of fossil organic matter at the Cretaceous-Paleogene (K-P) boundary. Geology 36, 355-358.

Hayes, J.M., 1993. Factors controlling ^{13}C contents of sedimentary organic compounds: principles and evidence. Marine Geology 113, 111–125.

Hayes, J.M., Strauss, H., Kaufman, A.J., 1999. The abundance of ^{13}C in marine organic matter and isotopic fractionation in the global biogeochemical cycle of carbon during the past 800 Ma. Chemical Geology 161, 103-125.

Hayes, J.M., 2001. Fractionation of Carbon and Hydrogen Isotopes in Biosynthetic Processes. Reviews in Mineralogy and Geochemistry 43, 225.

Helly, J.J., Levin, L.A., 2004. Global distribution of naturally occurring marine hypoxia on continental margins. Deep Sea Research Part I: Oceanographic Research Papers 51, 1159-1168.

Hildebrand, A.R., Penfield, G.T., Kring, D.A., Pilkington, M., Camargo Zanoguera, A., Jacobsen, S.B., Boynton, W.V., 1991. Chicxulub Crater; a possible Cretaceous/Tertiary boundary impact crater on the Yucatan Peninsula, Mexico. Geology 19, 867-871.

Hollis, C.J., Rodgers, K.A., Parker, R.J., 1995. Siliceous plankton bloom in the earliest Tertiary of Marlborough, New Zealand. Geology 23, 835-838.

Hollis, C.J., Strong, C.P., Rodgers, K.A., Rogers, K.M., 2003. Paleoenvironmental changes across the Cretaceous/Tertiary boundary at Flaxbourne River and Woodside Creek, eastern Marlborough, New Zealand. NEW ZEALAND JOURNAL OF GEOLOGY AND GEOPHYSICS 46, 177-198.

Hsü, K.J., He, Q., McKenzie, J.A., Weissert, H., Perch-Nielsen, K., Oberhansli, H., Kelts, K., LaBrecque, J., Tauxe, L., Krahenbuhl, U., Percival, S.F., Jr., Wright, R., Karpoff, A.M., Petersen, N., Tucker, P., Poore, R.Z., Gombos, A.M., Pisciotto, K., Carman, M.F., Jr., Schreiber, E., 1982. Mass Mortality and Its Environmental and Evolutionary Consequences. Science 216, 249-256.

Jarvis, I.A.N., Gale, A.S., Jenkyns, H.C., Pearce, M.A., 2006. Secular variation in Late Cretaceous carbon isotopes: a new d13C carbonate reference curve for the Cenomanian–Campanian (99.6–70.6 Ma). Geological Magazine 143, 561-608.

Jenkyns, H.C., 1980. Cretaceous anoxic events: from continents to oceans. Journal of the Geological Society 137, 171-188.

Jenkyns, H.C., Forster, A., Schouten, S., Damste, J.S., 2004. High temperatures in the Late Cretaceous Arctic Ocean. Nature(London) 432, 888-892.

Kaiho, K., Kajiwara, Y., Tazaki, K., Ueshima, M., Takeda, N., Kawahata, H., Arinobu, T., Ishiwatari, R., Hirai, A., Lamolda, M.A., 1999. Oceanic Primary Productivity and Dissolved Oxygen Levels at the Cretaceous/Tertiary Boundary: Their Decrease, Subsequent Warming, and Recovery. Paleoceanography 14, 511–524.

Kaiho, K., Lamolda, M.A., 1999. Catastrophic extinction of planktonic foraminifera at the Cretaceous-Tertiary boundary evidenced by stable isotopes and foraminiferal abundance at Caravaca, Spain. Geology 27, 355-358.

Kashiyama, Y., Ogawa, N.O., Kuroda, J., Shiro, M., Nomoto, S., Tada, R., Kitazato, H., Ohkouchi, N., 2008. Diazotrophic cyanobacteria as the major photoautotrophs during mid-Cretaceous oceanic anoxic events: Nitrogen and carbon isotopic evidence from sedimentary porphyrin. Organic Geochemistry In Press, Corrected Proof,

Katz, M.E., 2005. Biological overprint of the geological carbon cycle. Marine Geology 217, 323-338.

Keller, G., Barrera, E., Schmitz, B., Mattson, E., 1993. Gradual mass extinction, species survivorship, and long-term environmental changes across the Cretaceous-Tertiary boundary in high latitudes. Geological Society of America Bulletin 105, 979-997.

Keller, G., Li, L., MacLeod, N., 1995. The Cretaceous/Tertiary boundary stratotype section at El Kef, Tunisia: how catastrophic was the mass extinction? Palaeogeography, Palaeoclimatology, Palaeoecology 119, 221-254.

Keller, G., 2003. Biotic effects of impacts and volcanism. Earth and Planetary Science Letters 215, 249-264.

Keller, G., Adatte, T., Gardin, S., Bartolini, A., Bajpai, S., 2008. Main Deccan volcanism phase ends near the K-T boundary: Evidence from the Krishna-Godavari Basin, SE India. Earth and Planetary Science Letters 268, 293-311.

Knoll, A.H., Summons, R.E., Waldbauer, J.R., Zumberge, J.E., 2007. The Geological Succession of Primary Producers in the Oceans. In: F. P., K. A.H. (Eds.), The Evolution of Primary Producers in the Sea, Academic Press, Boston, pp. 133-163.

Kolonic, S., Wagner, T., Forster, A., Damste, J.S.S., Walsworth- Bell, B., Erba, E., Turgeon, S., Brumsack, H.J., Chellai, E.I., Tsikos, H., Kuhnt, W., Kuypers, M.M.M., 2005. Black shale deposition on the northwest African Shelf during the Cenomanian/Turonian oceanic anoxic event: Climate coupling and global organic carbon burial. Paleoceanography 20, PA1006, doi:10.1029/2003PA000950.

Koopmans, M.P., de Leeuw, J.W., Lewan, M.D., Sinninghe Damsté, J.S., 1996a. Impact of dia- and catagenesis on sulfur and oxygen sequestration of biomarkers as revealed by artificial maturation of an immature sedimentary rock. Organic Geochemistry 25, 391-426.

Koopmans, M.P., Koster, J., Van Kaam-Peters, H.M.E., Kenig, F., Schouten, S., Hartgers, W.A., de Leeuw, J.W., Sinninghe Damsté, J.S., 1996b. Diagenetic and catagenetic products of isorenieratene: Molecular indicators for photic zone anoxia. Geochimica et Cosmochimica Acta 60, 4467-4496.

Kring, D.A., 2007. The Chicxulub impact event and its environmental consequences at the Cretaceous-Tertiary boundary. Palaeogeography, Palaeoclimatology, Palaeoecology 255, 4-21.

Kuypers, M.M.M., Pancost, R.D., Sinninghe Damsté, J.S., 1999. A large and abrupt fall in atmospheric CO_2 concentration during Cretaceous times. Nature 399, 342-345.

Kuypers, M.M.M., Blokker, P., Erbacher, J., Kinkel, H., Pancost, R.D., Schouten, S., Sinninghe Damsté, J.S., 2001. Massive expansion of marine archaea during a mid-Cretaceous oceanic anoxic event. Science 293, 92-94.

Kuypers, M.M.M., Blokker, P., Hopmans, E.C., Kinkel, H., Pancost, R.D., Schouten, S., Sinninghe Damsté, J.S., 2002a. Archaeal remains dominate marine organic matter from the early Albian oceanic anoxic event 1b. Palaeogeography, Palaeoclimatology, Palaeoecology 185, 211-234.

Kuypers, M.M.M., Pancost, R.D., Nijenhuis, I.A., Sinninghe Damsté, J.S., 2002b. Enhanced productivity led to increased organic carbon burial in the euxinic North Atlantic basin during the late Cenomanian oceanic anoxic event. Paleoceanography 17, 1051, doi:10.1029/2000PA000569.

Kuypers, M.M.M., Lourens, L.J., Rijpstra, W.R.C., Pancost, R.D., Nijenhuis, I.A., Sinninghe Damsté, J.S., 2004a. Orbital forcing of organic carbon burial in the proto-North Atlantic during oceanic anoxic event 2. Earth and Planetary Science Letters 228, 465-482.

Kuypers, M.M.M., van Breugel, Y., Schouten, S., Erba, E., Sinninghe Damsté, J.S., 2004b. N_2-fixing cyanobacteria supplied nutrient N for Cretaceous oceanic anoxic events. Geology 32, 853-856.

Leckie, M., Bralower, T.J., Cashmann, R., 2002. Oceanic anoxic events and plankton evolution: Biotic response to tectonic forcing during the mid-Cretaceous. Paleoceanography 17, 1041, doi:10.1029/2001PA000623.

Lüning, S., Kolonic, S., Belhadj, E.M., Belhadj, Z., Cota, L., Baric, G., Wagner, T., 2004. Integrated depositional model for the Cenomanian-Turonian organic-rich strata in North Africa. Earth-Science Reviews 64, 51-117.

MacLeod, N., Rawson, P.F., Forey, P.L., Banner, F.T., Boudagher-Fadel, M.K., Bown, P.R., Burnett, J.A., Chambers, P., Culver, S., Evans, S.E., Jeffery, C., Kaminski, M.A., Lord, A.R., Milner, A.C., Milner, A.R., Morris, N., Owen, E., Rosen, B.R., Smith, A.B., Taylor, P.D., Urquhart, E., Young, J.R., 1997. The Cretaceous-Tertiary biotic transition. Journal of the Geological Society 154, 265-292.

McLean, D.M., 1985. Deccan traps mantle degassing in the terminal Cretaceous marine extinctions. Cretaceous Research 6, 235-259.

Meyer, K.M., Kump, L.R., 2008. Oceanic Euxinia in Earth History: Causes and Consequences. Annual Review of Earth and Planetary Sciences 36, 251-288.

Meyers, P.A., Simoneit, B.R.T., 1990. Global comparisons of organic matter in sediments across the Cretaceous/Tertiary boundary. Organic Geochemistry 16, 641-648.

Meyers, P.A., 2006. Paleoceanographic and paleoclimatic similarities between Mediterranean sapropels and Cretaceous black shales. Palaeogeography, Palaeoclimatology, Palaeoecology 235, 305-320.

Meyers, P.A., Bernasconi, S.M., Forster, A., 2006. Origins and accumulation of organic matter in expanded Albian to Santonian black shale sequences on the Demerara Rise, South American margin. Organic Geochemistry 37, 1816-1830.

Mita, H., Shimoyama, A., 1999. Characterization of n-alkanes, pristane and phytane in the Cretaceous/Tertiary boundary sediments at Kawaruppu, Hokkaido, Japan. Geochemical Journal 33, 285-294.

Mort, H., Jacquat, O., Adatte, T., Steinmann, P., Föllmi, K., Matera, V., Berner, Z., Stuben, D., 2007. The Cenomanian/Turonian anoxic event at the Bonarelli Level in Italy and Spain: enhanced productivity and/or better preservation? Cretaceous Research 28, 597-612.

Nederbragt, A.J., Thurow, J., Pearce, R., 2007. Sediment Composition and Cyclicity in the Mid-Cretaceous at Demerara Rise, ODP Leg 207. In: D.C. Mosher, J. Erbacher, M.J. Malone (Eds.), Proceedings of the Ocean Drilling Program, Scientific Results, 207, College Station, Texas, pp. 1-31.

Ohkouchi, N., Kashiyama, Y., Kuroda, J., Ogawa, N.O., Kitazato, H., 2006. The importance of diazotrophic cyanobacteria as primary producers during Cretaceous Oceanic Anoxic Event 2. Biogeosciences 3, 467-478.

Pagani, M., Freeman, K.H., Arthur, M.A., 1999. Late Miocene atmospheric CO2 concentrations and the expansion of C_4 grasses. Science 285, 876-879.

Pagani, M., Zachos, J.C., Freeman, K.H., Tipple, B., Bohaty, S., 2005. Marked Decline in Atmospheric Carbon Dioxide Concentrations During the Paleogene. Science 309, 600-603.

Pagani, M., Pedentchouk, N., Huber, M., Sluijs, A., Schouten, S., Brinkhuis, H., Damste, J.S.S., Dickens, G.R., Expedition-302-Scientists, 2006. Arctic hydrology during global warming at the Palaeocene/Eocene thermal maximum. Nature 442, 671-675.

Peters, K.E., Moldowan, J.M., 1991. Effects of source, thermal maturity and biodegradation on the distribution and isomerization of homohopanes in petroleum. Organic Geochemistry 17, 47-61.

Peters, K.E., Walters, C.C., Moldowan, J.M., 2005. The Biomarker Guide, 2nd edition. Cambridge University Press, Cambridge.

Pope, K.O., Ocampo, A.C., Duller, C.E., 1991. Mexican site for K/T impact crater? Nature 351, 105-105.

Pope, K.O., Baines, K.H., Ocampo, A.C., Ivanov, B.A., 1994. Impact winter and the Cretaceous/Tertiary extinctions: Results of a Chicxulub asteroid impact model. Earth and Planetary Science Letters 128, 719-725.

Pope, K.O., Baines, K.H., Ocampo, A.C., Ivanov, B.A., 1997. Energy, volatile production, and climatic effects of the Chicxulub Cretaceous/Tertiary impact. Journal of Geophysical Research 102, 21645–21664.

Pope, K.O., D'Hondt, S.L., Marshall, C.R., 1998. Meteorite impact and the mass extinction of species at the Cretaceous/Tertiary boundary. Proceedings of the National Academy of Sciences 95, 11028-11029.

Pope, K.O., 2002. Impact dust not the cause of the Cretaceous-Tertiary mass extinction. Geology 30, 99-102.

Poulsen, C.J., Barron, E.J., Peterson, W.H., Wilson, P.A., 1999. A reinterpretation of Mid-Cretaceous shallow marine temperatures through model-data comparison. Paleoceanography 14, 679-697.

Ryder, G., 1996. The unique significance and origin ofthe Cretaceous-Tertiary boundary: Historical context and burdens of proof. In: G. Ryder, D.E. Fastovsky, S. Gartner (Eds.), The Cretaceous-Tertiary Event and Other Catastrophes in Earth History, Geological Society of America, pp.

Schlanger, S.O., Jenkyns, H.C., 1976. Cretaceous oceanic anoxic events: causes and consequences. Geologie en Mijnbouw 55, 179-184.

Schlanger, S.O., Arthur, M.A., Jenkyns, H.C., Scholle, P.A., 1987. The Cenomanian-Turonian Oceanic Anoxic Event, I. Stratigraphy and distribution of organic carbon-rich beds and the marine $\delta^{13}C$ excursion. Geological Society, London, Special Publications 26, 371-399.

Schmitz, B., 1985. Metal precipitation in the Cretaceous-Tertiary boundary clay at Stevns Klint, Denmark. Geochimica et Cosmochimica Acta 49, 2361-2370.

Schmitz, B., Andersson, P., Dahl, J., 1988. Iridium, sulfur isotopes and rare earth elements in the Cretaceous-Tertiary boundary clay at Stevns Klint, Denmark. Geochimica et Cosmochimica Acta 52, 229-236.

Schmitz, B., Keller, G., Stenvall, O., 1992. Stable isotope and foraminiferal changes across the Cretaceous-Tertiary boundary at Stevns Klint, Denmark: Arguments for long-term oceanic instability before and after bolide-impact event. Palaeogeography, Palaeoclimatology, Palaeoecology 96, 233-260.

Schouten, S., Hopmans, E.C., Schefuss, E., Sinninghe Damste, J.S., 2002. Distributional variations in marine crenarchaeotal membrane lipids: a new tool for reconstructing ancient sea water temperatures? Earth and Planetary Science Letters 204, 265-274.

Schouten, S., Hopmans, E.C., Forster, A., van Breugel, Y., Kuypers, M.M.M., Sinninghe Damsté, J.S., 2003. Extremely high sea-surface temperatures at low latitudes during the middle Cretaceous as revealed by archaeal membrane lipids. Geology 31, 1069-1072.

Schouten, S., Ossebaar, J., Schreiber, K., Kienhuis, M.V.M., Langer, G., Benthien, A., Bijma, J., 2006. The effect of temperature, salinity and growth rate on the stable hydrogen isotopic composition of long chain alkenones produced by *Emiliania huxleyi* and *Gephyrocapsa oceanica*. Biogeosciences 3, 113-119.

Schulte, S., Mangelsdorf, K., Rullkötter, J., 2000. Organic matter preservation on the Pakistan continental margin as revealed by biomarker geochemistry. Organic Geochemistry 31, 1005-1022.

Sepkoski Jr, J.J., 1996. Patterns of Phanerozoic extinction: a perspective from global data bases. Global events and event stratigraphy. Springer, Berlin 35–52.

Sheehan, P.M., Hansen, T.A., 1986. Detritus feeding as a buffer to extinction at the end of the Cretaceous. Geology 14, 868-870.

Sheehan, P.M., Coorough, P.J., Fastovsky, D.E., 1996. Biotic selectivity during the K/T and Late Ordovician extinction events. In Ryder, G., Fastovsky, D., and Gartner, S., eds., The Cretaceous-Tertiary Event and Other Catastrophes in Earth History. Geological Society of America Special Paper 307 477-489.

Shimoyama, A., Kozono, M., Mita, H., Nomoto, S., 2001. Maleimides in the Cretaceous/Tertiary boundary sediments at Kawaruppu, Hokkaido, Japan. Geochemical Journal 35, 365-375.

Simoneit, B.R.T., Beller, H.R., 1987. Lipid geochemistry of Cretaceous/Tertiary boundary sediments, Hole 605, Deep Sea Drilling Project Leg 93, and Stevns Klint, Denmark. Initial Reports of the Deep Sea Drilling Project 93, 1211–1221.

Sinninghe Damsté, J.S., de Leeuw, J.W., 1990. Organically-bound sulphur in the geosphere: state of the art and future research. Organic Geochemistry 16, 1077-1101.

Sinninghe Damsté, J.S., Kenig, F., Koopmans, M.P., Köster, J., Schouten, S., Hayes, J.M., de Leeuw, J.W., 1995. Evidence for gammacerane as an indicator of water column stratification. Geochimica et Cosmochimica Acta 59, 1895-1900.

Sinninghe Damsté, J.S., Köster, J., 1998. A euxinic southern North Atlantic Ocean during the Cenomanian/Turonian oceanic anoxic event. Earth and Planetary Science Letters 158, 165-173.

Sinninghe Damsté, J.S., Kuypers, M.M.M., Schouten, S., Schulte, S., Rullkötter, J., 2003. The lycopane/C_{31}*n*-alkane ratio as a proxy to assess palaeoxicity during sediment deposition. Earth and Planetary Science Letters 209, 215-226.

Sinninghe Damsté, J.S., Kuypers, M.M.M., Pancost, R.D., Schouten, S., 2008. The carbon isotopic response of algae, (cyano)bacteria, archaea and higher plants to the late Cenomanian perturbation of the global carbon cycle: Insights from biomarkers in black shales from the Cape Verde Basin (DSDP Site 367). Organic Geochemistry In Press, Accepted Manuscript.

Stott, L.D., Kennett, J.P., 1989. New constraints on early Tertiary palaeoproductivity from carbon isotopes in foraminifera. Nature 342, 526-529.

Summons, R.E., Powell, T.G., 1987. Identification of aryl isoprenoids in source rocks and crude oils: Biological markers for the green sulphur bacteria. Geochimica et Cosmochimica Acta 51, 557-566.

Summons, R.E., Jahnke, L.L., Hope, J.M., Logan, G.A., 1999. 2-Methylhopanoids as biomarkers for cyanobacterial oxygenic photosynthesis. Nature 400, 554-557.

ten Haven, H.L., de Leeuw, J.W., Rullkötter, J., Sinninghe Damsté, J.S., 1987. Restricted utility of the pristane/phytane ratio as a paleoenvironmental indicator. Nature 330, 641-643.

ten Haven, H.L., Rohmer, M., Rullkötter, J., Bisseret, P., 1989. Tetrahymanol, the most likely precursor of gammacerane, occurs ubiquitously in marine sediments. Geochimica et Cosmochimica Acta 53, 3073-3079.

Turgeon, S.C., Creaser, R.A., 2008. Cretaceous oceanic anoxic event 2 triggered by a massive magmatic episode. Nature 454, 323-326.

van Breugel, Y., Baas, M., Schouten, S., Mattioli, E., Damste, J.S.S., 2006. Isorenieratane record in black shales from the Paris Basin, France: Constraints on recycling of respired CO_2 as a mechanism for negative carbon isotope shifts during the

Toarcian oceanic anoxic event Paleoceanography 21, DOI 10.1029/2006PA001305.

van der Meer, M.T.J., Baas, M., Rijpstra, W.I.C., Marino, G., Rohling, E.J., Sinninghe Damste, J.S., Schouten, S., 2007. Hydrogen isotopic compositions of long-chain alkenones record freshwater flooding of the Eastern Mediterranean at the onset of sapropel deposition. Earth and Planetary Science Letters 262, 594-600.

van der Meer, M.T.J., Sangiorgi, F., Baas, M., Brinkhuis, H., Sinninghe Damste, J.S., Schouten, S., 2008. Molecular isotopic and dinoflagellate evidence for Late Holocene freshening of the Black Sea. Earth and Planetary Science Letters 267, 426-434.

Venkatesan, M.I., Dahl, J., 1989. Organic geochemical evidence for global fires at the Cretaceous/Tertiary boundary. Nature 338, 57-60.

Wagner, T., Sinninghe Damsté, J.S., Hofmann, P., Beckmann, B., 2004. Euxinia and primary production in Late Cretaceous eastern equatorial Atlantic surface waters fostered orbitally driven formation of marine black shales. Paleoceanography 19, PA3009, doi:10.1029/2003PA000898. .

Wakeham, S.G., Lee, C., 1993. Production, transport, and alteration of particulate organic matter in the marine water column. Organic Geochemistry 145–169.

Wendler, J., Grafe, K.-U., Willems, H., 2002. Palaeoecology of calcareous dinoflagellate cysts in the mid-Cenomanian Boreal Realm: implications for the reconstruction of palaeoceanography of the NW European shelf sea. Cretaceous Research 23, 213-229.

Wendler, J., Willems, H., 2002. Distribution pattern of calcareous dinoflagellate cysts across the Cretaceous-Tertiary boundary (Fish Clay, Stevns Klint, Denmark): Implications for our understanding of species-selective extinction. Special Paper 356: Catastrophic events and mass extinctions: impacts and beyond 356, 265-275.

Wolbach, W.S., Gilmour, I., Anders, E., Orth, C.J., Brooks, R.R., 1988. Global fire at the Cretaceous- Tertiary boundary. Nature 334, 665-669.

Xie, S.C., Pancost, R.D., Yin, H.F., Wang, H.M., Evershed, R.P., 2005. Two episodes of microbial change coupled with Permo/Triassic faunal mass extinction. Nature 434, 494-497.

Zachos, J.C., Arthur, M.A., Dean, W.E., 1989. Geochemical evidence for suppression of pelagic marine productivity at the Cretaceous/Tertiary boundary. Nature 337, 61-64.

Zubkov, M.V., Tarran, G.A., 2008. High bacterivory by the smallest phytoplankton in the North Atlantic Ocean. Nature 455, 224-226.

CHAPTER II

Molecular-isotopic evidence of environmental and ecological changes across the Cenomanian-Turonian boundary in the Levant Platform of central Jordan

Julio Sepúlveda[1,2,*], Jens Wendler[3,§], Arne Leider[2], Hans-Joachim Kuss[3], Roger E. Summons[4], and Kai-Uwe Hinrichs[2]

Accepted for publication with moderate comments (August 2008)

in *Organic Geochemistry*

[1]International Graduate College – Proxies in Earth History (EUROPROX), University of Bremen, 28334 Bremen, Germany

[2]Organic Geochemistry Group, Department of Geosciences, University of Bremen, 28334 Bremen, Germany

[3]Geochronology Group, Department of Geosciences, University of Bremen, 28334 Bremen, Germany

[4]Department of Earth, Atmospheric and Planetary Sciences, Massachusetts Institute of Technology, Cambridge MA 02139, USA

*Corresponding author: Tel.: +49 421 218 65742; fax: 49 421 218 65715. E-mail address: sepulved@uni-bremen.de (J. Sepúlveda)

[§]Present address: Institute of Earth Sciences, Faculty of Chemistry and Earth Sciences, Friedrich-Schiller-Universität Jena, 07749 Jena, Germany

Keywords: Cretaceous, Cenomanian, Turonian, Jordan, oceanic anoxic event, euxinia, lipid biomarkers, stable isotopes, cyanobacteria.

ABSTRACT

We evaluated the structure of planktonic communities and paleoenvironmental conditions throughout the Cenomanian-Turonian Oceanic Anoxic Event (OAE2) by studying bulk geochemical properties and the molecular-isotopic composition of source-specific hydrocarbons from organic-rich sediments deposited in an intra-shelf basin at the Levant Platform, Central Jordan. High concentrations of desmethyl and 4-methyl steranes as well as dinosteranes indicated that marine algae including dinoflagellates were the main primary producing organisms. The presence of 2-methyl hopanes and low $\delta^{15}N$ values, in addition to isotopically enriched aryl isoprenoids, evidenced the contribution of N-fixing cyanobacteria and green-sulfur bacteria, respectively. Changes in the relative contribution of biomarkers revealed successions in planktonic communities associated with sea level changes and water column stratification. The OAE2 interval was characterized by a strong stratification of the water column, anoxic bottom waters, and a deep chemocline, as evidenced by high gammacerane and homohopane indices, and the absence of photic zone euxinia markers, respectively. However, the presence of isorenieratane and its derivatives in post-OAE black shales point to a shoaling of the chemocline and protracted euxinic conditions that extended into the photic zone. These sediments were also characterized by an exceptionally high abundance of chlorophyll-derived pristane and phytane (up to 2 mg g^{-1} TOC) likely as a result of high primary production and organic matter preservation. Our results provide further evidence for the importance of cyanobacteria and nitrogen fixation fueling primary production during the deposition of black shales, not only in open ocean settings but also in stratified/anoxic continental platforms during OAE2.

II.1. INTRODUCTION

Times of widespread deposition of organic-rich black shales in coastal and open ocean areas, as well as in epicontinental seas are known as Oceanic Anoxic Events (OAEs; (Jenkyns, 1980)). They are especially prominent during the Mesozoic and appear to coincide with extreme climatic and oceanographic conditions, such as exceptionally high sea surface temperatures (Bice et al., 2006; Forster et al., 2007; Schouten et al., 2003), rising sea level (e.g., (Arthur et al., 1987); (Schlanger et al., 1987)) and changes in oceanic circulation (e.g., (Erbacher et al., 2001)). OAEs are related to exceptional episodes of increased marine primary production, the depletion of oxygen and massive expansion of oxygen minimum zones, increased rates of organic carbon burial and a consequent perturbation of the global carbon cycle evidenced by a marked positive carbon isotopic excursion (CIE; (Jenkyns, 1980); (Arthur et al., 1987); (Schlanger et al., 1987), and perturbations in the ecology of primary producers (e.g., (2001; Kuypers et al., 1999; Kuypers et al., 2004b; Leckie et al., 2002)). Enhanced marine productivity due to an increased supply of nutrients and increased preservation due to water column stratification are among the main proposed models to explain the deposition of black shales during OAEs (e.g., (Meyers, 2006)). However, the relationship between marine productivity (e.g., (Kuypers et al., 2002b)) and preservation of organic matter under anoxic conditions (e.g., (Sinninghe Damsté & Köster, 1998)) remains contentious (Mort et al., 2007a).

Deciphering changes in communities of marine primary producers can provide a better understanding of paleoenvironmental conditions controlling primary production, nutrients and carbon cycling during these events. Here, the use of source-specific lipid biomarkers and their carbon isotopic composition have demonstrated to be of crucial importance in deciphering the role of organisms without hard skeletons such as prokaryotes (Kuypers et al., 2001; Kuypers et al., 2004b; Simons & Kenig, 2001); (Dumitrescu & Brassell, 2005); (Ohkouchi et al., 2006); (Knoll et al., 2007). Archaeal remains have been reported as the dominant component of the organic matter present in early Albian black shales deposited during the OAE1b in the North Atlantic Ocean, and

thus reflect their importance as constituents of the planktonic assemblage (Kuypers et al., 2001; 2002a). On the other hand, nitrogen-fixing cyanobacteria have been suggested to be a major autotrophic planktonic group in open ocean and costal areas during some OAEs, and are responsible for supplying nitrogen for other phytoplanktonic production (Kuypers et al., 2004b); (Dumitrescu & Brassell, 2005); (Ohkouchi et al., 2006); (Kashiyama et al., 2008).

Using a geochemical multi-proxy approach, we constrain the relationship between paleoenvironmental conditions associated with OAE2 (e.g., nutrient supply, euxinia, and sea level changes) and the paleoecology of primary producers in an intra-shelf basin in the southern Tethys ocean, i.e., the Levant Platform. Particularly, we evaluate the role of N-fixing cyanobacteria in fueling algal production in this coastal setting dominated by oxygen-depleted waters and loss of nitrogen via denitrification.

II.1.1. Prior Studies

A detailed geological, sedimentological and stratigraphical description (including platform sections further north and south) of the Levant Platform has been provided elsewhere (2005; Schulze et al., 2003). Biostratigraphic, paleontological and lithological analyses of the outcrop sections used in the present study are part of a companion paper (Wendler et al., in review). The Levant carbonate platform extended over the passive margin of the Arabo-Nubian shield during Cenomanian-Turonian (C-T) times. The outcrop sections in this area represent deposits of an intra-platform basin (Karak-Silla Basin), which was only intermittently disconnected from the open marine environment as evidenced by the formation of occasional evaporites (Kuss et al., 2003). The prevailing platform carbonates document a neritic depositional environment while restricted water circulation and a deep subtidal environment characterized by dysoxic/anoxic episodes occurred during transgressions and OAE2 (Schulze et al., 2005). Bituminous black shales, thin laminations, organic-rich mudstones, and the presence of small opportunistic benthic foraminifers are all consistent with the prevalence of dysoxic conditions (Schulze et al., 2005).

II.2. MATERIALS AND METHODS

II.2.1. Samples

The outcrop sections, Ghawr Al Mazar (GM3) and Kuthrubbah (KB3) are about 30 km apart (Fig. II.1.) and approximately 150 km distant from the paleo-coastline. Section GM3 was proximal to the intra-platform basin rim and is characterized, from bottom to top, by green clays and marls, dolomites, transitioning into a platy, bituminous limestone beds, brown marly clays, grey marls capped by limestones at the top (Fig. II.2.). Section KB3 represents deeper parts of the Karak-Silla intraplatform basin and comprised of an extended series of organic-rich black shales. A total of 150 samples were collected from the 36 m thick GM3 C-T boundary section (31°15'34" N; 35°35'41" E; Fig. II.1.) at sample spacing of 10 to 25 cm. For bulk geochemical analyses, 150 were analyzed for total organic carbon (TOC) and 118 for carbonate carbon isotopes ($\delta^{13}C_{carb}$) ((Wendler et al., in review)), whereas 38 were analyzed for organic carbon ($\delta^{13}C_{org}$) and nitrogen ($\delta^{15}N_{org}$) isotopes. For lipid biomarkers, we selected 8 samples of organic-rich sequences from the GM3 section spawning the Late Cenomanian, the C-T Boundary, and Early Turonian (127-239; Table II.1.). Their lithology varied from black shales, dark marls, and laminated bituminous marls (Table II.1.), whereas their deposition occurred during variable sea-level conditions, spanning roughly one 3rd order sequence (Schulze et al., 2005); J. Wendler, pers. commun.). Additionally, two organic-rich black shales, taken from the Early Turonian interval of the 25 m thick KB3 section (31°09'13" N; 35°36'06" E) were analyzed. These samples represent an expanded counterpart of the post-OAE2 black-shale interval typified by sample 238 in GM3 section (J. Wendler, pers. commun.).

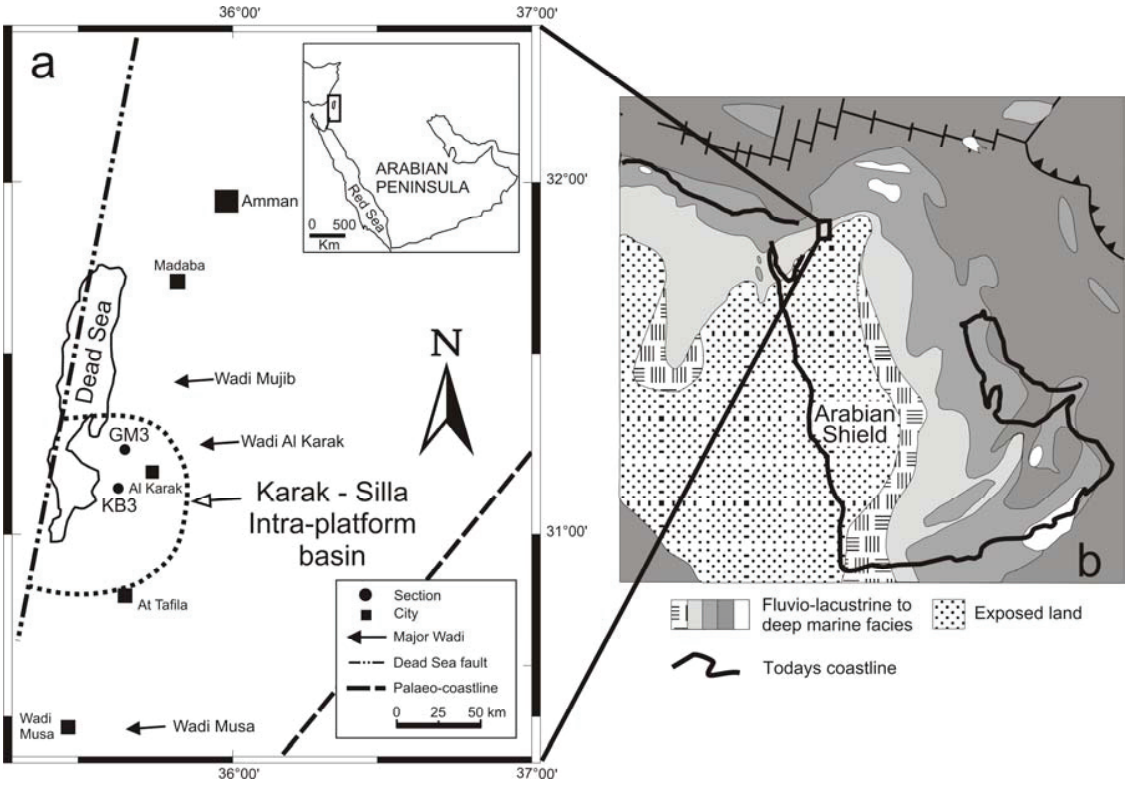

Figure II.1. a) Study area showing the location of sections GM3 and KB3 (filled circles). Insert represents an expanded view of the Arabian Peninsula. b) Configuration of the Levant Platform during the Late Cenomanian (after Philip et al., 2000).

II.2.2. Bulk measurements

Rock samples were cleaned by removing their outer parts with a saw and then crushed to powder in an agate mortar. TOC and $\delta^{13}C_{carb}$ measurements are described elsewhere (Wendler et al., in review). Powdered samples prepared for carbonate-free organic carbon and nitrogen isotopes were decalcified using solvent-washed HCl 10% until no further reaction was observed. Subsequently, the residues were rinsed with solvent-washed Milli-Q water, centrifuged, and dried for 72 hours at 60 °C. The isotopic analyses were carried out using a Finnigan MAT Delta Plus coupled to a Carlo-Erba element analyzer at the University of Bremen.

II.2.3. Lipid analysis

Rock samples were cleaned further by sonication for 5 minutes in solvent-rinsed Milli-Q water. Samples were then dried overnight at 60 °C. Between 5 and 10 g of rock were ground to powder in an agate mortar and homogenized. Samples were extracted in a MARS microwave system (CEM Corporation) using a solvent mixture of dichloromethane:methanol (DCM:MeOH) 3:1 (at least 3x, until the solvent extracts became colorless) at 80°C for 20 minutes. Before extraction, 2 μg of hexatriacontane, behenic acid methyl esther, 1-nonadecanol and 2-methyl octadecanoic acid were added as internal standards. Total lipid extracts (TLE) were combined after centrifugation and concentrated under a stream of nitrogen using a Turbovap. TLEs were then separated into asphaltenes and maltenes using small Pasteur pipettes filled with combusted glass wool and $NaSO_4$, and eluted with hexane and DCM, respectively. Elemental sulfur was removed from the maltenes using acid-activated copper (4 N HCl, rinsed consecutively with Milli-Q, MeOH, DCM, and *n*-hexane). The maltenes were fractionated into four fractions of different polarities using Supelco LC-NH2 glass cartridges (500 mg sorbent; (Hinrichs et al., 2000)). Hydrocarbons were identified by coupled gas chromatography-mass spectrometry (GC-MS) using a Thermo Electron Trace instrument equipped with a 30-m DB-5MS fused silica capillary column (0.32 mm ID, 0.25 μm film thickness), and using helium as the carrier gas. The GC temperature program used was: injection at 60°C, 2 min. isothermal; from 60°C to 150°C at 15°C min^{-1}; from 150°C to 320°C at 4°C min^{-1}; 20 min. isothermal. Identification of compounds was based on GC retention times and mass spectral comparisons to literature reference data.

Saturated hydrocarbons and aromatics were also analyzed by GC-MS in metastable reaction monitoring (MRM-GC-MS) and selected ion monitoring (SIM-GC-MS) modes respectively. For this we used a Micromass AutoSpec-Ultima mass spectrometer interfaced to an Agilent 6890N gas chromatograph. The GC was fitted with a DB-1 fused silica capillary column (60 m; 0.25 mm I.D.; 0.25 μm film thickness; J & W Scientific) and the carrier gas was helium. The GC temperature program used was: injection at 60°C, 2 min. isothermal; from 60°C to 150°C at 10°C min^{-1}; from 150°C to 315°C at 3°C min^{-1}; 24 min isothermal. The AutoSpec source was operated in EI-mode at

250° C, 70 eV ionization energy, and 8 kV accelerating voltage. Data were acquired and processed using MassLynx 4.0 (Micromass Ltd.).

Compound-specific isotope analyses were performed by gas chromatography-combustion-isotope ratio mass spectrometry (GC-C- irm-MS) consisting of a Thermo Electron Trace GC coupled via a Thermo Electron GCC-II-interface to a Thermo Electron Delta Plus XP mass spectrometer. GC conditions were identical to those described above. Carbon isotope ratios are reported as δ values ($\delta^{13}C$, in ‰) relative to the VPDB standard. Multiple CO_2-pulses of known $\delta^{13}C$ value at the beginning and end of each run were used for calibration. Instrument precision (~ 0.22‰ or better) was regularly checked by injecting a mixture of *n*-alkanes (*n*-C_{15} to *n*-C_{29}) with known isotopic compositions.

II.2.4. Desulfurization and ether cleavage

Raney nickel desulfurization was performed in asphaltenes and polar fractions of selected samples at MIT as described elsewhere (Grice et al., 1998b). Our main goal was to evaluate preferential preservation of phytane due to sulfurization during early diagenesis. 2 μg of 3-*n*-Octadecylthiophene (CHIRON AS), 7-methylbenzo[b]naphthol [2,3-d]thiophene (CHIRON AS), and hexatriacontane were added as internal standards. The residue was extracted 3x with DCM, concentrated, loaded in small silica columns and separated in five fractions using the following elution sequence: a) 3/8 dead volume (DV) of hexane for saturated and unsaturated hydrocarbons; b) 2 DV of hexane/DCM 8/2 for aromatics; c) 2 DV of DCM for ketones; d) 2 DV of DCM/EtOAc 8/2 for alcohols; e) 2 DV of /EtOAc for acids. Hydrocarbons and aromatics were analyzed by GC-MS in full scan mode on a Micromass AutoSpec-Ultima as described above for MRM-GCMS, over a mass range of 50 to 600 Daltons. Data were acquired and processed using MassLynx 4.0 (Micromass Ltd.).

Ether bond cleavage was carried out in selected polar fractions as described elsewhere (Summons et al., 1998), in order to evaluate the potential contribution of phytane from archaeal diethers. Cleavage products were subsequently extracted with *n*-hexane (3x) and *n*-hexane/DCM 4/1 (2x) using a Pasteur pipette. Samples were loaded

onto silica columns and separated into hydrocarbons and polar fractions using *n*-hexane and EtOAc as eluents, respectively. Hydrocarbons were analyzed by GC-MS as described above for desulfurization products. 2 μg of hexatriacontane was used as standard for quantification.

II.3. RESULTS AND DISCUSSION

II.3.1. Bulk geochemistry

The TOC content varied between close to zero and 3.10 % along the section with the highest values found at 57-70 and 75-79 meters (Fig. II.2.). The TOC content of samples from KB3 was comparatively higher than at GM3 (up to 6.8%; Table II.1.). $\delta^{13}C_{carb}$ in GM3 fluctuated between -4 and +4‰ with a sharp negative excursion at the lower part of the section, followed by a marked positive carbon isotopic excursion (CIE) between 55 and 70 meters (grey area in Figure II.2.). Rather uniform values around +1‰ characterized the post-CIE interval. $\delta^{13}C_{carb}$ values of samples from KB3 section were slightly lower than those from GM3 (Table II.1.). The $\delta^{13}C_{carb}$ record was correlated with the Pueblo (USA) stratotype section that defines the position and duration of 500-600 ka of OAE2 (gray area in Figure 2; (Wendler et al., in review)). The $\delta^{13}C_{org}$ varied between -27 and -22‰. Despite its coarser resolution (Fig. II.2.), the organic values track the $\delta^{13}C_{carb}$ record reasonably faithfully with a negative CIE to values around -26‰ just prior to the OAE and a positive CIE to values around -22 to -25‰ in the OAE. The $\delta^{13}C_{org}$ in KB3 samples displayed values around -25‰ (Table II.1.). The CIE reflects a perturbation in the global carbon cycle and encodes the C-isotopic discrimination by phytoplankton during photosynthesis under conditions of increased marine productivity and the enhanced global burial of organic matter during OAE2 (Arthur et al., 1988; Scholle & Arthur, 1980).

Table II.1. Geochemical characterization of sediments used for this study.

Sample	[a]Depth (meters)	Lithology	Relative Stratigraphy	TOC (%)	[b]CaCO3 (%)	[b]Tmax (°C)	$\delta^{13}C_{carb}$	$\delta^{13}C_{carb}$	[c]$\delta^{15}N_{org}$
KB3-70*	18.6	black shale	Post-OAE2	6.5	85.9	-	1.3	-25.0	-0.6
KB3-68*	17.4	black shale	Post-OAE2	6.9	86.4	-	0.8	-25.3	-1.2
GM3-239	77.17	laminated, bituminous brown marl	Post-OAE2	1.3	49.9	425	5.5	-23.9	1.7
GM3-238*	76.87	laminated, bituminous brown marl	Post-OAE2	2.9	54.8	425	2.2	-24.2	1.1
GM3-237	76.60	laminated, bituminous brown marl	Post-OAE2	0.8	59.0	433	3.2	-24.4	0.1
GM3-232	74.95	laminated, bituminous brown marl	Post-OAE2	1.8	66.9	432	2.1	-24.3	0.0
GM3-213	69.60	bituminous dark-brown marly claystone	OAE2	1.9	64.6	432	2.4	-24.6	-0.1
GM3-188	62.73	brown marl	OAE2	1.5	70.0	433	2.8	-23.3	0.9
GM3-159	58.36	dark-brown marl	OAE2	3.1	63.5	436	4.4	-24.1	2.0
GM3-127	52.40	black shale	Pre-OAE2	0.8	18.3	462	2.0	-26.1	0.5

*Corresponding samples representing the same time interval (J. Wendler, pers. commun.)
[a]Low numbers indicate low position in the outcrop.
[b]Jens Wendler (unpublished data)
[c]Measured on decalcified samples and assumed to represent mostly organic material although inorganic nitrogen can not be excluded

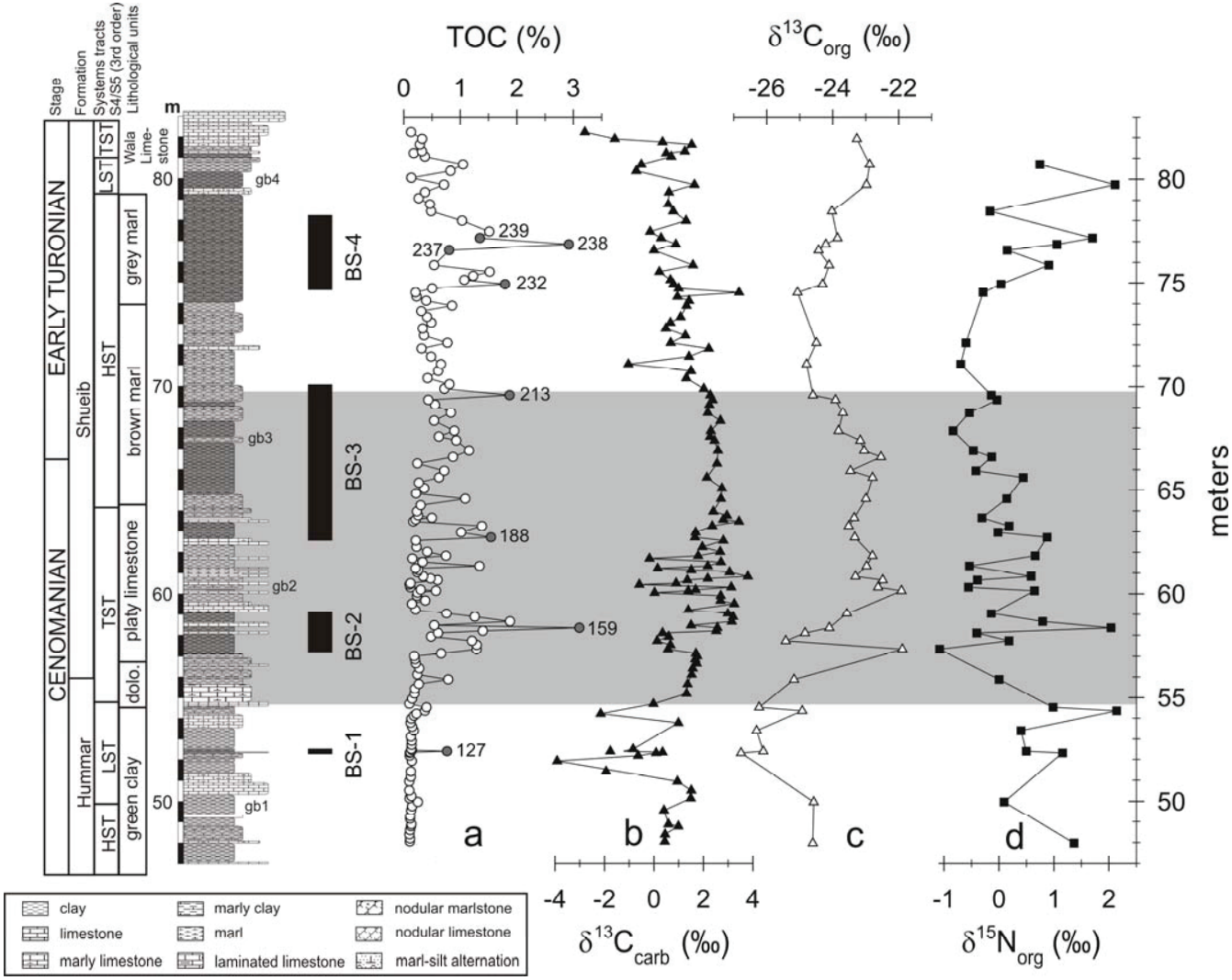

Figure II.2. Lithology and bulk geochemistry of section GM3. Vertical bars on the left panel refer to the lithographic and sequence stratigraphic subdivisions, and sea level tracks of Wendler et al (in review). Filled vertical bars represent four major black shale (BS) units with eight samples (127-239) used for lipid biomarkers. HST = highstand systems tract; LST = lowstand systems tract; TST = transgressive systems tract; dolo = dolomite unit; gb = gypsum bed. Geochemistry is indicated as follows: a) percentage of total organic carbon; b) $\delta^{13}C$ of bulk carbonates; c) $\delta^{13}C$ of organic matter; d) $\delta^{15}N$ of decalcified samples. The grey area represents the positive isotopic excursion defining OAE2.

The $\delta^{15}N_{org}$ record fluctuated between -1 and +2‰, with positive values prior to the CIE and towards the top of the section, and the most depleted values during OAE2 (Fig. II.2.). In KB3 samples $\delta^{15}N$ values ranged between -1.2 and -0.6‰ (Table II.1.). The $\delta^{15}N$ of bulk sediments has been used for assessing the occurrence of nitrogen fixation (e.g., (Kuypers et al., 2004b); (Ohkouchi et al., 2006)), and denitrification (Jenkyns et al., 2007) during the deposition of Cretaceous black shales. Due to the low N-isotopic fractionation of cyanobacteria during N_2 fixation, $\delta^{15}N_{org}$ values between 0 and -3 ‰ are characteristic of sediments with high predominance of cyanobacterial markers (Kuypers et al., 2004b); (Ohkouchi et al., 2006); (Kashiyama et al., 2008). On the other hand, denitrification leads to enriched values in marine sediments as observed in Quaternary sediments of upwelling areas (e.g., (Ganeshram et al., 2000)). Although $\delta^{15}N_{org}$ is influenced by multiple factors, we can surmise that diazotrophy was an important process in the study area during OAE2 However, the scattered nature of the data suggests that relative importance of this process varied over time (Fig. II.2.).

II.3.2. Hydrocarbons and their biological sources

The aliphatic fraction of the samples from GM3 was dominated by desmethyl steranes, 4-methyl steranes, triterpanes, *n*-alkanes, branched alkanes and phytane and pristane (Fig. II.3.). However, their relative abundances varied greatly through the section (Fig. II.4.). Sample 238, as well as coeval samples from the KB3 section, exhibited a unique distribution of biomarkers characterized by a minor contribution of hopanes, a high abundance of saturated and unsaturated steroidal compounds, and a high abundance of Ph and Pr (Figs. II.3., II.4.). The total summed concentration of hydrocarbon compounds displayed maximum values in sample GM3-238 (one order of magnitude higher than other samples) (Fig. II.4.).

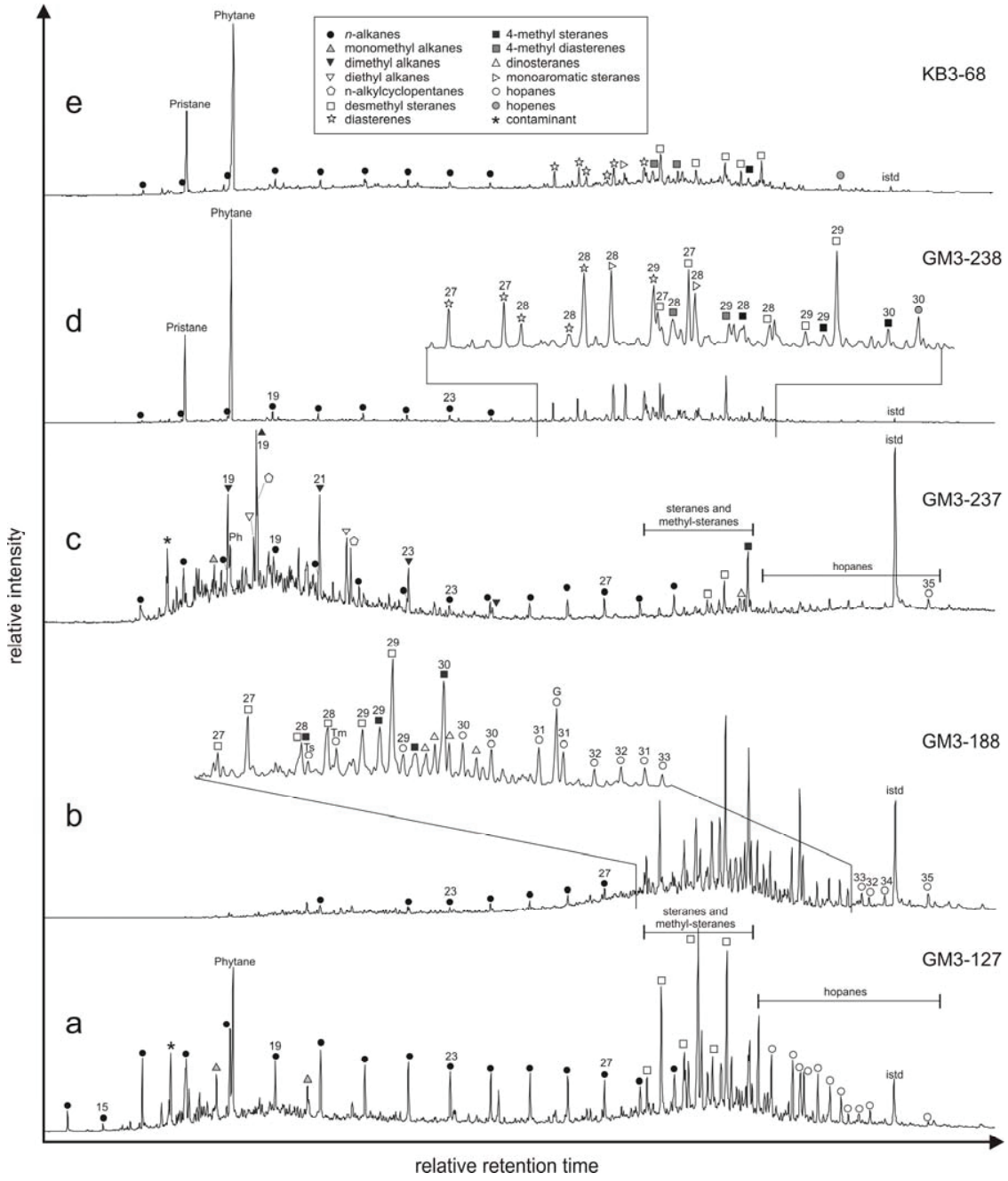

Figure II.3. Total ion chromatograms from GC-MS analysis of five characteristic aliphatic fractions from the GM3 and KB3 sections. a) sample GM3-127 located below the isotopic excursion of OAE2; b) sample GM3-188 located in the middle of the isotopic excursion; c) sample GM3-237 positioned above the isotopic excursion; d) sample GM3-238 positioned above the isotopic excursion and with a characteristic high abundance of pristane and phytane; e) sample KB3-68, equivalent to sample 238 in GM3 and also exhibiting high pristane and phytane. Inserts in figures b and d show the area dominated by steranes and hopanes in greater detail. See legend for compounds identification and Table 1 for identities of samples.

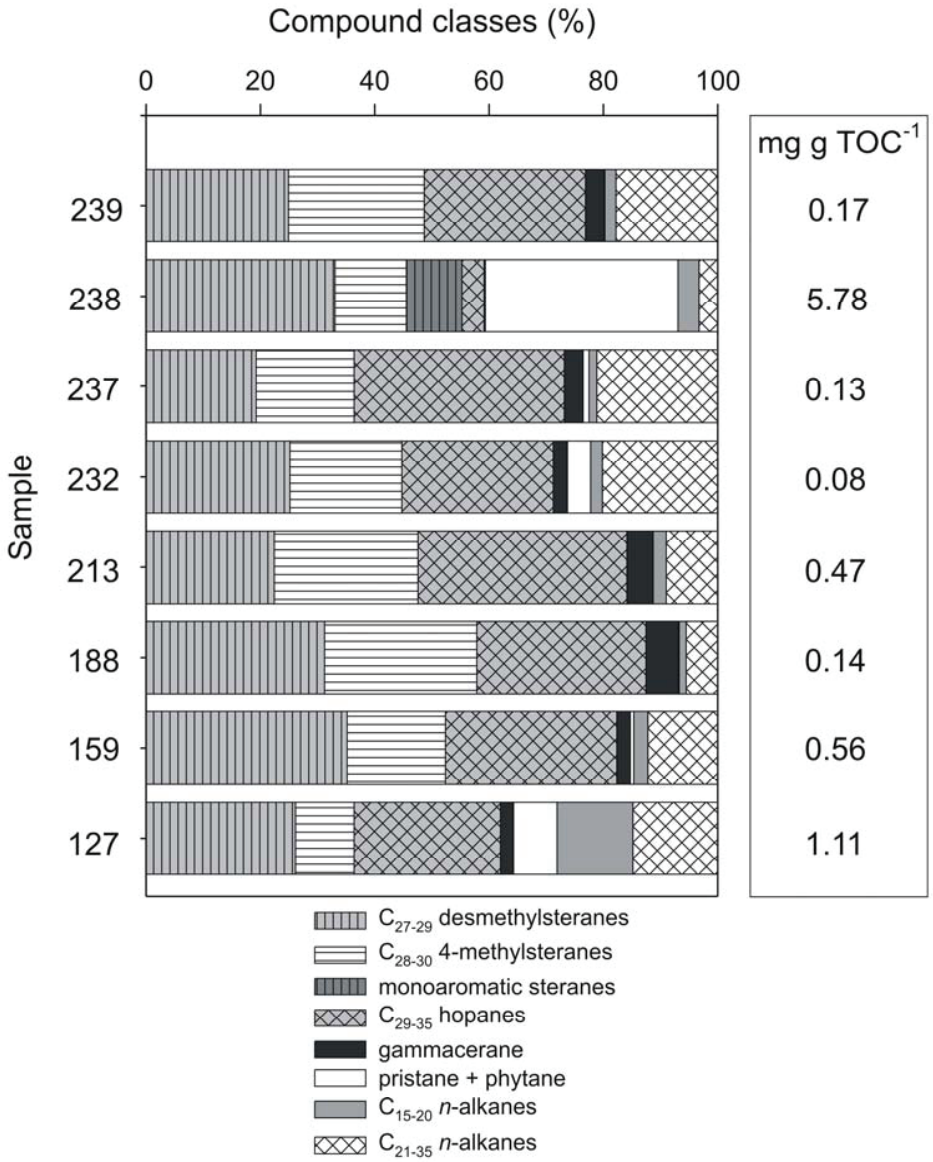

Figure II.4. Relative percentage contribution of main compound classes found in the aliphatic fractions in GM3 section. Numbers in the right represent the concentration of hydrocarbons standardized by TOC.

II.3.2.1. Normal, branched and isoprenoid alkanes

n-Alkanes were mainly represented by C_{15-35} homologues and their distribution through the section did not show a clear trend, with neither unimodal nor bimodal

distributions dominating. In general, concentrations of short-chain homologues (< *n*-C_{20}; SC) were low compared to mid- (*n*-C_{21-25}; MC) and long-chain (> *n*-C_{26}; LC) counterparts (Table II.2.), except for the majority of non-OAE samples which maximized at *n*-C_{18} or *n*-C_{19}. LC maximized at C_{27}, C_{29}, and C_{31} and exhibited a slight odd-over-even predominance, except for sample 238 with no preference, whereas MC exhibited a marked even-over-odd predominance as evidenced by their carbon preference index (CPI in Table II.2.). Samples from KB3 showed mostly SC and MC homologues. SC *n*-alkanes are mostly derived from aquatic algae and microorganisms (Cranwell et al., 1987), whereas LC homologues with a pronounced odd-over-even predominance are characteristic of epicuticular waxes of vascular plants (Eglinton & Hamilton, 1967). The observed slight odd-over-even preference of LCs, the high abundance of those in the C_{15-25} range and the absence of other biomarkers typical of terrestrial contribution (e.g., oleanane), point to a mainly mixed algal/microbial origin of the organic matter.

Acyclic isoprenoids were represented by phytane (Ph) and pristane (Pr), although the latter was almost absent in most of the samples from GM3 section. These two compounds were unusually concentrated in sample 238 representing up to 33% of the total hydrocarbon fraction and accounting up to 2.2 mg g TOC^{-1} (Figs. II.3., II.4.). This signal was widespread with the same pattern observed in corresponding samples from KB3. We discuss this further in section 3.6.

Two series of odd-carbon numbered C_{19-25} 5,5-diethylalkanes and C_{19} and C_{21} 3,3-diethylalkanes were detected in samples 232 and 237 using the m/z 127 and 99, respectively (Fig. II.3.). Series of branched alkanes with one or two quaternary carbon atoms (BAQCs) are commonly found in geological samples and have been suggested to have a biological source (most likely bacterial; see (Kenig et al., 2003); (2005) for a detailed review), although their source as contaminants from plastic bags commonly used during sampling of geological material has been reported recently (Grosjean & Logan, 2007). C_{18} and C_{20} alkylcyclopentanes were also found in samples 232 and 237 (Fig. II.3.). Such compounds have been also suggested to originate as the result of contamination by plastic bags (Grosjean & Logan, 2007). An even carbon numbered series of C_{18-22} 3-methyl alkanes was observed in few samples, although most prominently in sample 232.

Mono methyl alkanes are commonly found in cyanobacterial mats and cultures and are thus used as biomarkers for these organisms (e.g., (Kenig et al., 1995b); (Köster et al., 1999)).

Table II.2. Selected biomarker ratios.

Sample	*n*-C_{15-20}/ *n*-C_{15-35}	*n*-C_{21-26}/ *n*-C_{15-35}	*n*-C_{27-35}/ *n*-C_{15-35}	[a]CPI_{25-35}	[b]C_{27}-ster %	[c]C_{28}-ster %	[d]C_{29}-ster %	C_{29} ααα steranes 20S/(20S + 20R)	C_{31} αβ hopanes 22S/(22S + 22R)	Ts/ (Ts + Tm)	[e]AI
KB3-70*	-	-	-	-	52.1	21.5	26.4	0.04	0.09	0.19	++
KB3-68*	-	-	-	-	45.8	22.8	31.4	0.04	0.27	0.14	++
GM3-239	0.0	0.3	0.6	1.2	32.3	21.2	46.5	0.09	0.29	0.27	n.d.
GM3-238*	0.2	0.4	0.2	1.0	39.2	22.3	38.5	0.05	0.11	0.08	++
GM3-237	0.3	0.2	0.2	1.2	20.5	20.8	58.6	0.08	0.19	0.08	n.d.
GM3-232	0.3	0.2	0.4	1.4	19.2	20.8	60.0	0.08	0.20	-	n.d.
GM3-213	0.0	0.5	0.4	1.4	39.7	22.9	37.5	0.07	0.21	0.12	n.d.
GM3-188	0.1	0.3	0.6	1.3	27.0	22.5	50.6	0.09	0.21	0.13	n.d.
GM3-159	0.0	0.4	0.4	1.2	37.8	33.5	28.7	0.06	0.14	0.06	n.d.

*Corresponding samples representing the same time interval (J. Wendler, pers. commun.)
[a]Carbon Preference Index (CPI2; (Marzi et al., 1993)) = $((C_{25}+C_{27}+C_{29}+C_{31})+(C_{27}+C_{29}+C_{31}+C_{33})) / ((2 \times (C_{26}+C_{28}+C_{30}+C_{32}))$
[b]Relative contribution of C_{27} steranes = C_{27} ααα *S* + *R* / (C_{27-29} ααα *S* + *R*)
[c]Relative contribution of C_{28} steranes = C_{28} ααα *S* + *R* / (C_{27-29} ααα *S* + *R*)
[d]Relative contribution of C_{29} steranes = C_{29} ααα *S* + *R* / (C_{27-29} ααα *S* + *R*)
[e]Aryl Isoprenoids = ++, abundant; +, present; n.d., not detected

II.3.2.2. Steroids

All bitumens presented abundant desmethyl steranes and 4-methyl steranes including dinosteranes (Fig. II.3.). The dominant compounds were C_{27-29} 5α, 14α, 17α(H)-20*R* desmethyl steranes with small contribution from the 5α, 14α, 17α(H)-20*S* counterparts (Fig. II.3.). 24-Ethylcholestane was dominant from the base of the isotopic excursion to the top and maximized in samples 232 and 237 (Table II.2.). 4-Methylcholestanes and ergostanes along with 4-methyl-24-ethylcholestanes and dinosteranes were in evidence. Dinosteranes were identified by their mass spectra and by comparing their elution order with published data (Summons et al., 1987); (van Kaam-Peters et al., 1997); (Grice et al., 1998b). The abundances of total 4-methyl steranes and dinosteranes was tightly correlated along the section (r^2 = 0.98), whereas their relative abundance increased up section and remained high from the end of OAE2 onwards, except for a decrease in sample 238 (Fig. II.5.). Sample 238, and those from the KB3 section, showed a distinctive pattern. Apart from the presence of desmethyl steranes and 4-methyl steranes, rearranged C_{27-29} diaster-13(17)-enes (m/z 257), C_{27-29} 4-methyl sterenes (m/z 271), and C-ring monoaromatic steranes (m/z 253) and methyl monoaromatic steranes (m/z 267) were abundant (Fig. II.3.). With the exception of sample 238 (where Ph dominated), steroidal compounds were the dominant terpenoids in the hydrocarbon fraction in most of the bitumens, were present at relatively high concentrations during OAE2, and maximized in sample 238 and in those from the KB3 section (Figs. II.3., II.4.).

Sterols are produced by eukaryotic algae, protists and multicellular eukaryotes (e.g., (Volkman et al., 1998)). Algae and metazoa are the likely main producers of C_{27} sterols whereas C_{29} sterols are often attributed to marine green algae (Knoll et al., 2007), freshwater microalgae (e.g., (Volkman et al., 1999); (Kodner et al., 2008)), and land-plants (e.g., (Volkman et al., 1998)). 4-Methyl-24-ethyl cholestane and dinosteranes derive mostly from dinoflagellates (de Leeuw et al., 1983); (Summons et al., 1987)). Other side-chain alkylated 4-methyl steranes are positively correlated with dinosteranes and dinoflagellate remains and thus assumed to originate from the same biological

precursors (e.g., (Grice et al., 1998b)). Apart from those compounds specifically identified as originating from methane oxidizing bacteria (Jahnke et al., 1999), 4-methyl steroids are mostly algal in origin (e.g., (de Leeuw et al., 1983)). In addition to marine samples, they are commonly found in evaporitic (e.g., (Grice et al., 1998b)) and freshwater (e.g., (Goodwin et al., 1988); (Grice et al., 1998b)) environments indicating a wide tolerance of their predominantly dinoflagellate source organisms. The high abundance of $C_{27\text{-}29}$ desmethyl steranes, 4-methyl steranes and dinosteranes indicates that autochthonous phytoplankton, including dinoflagellates, were an important component of the organic matter produced and preserved during the deposition of these black shales. Changes in the composition of steroids point towards successions in assemblage of primary producers due to environmental changes (Knoll et al., 2007). The relative contribution of $C_{27\text{-}29}$ desmethyl steranes relative to $C_{30\text{-}35}$ hopanes exhibited a general decrease up section, except for a maximum in sample 238 (Fig. II.5.). This trend is inversely correlated with the relative contribution of 4-methyl steranes and dinosteranes, which increased from the base of the CIE upwards except for a minimum in sample 238 (Fig. II.5.), and is likely to represent the development of specific paleoenvironmental conditions (Thomas et al., 1993). Dinoflagellates evidently became an increasingly important component of the phytoplanktonic community in conjunction with the development of water column stratification (Fig. II.5.; see section 3.7), and a transgressional phase and sea level high stand associated with the development of more open marine conditions during OAE2 (Wendler et al., in review).

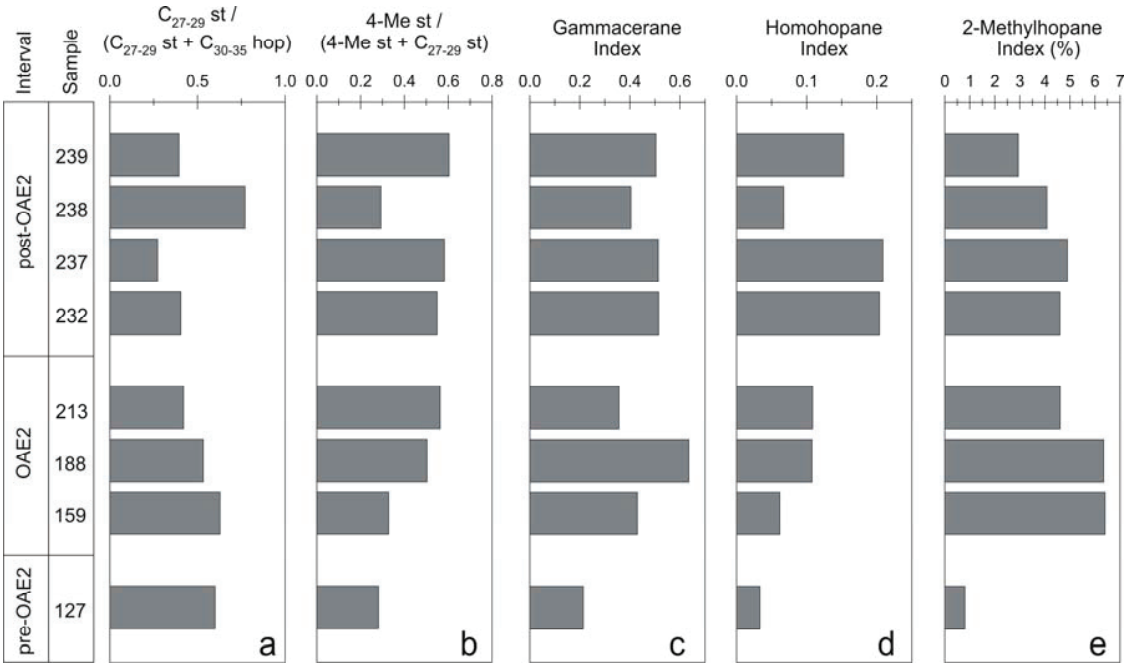

Figure II.5. Selected biomarker ratios. a) Steranes over hopanes ratio = C_{27-29} ααα steranes / C_{30-35} Hopanes; indicates the relative contribution of eukaryotic versus bacterial organic matter. b) Relative contribution of 4-methyl steranes = C_{28-30} 4-methyl steranes / (C_{28-30} 4-methyl steranes + C_{27-29} ααα steranes); indicates the relative contribution of dinoflagellates to the total eukaryotic assemblage. c) Gammacerane Index = gammacerane / (gammacerane + C_{30} αβ *S* + C_{30} αβ *R*); indicative of water column stratification. d) Homohopane Index = C_{35}/ (C_{31-35} 17α, 21β(H) and 17β, 21α(H) S + R homohopanes); indicative of water column stratification, hypersalinity and euxinia. e) 2-Methyl Hopane Index = C_{31} αβ-hopane/ (C_{31} 2-Me αβ-hopane + C_{30} αβ-hopane); indicates the relative contribution of cyanobacteria.

II.3.2.3. Pentacyclic triterpenoids

Series of 17α, 21β(H) and 17β, 21α(H)-C_{27-35} hopanes, with minor 17β, 21β(H) isomers and C_{28} almost absent, were identified in all samples based on the m/z 191 ion chromatogram (Fig. 6). C_{30} αβ-hopane was dominant in the lowermost two samples, whereas gammacerane dominated in the rest, except in sample 238 (Fig. II.6.). As well, C_{30} and C_{31} hop-17(21)-enes were present and their relative contributions increased upwards. Sample 238 and those from the KB3 section exhibited a more important contribution of C_{29}-C_{30} hop-17(21)-enes. The high abundance of hopanes in our samples (generally between 25 and 36 % of the GC-amenable hydrocarbons; Fig. II.4.) indicates an important input of bacterial biomass (Ourisson et al., 1987), (Rohmer et al., 1984). The contribution of hopanes in relation to steroidal compounds was higher towards the end of OAE2 and afterwards, except for a minimum in sample 238 (Fig. II.5.). The latter

is consistent with an increase in the relative contribution of extended C_{31-35} hopanes up section reaching a maximum in samples 232 and 237 as expressed by the homohopane index (HHI; Fig. II.5.). This could represent an increasing contribution of cyanobacteria, also indicated by the presence of C_{18-22} 3-methyl alkanes (particularly in samples 232 and 237).

C_{31} 2-methylhopane was identified and quantified using the m/z 426 → 205 reaction from MRM-GC-MS analysis. The 2-methylhopane index (2MeHI) increased sharply from a minimum at the base of the section to maximum values during the CIE, whereas fairly stable values between 4 and 5% were observed until samples 238, followed by a slight decrease at the top of the section (Figure II.5.). In section KB3, the 2MeHI varied between 5 and 7%. 2-Methyl hopanes are proposed as diagnostic markers of cyanobacteria (Summons et al., 1999) and have been previously described as important biomarkers in black shales deposited during OAEs (Kuypers et al., 2004b); (Dumitrescu & Brassell, 2005). Values of the 2MeHI up to 6 identify the presence of cyanobacteria in the environment, as well as their role as producers of extended hopanes. Co-occurring low $\delta^{15}N_{org}$ values are also consistent with nitrogen fixation by cyanobacteria (Table II.1.). A recent study (Rashby et al., 2007) found an unusual array of triterpenoids including 2-methyl bacteriohopanetetrol, non-methylated BHP, tetrahymanol and additional methylated triterpenoids of the gammacerane type in the non-marine purple bacterium *Rhodopseudomonas palustris*. Methylated tetrahymanols and hopanoids have also been reported in a closely-related soil bacterium, *Bradyrhizobium japonicum* (Bravo et al., 2001), reinforcing the knowledge that sources of 2-methylhopanes encompass organisms other than cyanobacteria. However, despite encountering abundant gammaceranes in all OAE2 samples (see below), our GC-MS data show no evidence of methylated gammaceranes. Thus, *R. palustris* cannot readily be invoked as the source of co-occurring 2-methylhopanes. Moreover, there do not appear to be any previous reports of methylated gammaceranes in modern or ancient sediments.

Gammacerane is commonly found in anoxic and hypersaline environments (de Leeuw & Sinninghe Damsté, 1990), it derives from tetrahymanol (ten Haven et al., 1989), and is synthesized by bacterivorous ciliates or purple bacteria living at or below a chemocline. It is often used as an indicator of water column stratification and anoxia

(Sinninghe Damsté et al., 1995a; 1995b). Gammacerane was abundant in all analyzed samples, indicating the presence of a stratified water column during the time of deposition of black shales. Redox conditions are discussed in detail in section 3.7.

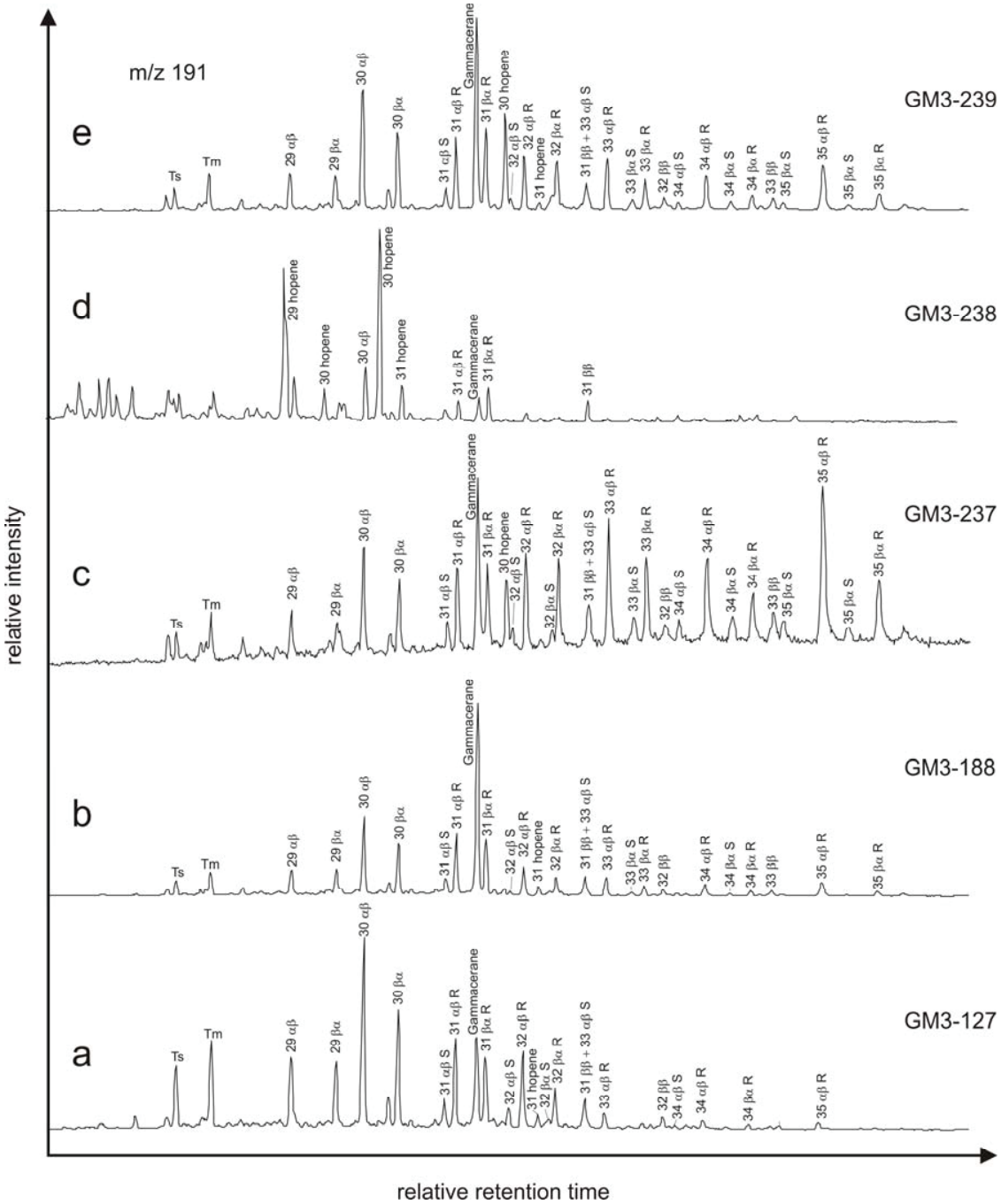

Figure II.6. Selected ion chromatograms (m/z 191) showing the distribution of triterpenoids in GM3 section.

II.3.2.4. Isorenieratane and derivatives

Isorenieratane was found in trace amounts in sample 127 at the base of the section and most notably in sample 238. The latter, together with samples from KB3 section, exhibited a notable contribution of isorenieratane and its diagenetic products, aryl and diaryl isoprenoids (Summons & Powell, 1987); (Koopmans et al., 1996b); (Sinninghe Damsté et al., 2001); Fig. II.7.). Aryl and diaryl isoprenoids were present in the range C_{13}-C_{22} and C_{18}-C_{22}, respectively, and all samples displayed a similar distribution (Fig. II.7.), although concentrations were higher in KB3 samples than in 238. A C_{33} diaryl isoprenoid was also identified as an important component of the m/z 133 and 134 ion chromatograms (Fig. II.7.). Isorenieratane derives from photosynthetic green sulfur bacteria (Chlorobiaceae producing isorenieratene) living in stratified water columns with a relatively shallow chemocline. They are strict anaerobes and simultaneously require light and H_2S for growth (e.g., (Liaaen-Jensen, 1978); (Summons & Powell, 1987); (Koopmans et al., 1996b); (Sinninghe Damsté et al., 2001)). Isorenieratane and its diagenetic derivatives are generally interpreted as indicators of euxinic conditions in the photic zone and are common in Cretaceous black shales, especially those deposited during the C-T interval (e.g., (Sinninghe Damsté & Köster, 1998); (Kuypers et al., 2004a); (Kolonic et al., 2005)). Thus, the presence of isorenieratane and aryl isoprenoids in these samples indicates the presence of Chlorobiaceae as a component of the planktonic assemblage, also confirmed by their ^{13}C-enriched nature (see section 3.5).

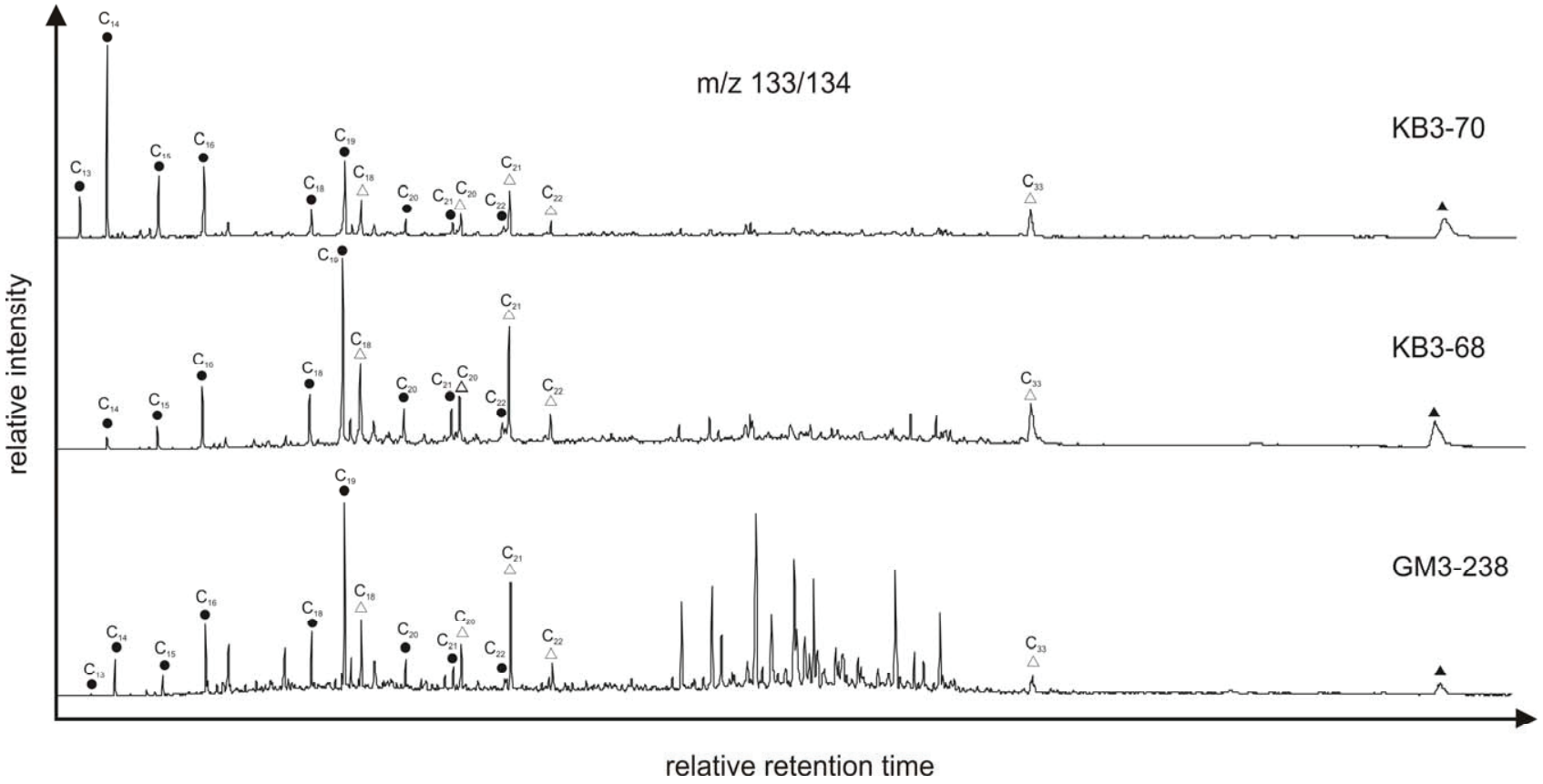

Figure II.7. Selected ion chromatograms (m/z 133/134) of hydrocarbon fractions from sample GM3-238, KB3-68, and KB3-70 showing the distribution of isorenieratane (filled triangle), aryl (filled circle) and diaryl (open triangle) isoprenoids. Peaks in the middle of chromatogram from sample GM3-238 correspond to steroidal compounds.

II.3.3. Thermal maturity

The high proportion of 17α, 21β(H) and 17β, 21α(H) hopanes with a marked 22R over 22S predominance indicates that the organic matter is relatively immature (Fig. II.6.). The presence of 17β, 21β(H) hopanes, although in small amounts, supports this. The 22S/(22S + 22R) ratio of C_{31} 17α, 21β(H) hopane varied between 0.1 and 0.3 (Table II.2.) and far from the end-point value of ~ 0.6 (Peters et al., 2005). The relationship between C_{27} 18α-trisnorhopane (Ts) and C_{27} 17α-trisnorhopane (Tm), expressed as the Ts/(Ts + Tm) ratio, displayed values ranging from 0.02 to 0.27 (Table II.2.). The relationship between C_{29} ααα 22S/(22S + 22R) steranes generally varied between 0.03 ad 0.09 (Table II.2.). These values are also well below the end-point of 0.5 (Peters et al., 2005) and indicate relatively immature organic matter. The presence of rearranged diasterenes, sterenes, and 4-methyl sterenes in sample 238 and in those from KB3 section support this conclusion as do low T_{max} values obtained from Rock-Eval pyrolysis (J. Wendler, unpublished data; Table II.1.).

II.3.4. Isotopic composition of selected biomarkers and potential sources

The compound-specific C-isotopic composition of selected biomarkers was compared to the $\delta^{13}C_{org}$ record to gain information regarding their potential biological precursors (Fig. II.8.). The C_{27-29} steranes exhibited similar values through the section and these fluctuated between -30.9 and -27.7‰; like the $\delta^{13}C_{org}$ record they showed a positive excursion of ~ 2‰ at the base of OAE2 and returned to pre-OAE2 values in the upper part of the CIE, except for a second maximum at the top of the section (Fig. II.8.). The almost identical isotopic composition of the three major steranes points toward a common biological source likely being an algal community typical of Cretaceous surface waters (e.g. (Kuypers et al., 2002a), (2002b); (Dumitrescu & Brassell, 2005)). A significant contribution of C_{29} from terrestrial plants thus appears unlikely. C_{30} αβ-hopane varied from -28.7 to -24.3‰ and presented a positive excursion of ~3.2‰ at the beginning of OAE2 and peaked in the middle of the CIE. A second maximum, as for the steranes, was

observed at the top of the section (Fig. II.8.). The $\delta^{13}C$ of gammacerane varied between -27 and -22‰ and displayed a similar trend than C_{30} αβ-hopane although with a smaller positive excursion (~1.6‰; Fig. II.8.). The ^{13}C-enriched nature of gammacerane compared to steranes and hopanes, is consistent with its origin from heterotrophic organisms (bacteria or ciliates) living near the chemocline and partially feeding on ^{13}C-enriched organic matter (Kenig et al., 1995a); (Sinninghe Damsté et al., 1995a). In general, biomarkers tracked the $\delta^{13}C_{org}$ profile, and except for gammacerane, they were isotopically depleted (Fig. II.8.). C_{27-29} steranes and C_{30} αβ-hopane presented an offset of ~ 4-6‰ and 0.4-1.7‰ from TOC values, respectively, consistent with the depleted nature of lipids relative to the total biomass (Hayes, 2001). $\delta^{13}C$ values for C_{30} αβ-hopane and gammacerane fell close to TOC suggesting that these compounds have their origins in common with the bulk of the preserved organic matter likely comprising heterotrophic bacteria, ciliates, and cyanobacteria (Fig. II.8.). Relatively ^{13}C-enriched bacterial products compared to those of eukaryotic photoautotrophs has been previously described in environments dominated by cyanobacteria, such as the Vena del Geso evaporitic sequence in Italy (e.g., (Kenig et al., 1995a)), and the C-T boundary in the Equatorial Atlantic (Kuypers et al., 2004b). Moreover, heavy $\delta^{13}C_{org}$ values were observed in rocks from the C-T boundary in Italy dominated by diazotrophic cyanobacteria (Kashiyama et al., 2008). Cyanobacteria possess an extremely effective CO_2 concentrating mechanism (Badger & Price, 2003) and their derived lipids are less depleted than eukaryotic counterparts due to the reduced carbon isotopic fractionation during carbon fixation (Sakata et al., 1997). Evidence of cyanobacterial contribution to organic matter in our samples is supported by the 2MeHI, which exhibited higher values (3 to 6) during OAE2 and the post-OAE2 interval (Fig. II.5.) together with relatively depleted $\delta^{15}N_{org}$ values (Table II.2.) suggestive of N_2 fixation. The latter implies that a deficiency in N as opposed to P occurred (N/P lower than Redfield), i.e., conditions beneficial to nitrogen fixing cyanobacteria (Tyrrell, 1999). Depletion of oxygen in the water column through respiration of organic matter during the onset of OAE2 would have promoted denitrification with the subsequent removal of nitrate and release of phosphate, both necessary factors promoting the expansion of N-fixing cyanobacteria. Sulfidic conditions in deep waters may have impacted the availability of trace metals crucial for enzymes

associated with the biological N-cycle (Anbar & Knoll, 2002). N-fixing cyanobacteria may have been critical for sustaining elevated levels of primary production and export of organic carbon to the sea floor during OAEs (Kuypers et al., 2004b). The high abundances of steroidal hydrocarbons and complexity of their distribution suggest that productivity by eukaryotic algae flourished. However, since our samples would have integrated long periods of time (~10^4 yr), it is not possible to discern any particular spatial or secular successions in phytoplankton communities.

Among aryl isoprenoids, isotopic data were only obtained for C_{14} compounds in KB3 samples. This is because a relatively high concentration and reduced co-elution in these samples allowed for higher precision measurements. The C_{14} aryl isoprenoid showed the most enriched $\delta^{13}C$ values among all the studied compounds (~ -17‰; Table 3), consistent with an origin from green sulfur bacteria using the reversed tricarboxylic acid cycle for carbon fixation ((Evans et al., 1966). The $\delta^{13}C$ of Ph and Pr in sample GM3-238 and its counterparts from KB3 are remarkably similar and suggestive of a common source (Table II.3.). The latter is supported by similar hydrogen isotopic values (J. Sepúlveda, unpublished data).

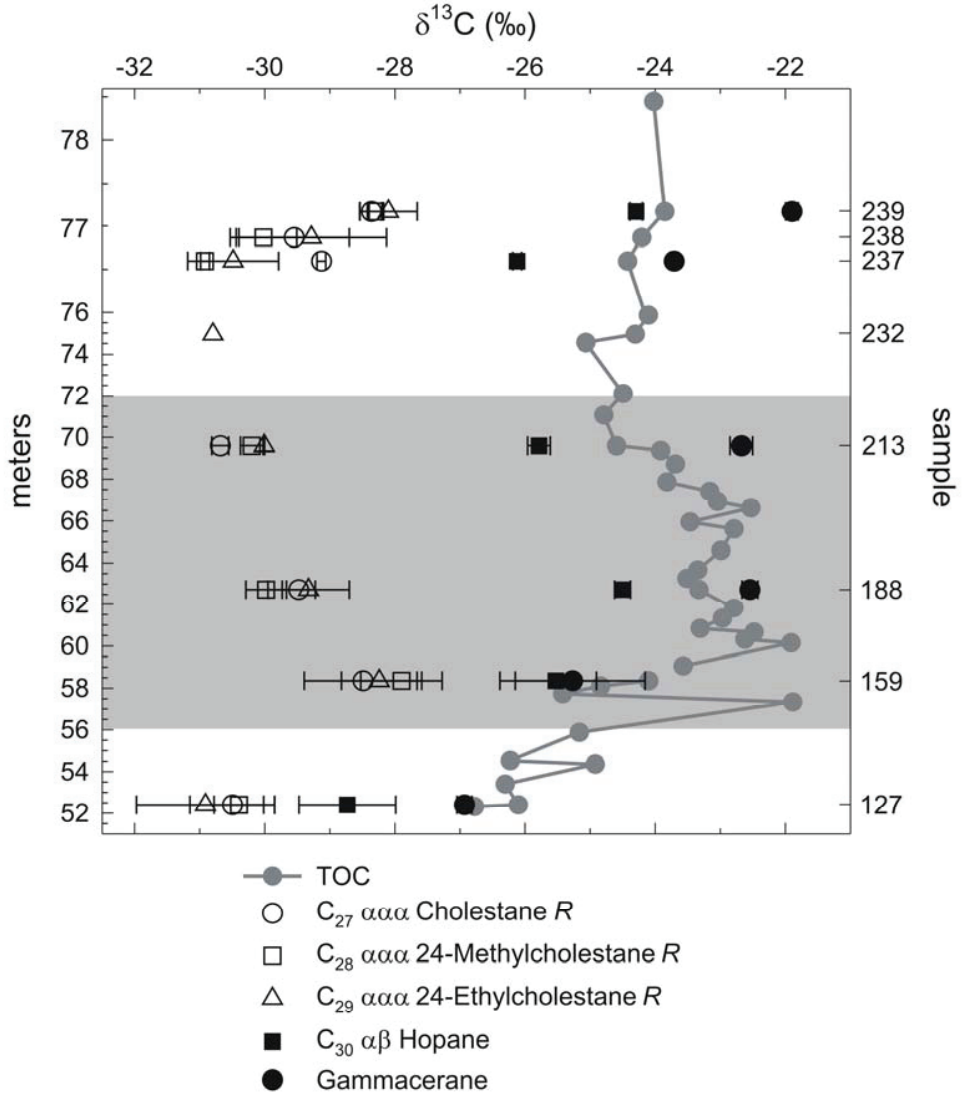

Figure II.8. $\delta^{13}C$ of bulk organic carbon and compound-specific $\delta^{13}C$ values of selected biomarkers from GM3 section. Axis "Y" was zoomed in between 76 and 78.5 meters. Grey area represents the OAE2 interval.

Table II.3. Compound-specific carbon isotopic composition of pristane, phytane, and C_{14} aryl isoprenoids in post-OAE2 samples.

Sample	Phytane $\delta^{13}C$ (‰)	Pristane $\delta^{13}C$ (‰)	C_{14} Aryl Isoprenoid $\delta^{13}C$ (‰)
GM3-238	-28.0 ± 1.6	-28.7 ± 0.7	-
KB3-70	-27.8 ± 0.8	-28.7 ± 0.5	-17.1 ± 0.1
KB3-68	-28.3 ± 0.9	-29.0 ± 0.8	-17.4 ± 2.5

II.3.5. Sulfur-bound lipids

The desulfurization of asphaltenes and polar fractions of selected samples from both sections only yielded small amounts of hydrocarbons, namely $C_{18\text{-}24}$ *n*-alkanes with an odd-over-even predominance and maximum at *n*-$C_{21}H_{44}$, and phytane. The m/z 133 and 134 chromatograms of aromatic fractions did not reveal isorenieratane or its derivatives. The low yield of hydrocarbons after Raney-Nickel desulfurization suggests that the sulfurization of functionalized lipids during the early stages of diagenesis was minor either due to low concentrations of reactive sulfur species or due to high iron content (Sinninghe Damsté & de Leeuw, 1990). Alternatively, postdepositional processes can also affect the stability of sulfur-bound compound formed during early diagenesis. Desulfurization through thermal cleavage, as evidenced by the relatively weak nature of S-S and C-S bonds after hydrous pyrolysis (< 260°C), has also been invoked as a mechanism affecting the release of sulfur-bound hydrocarbons during catagenesis (Koopmans et al., 1996a). However, this mechanism can be excluded for the thermally immature samples (Tables II.1. and II.2.; Fig. II.3.d).

II.3.6. Sources of pristane and phytane

Ph and Pr derive from the degradation of the phytyl side chain of chlorophyll-*a* from photosynthetic algae and cyanobacteria, as well as from bacteriochlorophyll-*a* and -*b* from purple sulfur bacteria (Brooks et al., 1969). Additional sources could possibly include lipids from methanogenic and halophilic archaea (e.g., (Rowland, 1990), as well as tocopherols for Pr (Goossens et al., 1984). We interpret the high amount of Ph and Pr in sample 238 and those from KB3 to mostly derive from the phytyl chain of chlorophyll-a from photosynthetic algae (eukaryotic phytoplankton) based on the following criteria: a) The isotopic composition of Ph and Pr is similar to steroidal compounds of eukaryotic source; b) the corresponding high concentration of distinctive steroidal compounds from algae and the relatively low contribution of hopanes characteristic of cyanobacteria; and c) the absence of Ph and biphythane after ether-cleavage of polar fractions suggesting that a contribution of Ph from archaeol and caldarchaeol representative of marine planktonic archaea (e.g., (Kuypers et al., 2002a)), is not likely.

To our knowledge, such a high predominance of Ph and Pr has only been reported in few cases and associated with euxinic environments where sulfurization of functional lipids takes place ((Keely et al., 1993); (Grice et al., 1996; 1998a; 1998b); (Kenig et al., 1995a)). Extremely high concentrations of Ph (up to 9000 μg $gTOC^{-1}$) were found in a marl sequence from the Oligocene Mulhouse Basin, France (Keely et al., 1993) and explained to result from sulfurization during early diagenesis and subsequent temperature cleavage of the sulfur bonds during catagenesis. High concentrations of Ph and steroids, and a lack of even over odd predominance of *n*-alkanes (as observed in sample GM3-238 and those from KB3) have been explained by the same mechanisms in immature and sulfur-rich rocks (Koopmans et al., 1996a). However, as explained in section 3.5, this desulfurization mechanism is contradictory to the immature nature of our samples. Although the desulfurization of polar fractions and asphaltenes yielded insignificant amounts of hydrocarbons, it does not exclude the occurrence of sulfurization during early diagenesis. Chemical weathering can also account for unselective alteration of organic matter (Petsch et al., 2000). Additionally, the abiotic reduction (hydrogenation) of functionalized lipid into partly reduced counterparts under the presence of H_2S/HS^-, with

or without an intermediate sulfurization step, has been proposed as a major preservation pathway of organic carbon at a molecular level (Hebting et al., 2006).

Sample GM3-238 and its counterparts from KB3 were deposited under high algal productivity and the accumulation of organic matter under euxinic conditions. High concentrations of H_2S might have favored the presence of a simple trophic structure with low heterotrophic activity, and a diminished degradation of organic matter in the water column and sediments, allowing the preservation of a relatively unaltered algal lipid composition. Chlorophyll-*a* can be found in high proportion compared to sterols in certain marine dinoflagellates (Hallegraeff et al., 1991). Temporary limitation of specific resources can also contribute to the high occurrence of pigment-derived lipids compared to membrane-derived lipids in their precursors. Under conditions of scarce resources such as light and nutrients, slow-growing phytoplankton can synthesize additional "resource acquisition machinery" components such as pigments, consequently influencing the cellular stoichiometry (Klausmeier et al., 2004); (Arrigo, 2005).

II.3.7. Redox conditions and paleoenvironmental reconstruction

The presence of gammacerane in the entire set of analyzed samples suggests the presence of a stratified and anoxic water column during their deposition, whereas changes in its relative contribution can be interpreted as variations in the degree of stratification (e.g., (Sinninghe Damsté et al., 1995a). The gammacerane index (GI) exhibited relatively low values at the base of the section, increased and reached a maximum in the middle of the CIE and remained high upward (Fig. II.5.). The relative contribution of extended $C_{31\text{-}35}$ hopanes increased up section and reached a maximum in samples 232 and 237 (Fig. II.5.). An increased contribution of extended hopanes probably indicates an better preservation of their precursor bacteriohopanetetrol in sulfide-rich and anoxic sediments (Peters & Moldowan, 1991), and hypersaline environments (de Leeuw & Sinninghe Damsté, 1990). Both indices indicate a progressive increase of salinity and/or thermal stratification of the water column and euxinic conditions in the bottom during the deposition of black shales. The Pr/Ph ratio was only calculated in sample 238 (0.33) and in those from KB3 section (0.34 – 0.44) (Table II.3.) and is indicative of

strongly reducing conditions during deposition (Didyk et al., 1978); (de Leeuw & Sinninghe Damsté, 1990); (ten Haven et al., 1985), (1987). A low total phosphorous content has been found in samples deposited during and after OAE2 in GM3 section (J. Wendler, unpublished data) and corroborates the presence of anoxic conditions at the water-sediment interface during these intervals (Mort et al., 2007b).

The presence of isorenieratane and its diagenetic products, the isotopically enriched aryl isoprenoids, found in sample 238 and in KB3 section point to the presence of Chlorobiaceae and the existence of photic zone euxinia (e.g., (Sinninghe Damsté et al., 1995a); (van Kaam-Peters & Sinninghe Damsté, 1997). Gammacerane and isorenieratane have been used for reconstructing changes of the depth of the chemocline in ancient environments (e.g., (Sinninghe Damsté et al., 1995a). The occurrence of gammacerane and the absence of isorenieratane in most samples from the section reflect the occurrence of a stratified water column with a chemocline positioned below the photic zone. On the other hand, the presence of both gammacerane and isorenieratane (as observed in sample 238 and KB3 section) points to a stratified water column with a shallow chemocline in the photic zone. A conceptual model for the Levant platform during the deposition of organic-rich sediments is proposed in Figure II.9. A likely mechanisms triggering water column stratification and bathymetrical changes of the chemocline is salinity stratification as a result of changes in sea level, water circulation, and/or evaporation, as observed in semi-restricted environments (Kenig et al., 1995a); (Sinninghe Damsté et al., 1995a). Due to the "intra-platform" configuration of the Karak-Silla-Basin, the study area was sensitive to sea-level fluctuations and experienced different periods of connection and isolation from open marine conditions (Kuss et al., 2003). The presence of four "gypsum beds" along the section indicates evaporitic conditions during low sea level conditions (gb1-4 in Fig. II.2.), whereas geochemical and microfossil data indicate temporally restricted lagoonal and brackish conditions in the lower part of GM3 section, and a maximum flooding shortly below the C-T boundary (Wendler et al., in review). We interpret the flooding event associated with the isotopic excursion to have favored the formation of dense waters that filled the intrashelf-basin of the Levant Platform and resulted in the observed stratification and anoxia in both the water column and the sediments (Fig. II.9.). This maximum sea level has been indicated as one of the major

forcing mechanisms triggering high productivity and the deposition of organic carbon in globally widespread basins (e.g., (Arthur et al., 1987). The flooding of extended coastal areas in arid low latitude environments, together with high evaporation and generation of warm and salty waters in marginal seas are considered as important processes leading to the generation of dense deep and intermediate waters responsible for stratification during OAEs (e.g., (Brass et al., 1982); (Arthur et al., 1987).

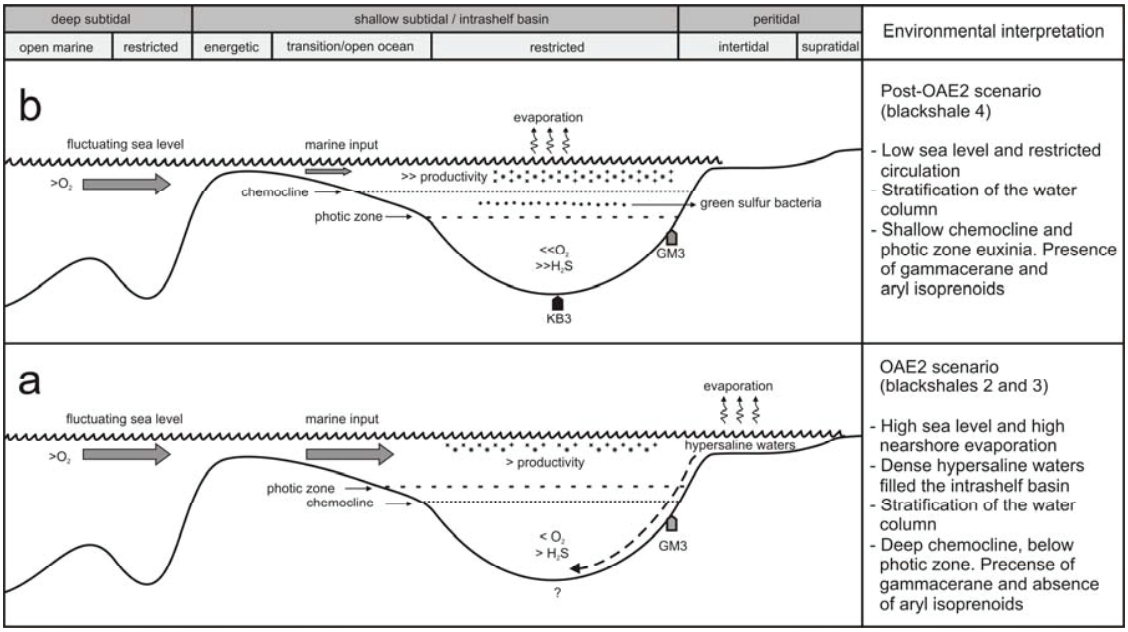

Figure II.9. Conceptual model of two representative depositional environments. a) An OAE2 scenario would represent transgressive and high-stand conditions, flooding of coastal areas, and formation of dense waters and stratification of the water column. The sea level rise exchanged surface waters with the neighboring open ocean supplying nutrients that supported high rates of primary production. Nitrate was removed by denitrification in anoxic waters hence favoring nitrogen fixation. Photic zone euxinia was likely precluded by a deepening of the chemocline. b) The post-OAE2 scenario (samples GM3-238, KB3-68, and KB3-70) represents decreasing sea level where restricted conditions are established. Photic zone euxinia developed due to shoaling of the chemocline. The bathymetrical profile was modified from Schulze et al. (2005) and exaggerated for schematic reasons. Dark and light grey boxes on top represent facies belts and reconstructed depositional environments, respectively, according to Schulze et al. (2005).

II.4. CONCLUSIONS

Source-specific biomarker parameters obtained from bitumens of organic-rich rocks from the Cenomanian-Turonian boundary of west-central Jordan indicated the presence of immature marine organic matter, mostly derived from algae including dinoflagellates, as well as photosynthetic bacteria such as cyanobacteria and Chlorobiaceae, and bacterivorous ciliates. Terrestrial input was apparently minimal. Successions in planktonic communities seem to be strongly associated with sea level changes and water column stratification, e.g. the direct relationship between water column stratification and the relative contribution of dinoflagellates. The carbon isotopic composition of hopanes, together with the presence of low $\delta^{15}N_{org}$ values and the occurrence of 2-methyl hopanes suggest that N-fixing cyanobacteria were an important component of the planktonic assemblage, accounting for an essential part of the organic carbon deposited in the black shales. We provide further evidence about the important role of these microorganisms as primary producers as well as nitrogen fixation for fueling primary production in stratified/anoxic coastal environments during OAEs.

Redox parameters, such as the Pr/Ph ratio and the gammacerane and homohopane indexes, indicate the presence of a stratified, euxinic and likely hypersaline water column throughout OAE2 and after. A shoaling of the chemocline and the development of photic zone euxinia occurred in a post-OAE interval as evidenced by the presence of isorenieratane and isotopic enrichment of the C_{14} aryl isoprenoid. This event was characterized by high concentrations of phytane and pristine of algal origin, likely to represent high primary production under conditions of environmental stress and the preservation of lipids under euxinic conditions.

Two main conceptual models to explain stratification of the water column and the development of anoxia during the C-T boundary are proposed. 1) Throughout OAE2, the flooding of extended areas associated to the rising sea level, and the expected high evaporation due to increased temperatures, probably promoted the formation of salty-dense water masses in shallow coastal areas that filled the basin creating strong salinity

stratification. 2) During the deposition of post-OAE2 black shales, intermittent isolation of the basin and restricted circulation during low sea level stages most likely triggered stratification of the water column and a shoaling of the chemocline promoting photic zone euxinia.

II.5. ACKNOWLEDGEMENTS

This research was funded by the Deutsche Forschungsgemeinschaft (DFG) as part of the European Graduate College "Proxies in Earth History" (EUROPROX) and the DFG project Ku642-221. We thank X. Prieto, S. Tille, L. Sherman, C. Colonero, M. Segl, U. Beckert, and P. Simundic for their valuable laboratory assistance, D. Birgel and M. Elvert for helpful discussion and assistance in mass spectrometry, R. Stein at the Alfred Wegener Institute, Bremerhaven for laboratory facilities, and A. Masri and the Jordan Geological Survey (NRA) for providing ideal field campaign logistics. R.E. Summons was supported by the NASA Exobiology Program, the Hanse-Wissenschaftskolleg, and the Alexander von Humboldt-Stiftung Foundation. J. Sepúlveda acknowledges the DFG and the EUROPROX program for supporting his doctoral studies and a six month research visit to the Summons Laboratory at MIT.

II.6. REFERENCES

Anbar, A.D., Knoll, A.H., (2002) Proterozoic Ocean Chemistry and Evolution: A Bioinorganic Bridge? *Science*, 297(5584), 1137-1142.

Arrigo, K.R., (2005) Marine microorganisms and global nutrient cycles. *Nature*, 437, 349-355.

Arthur, M.A., Dean, W.E., Pratt, L.M., (1988) Geochemical and climatic effects of increased marine organic carbon burial at the Cenomanian/Turonian boundary. *Nature*, 335(6192), 714-717.

Arthur, M.A., Schlanger, S.O., Jenkyns, H.C., (1987) The Cenomanian-Turonian Oceanic Anoxic Event, II. Palaeoceanographic controls on organic-matter production and preservation. *Geological Society, London, Special Publications*, 26(1), 401-420.

Badger, M.R., Price, G.D., (2003) CO_2 concentrating mechanisms in cyanobacteria: molecular components, their diversity and evolution. *Journal of Experimental Botany*, 54(383), 609-622.

Bice, K.L., Birgel, D., Meyers, P.A., Dahl, K.A., Hinrichs, K.-U., Norris, R.D., (2006) A multiple proxy and model study of Cretaceous upper ocean temperatures and atmospheric CO_2 concentrations. *Paleoceanography*, 21, PA2002, doi:10.1029/2005PA001203.

Brass, G.W., Southam, J.R., Peterson, W.H., (1982) Warm saline bottom water in the ancient ocean. *Nature*, 296(5858), 620-623.

Bravo, J.-M., Perzl, M., Hartner, T., Kannenberg, E.L., Rohmer, M., (2001) Novel methylated triterpenoids of the gammacerane series from the nitrogen-fixing bacterium Bradyrhizobium japonicum USDA 110. *European Journal of Biochemistry*, 268(5), 1323-1331.

Brooks, J.D., Gould, K., Smith, J., (1969) Isoprenoid hydrocarbons in coal and petroleum. *Nature*, 222, 257-259.

Cranwell, P.A., Eglinton, G., Robinson, N., (1987) Lipids of aquatic organisms as potential contributors to lacustrine sediments-II. *Organic Geochemistry*, 11(6), 513-527.

de Leeuw, J.W., Rijpstra, W.I.C., Schenck, P.A., Volkman, J.K., (1983) Free, esterified and residual bound sterols in Black Sea Unit I sediments. *Geochimica et Cosmochimica Acta*, 47(3), 455-465.

de Leeuw, J.W., Sinninghe Damsté, J.S., (1990) Organic sulphur compounds and other biomarkers as indicators of palaeosalinity. In: W.L. Orr, C.M. White (Eds.), *Geochemistry of Sulfur in Fossil Fuels, ACS Symposium Series 429* (Ed. by W.L. Orr, C.M. White), pp. 417-443. American Chemical Society, Washington DC.

Didyk, B.M., Simoneit, B.R.T., Brassell, S.C., Eglinton, G., (1978) Organic geochemical indicators of palaeoenvironmental conditions of sedimentation. *Nature*, 272, 216-222.

Dumitrescu, M., Brassell, S.C., (2005) Biogeochemical assessment of sources of organic matter and paleoproductivity during the early Aptian Oceanic Anoxic Event at Shatsky Rise, ODP Leg 198. *Organic Geochemistry*, 36(7), 1002-1022.

Eglinton, G., Hamilton, R.J., (1967) Leaf epicuticular waxes. *Science*, 156, 1322-1335.

Erbacher, J., Huber, B.T., Norris, R.D., Markey, M., (2001) Increased thermohaline stratification as a possible cause for an ocean anoxic event in the Cretaceous period. *Nature*, 409(6818), 325-327.

Evans, M.C.W., Buchanan, B.B., Arnon, D.I., (1966) A New Ferredoxin-Dependent Carbon Reduction Cycle in a Photosynthetic Bacterium. *Proceedings of the National Academy of Sciences*, 55(4), 928-934.

Forster, A., Schouten, S., Moriya, K., Wilson, P.A., Sinninghe Damsté, J.S., (2007) Tropical warming and intermittent cooling during the Cenomanian/Turonian oceanic anoxic event 2: Sea surface temperature records from the equatorial Atlantic. *Paleoceanography*, 22, PA1219, doi:10.1029/2006PA001349.

Ganeshram, R.S., Pedersen, T.F., Calvert, S.E., McNeill, G.W., Fontugne, M.R., (2000) Glacial-Interglacial Variability in Denitrification in the World's Oceans: Causes and Consequences. *Paleoceanography*, 15(4), 361–376.

Goodwin, N.S., Mann, A.L., Patience, R.L., (1988) Structure and significance of C_{30} 4-methyl steranes in lacustrine shales and oils. *Organic Geochemistry*, 12(5), 495-506.

Goossens, H., de Leeuw, J.W., Schenck, P.A., Brassell, S.C., (1984) Tocopherols as likely precursors of pristane in ancient sediments and crude oils. *Nature*, 312, 440-442.

Grice, K., Schaeffer, P., Schwark, L., Maxwell, J.R., (1996) Molecular indicators of palaeoenvironmental conditions in an immature Permian shale (Kupferschiefer, Lower Rhine Basin, north-west Germany) from free and S-bound lipids. *Organic Geochemistry*, 25(3-4), 131-147.

Grice, K., Schouten, S., Nissenbaum, A., Charrach, J., Damste, J.S.S., (1998a) Isotopically heavy carbon in the C-21 to C-25 regular isoprenoids in halite-rich deposits from the Sdom Formation, Dead Sea Basin, Israel. *Organic Geochemistry*, 28(6), 349-359.

Grice, K., Schouten, S., Peters, K.E., Sinninghe Damste, J.S., (1998b) Molecular isotopic characterisation of hydrocarbon biomarkers in Palaeocene-Eocene evaporitic, lacustrine source rocks from the Jianghan Basin, China. *Organic Geochemistry*, 29(5-7), 1745-1764.

Grosjean, E., Logan, G.A., (2007) Incorporation of organic contaminants into geochemical samples and an assessment of potential sources: Examples from Geoscience Australia marine survey S282. *Organic Geochemistry*, 38(6), 853-869.

Hallegraeff, G.M., Nichols, P.D., Volkman, J.K., Blackburn, S.I., Everitt, D.A., (1991) Pigments, fatty acids, and sterols of the toxic dinoflagellate *Gymnodinium catenatum*. *Journal of Phycology*, 27(5), 591-599.

Hayes, J.M., (2001) Fractionation of Carbon and Hydrogen Isotopes in Biosynthetic Processes. *Reviews in Mineralogy and Geochemistry*, 43(1), 225.

Hebting, Y., Schaeffer, P., Behrens, A., Adam, P., Schmitt, G., Schneckenburger, P., Bernasconi, S.M., Albrecht, P., (2006) Biomarker Evidence for a Major Preservation Pathway of Sedimentary Organic Carbon. *Science*, 312(5780), 1627-1631.

Hinrichs, K.-U., Summons, R.E., Orphan, V., Sylva, S.P., Hayes, J.M., (2000) Molecular and isotopic analysis of anaerobic methane-oxidizing communities in marine sediments. *Organic Geochemistry*, 31(12), 1685-1701.

Jahnke, L.L., Summons, R.E., Hope, J.M., Des Marais, D.J., (1999) Carbon isotopic fractionation in lipids from methanotrophic bacteria II: the effects of physiology and environmental parameters on the biosynthesis and isotopic signatures of biomarkers. *Geochimica et Cosmochimica Acta*, 63(1), 79-93.

Jenkyns, H.C., (1980) Cretaceous anoxic events: from continents to oceans. *Journal of the Geological Society*, 137(2), 171-188.

Jenkyns, H.C., Matthews, A., Tsikos, H., Erel, Y., (2007) Nitrate reduction, sulfate reduction, and sedimentary iron isotope evolution during the Cenomanian-Turonian oceanic anoxic event. *Paleoceanography*, 22, PA3208.

Kashiyama, Y., Ogawa, N.O., Kuroda, J., Shiro, M., Nomoto, S., Tada, R., Kitazato, H., Ohkouchi, N., (2008) Diazotrophic cyanobacteria as the major photoautotrophs during mid-Cretaceous oceanic anoxic events: Nitrogen and carbon isotopic evidence from sedimentary porphyrin. *Organic Geochemistry*, 39(5), 532-549.

Keely, B.J., Sinninghe Damste, J.S., Betts, S.E., Yue, L., de Leeuw, J.W., Maxwell, J.R., (1993) A molecular stratigraphic approach to palaeoenvironmental assessment

and the recognition of changes in source inputs in marls of the Mulhouse Basin (Alsace, France). *Organic Geochemistry*, 20(8), 1165-1186.

Kenig, F., Simons, D.-J.H., Crich, D., Cowen, J.P., Ventura, G.T., Rehbein-Khalily, T., (2005) Structure and distribution of branched aliphatic alkanes with quaternary carbon atoms in Cenomanian and Turonian black shales of Pasquia Hills (Saskatchewan, Canada). *Organic Geochemistry*, 36(1), 117-138.

Kenig, F., Simons, D.-J.H., Crich, D., Cowen, J.P., Ventura, G.T., Rehbein-Khalily, T., Brown, T.C., Anderson, K.B., (2003) Branched aliphatic alkanes with quaternary substituted carbon atoms in modern and ancient geologic samples. *Proceedings of the National Academy of Sciences*, 100(22), 12554-12558.

Kenig, F., Sinninghe Damste, J.S., Frewin, N.L., Hayes, J.M., De Leeuw, J.W., (1995a) Molecular indicators for palaeoenvironmental change in a Messinian evaporitic sequence (Vena del Gesso, Italy). II: High-resolution variations in abundances and 13C contents of free and sulphur-bound carbon skeletons in a single marl bed. *Organic Geochemistry*, 23(6), 485-526.

Kenig, F., Sinninghe Damste, J.S., Kock-van Dalen, A.C., Rijpstra, W.I.C., Huc, A.Y., de Leeuw, J.W., (1995b) Occurrence and origin of mono-, di-, and trimethylalkanes in modern and Holocene cyanobacterial mats from Abu Dhabi, United Arab Emirates. *Geochimica et Cosmochimica Acta*, 59(14), 2999-3015.

Klausmeier, C.A., Litchman, E., Daufresne, T., Levin, S.A., (2004) Optimal nitrogen-to-phosphorus stoichiometry of phytoplankton. *Nature*, 429(6988), 171-174.

Knoll, A.H., Summons, R.E., Waldbauer, J.R., Zumberge, J., (2007) The Geological Succession of Primary Producers in the Oceans. In: P. Falkowski, A.H. Knoll (Eds.), *The Evolution of Primary Producers in the Sea* (Ed. by P. Falkowski, A.H. Knoll), pp. 133–163. Academic Press, Boston.

Kodner, R.B., Summons, R.E., Pearson, A., Knoll, A.H., (2008) Sterols in red and green algae: quantification, phylogeny and relevance for the interpretation of geologic steranes. *Geobiology (In Press)*.

Kolonic, S., Wagner, T., Forster, A., Damste, J.S.S., Walsworth- Bell, B., Erba, E., Turgeon, S., Brumsack, H.J., Chellai, E.I., Tsikos, H., Kuhnt, W., Kuypers, M.M.M., (2005) Black shale deposition on the northwest African Shelf during the Cenomanian/Turonian oceanic anoxic event: Climate coupling and global organic carbon burial. *Paleoceanography*, 20(1).

Koopmans, M.P., de Leeuw, J.W., Lewan, M.D., Sinninghe Damsté, J.S., (1996a) Impact of dia- and catagenesis on sulfur and oxygen sequestration of biomarkers as revealed by artificial maturation of an immature sedimentary rock. *Organic Geochemistry*, 25, 391-426.

Koopmans, M.P., Koster, J., Van Kaam-Peters, H.M.E., Kenig, F., Schouten, S., Hartgers, W.A., de Leeuw, J.W., Sinninghe Damste, J.S., (1996b) Diagenetic and catagenetic products of isorenieratene: Molecular indicators for photic zone anoxia. *Geochimica et Cosmochimica Acta*, 60(22), 4467-4496.

Köster, J., Volkman, J.K., Rullkotter, J., Scholz-Bottcher, B.M., Rethmeier, J., Fischer, U., (1999) Mono-, di- and trimethyl-branched alkanes in cultures of the filamentous cyanobacterium Calothrix scopulorum. *Organic Geochemistry*, 30(11), 1367-1379.

Kuss, J., Bassiouni, A., Bauer, J., Bachmann, M., Marzouk, A., Scheibner, C., Schulze, F., (2003) Cretaceous-Paleogene sequence stratigraphy of the Levant Platform (Egypt, Sinai, Jordan). In: E. Gili, H. Negra, P.W. Skelton (Eds.), *North African cretaceous carbonate platform systems*, *28* (Ed. by E. Gili, H. Negra, P.W. Skelton), pp. 171-187. Nato Science Series.

Kuypers, M.M.M., Blokker, P., Erbacher, J., Kinkel, H., Pancost, R.D., Schouten, S., Sinninghe Damsté, J.S., (2001) Massive expansion of marine archaea during a mid-Cretaceous oceanic anoxic event. *Science*, 293(5527), 92-94.

Kuypers, M.M.M., Blokker, P., Hopmans, E.C., Kinkel, H., Pancost, R.D., Schouten, S., Sinninghe Damsté, J.S., (2002a) Archaeal remains dominate marine organic matter from the early Albian oceanic anoxic event 1b. *Palaeogeography, Palaeoclimatology, Palaeoecology*, 185(1-2), 211-234.

Kuypers, M.M.M., Lourens, L.J., Rijpstra, W.R.C., Pancost, R.D., Nijenhuis, I.A., Sinninghe Damsté, J.S., (2004a) Orbital forcing of organic carbon burial in the proto-North Atlantic during oceanic anoxic event 2. *Earth and Planetary Science Letters*, 228(3-4), 465-482.

Kuypers, M.M.M., Pancost, R.D., Nijenhuis, I.A., Sinninghe Damsté, J.S., (2002b) Enhanced productivity led to increased organic carbon burial in the euxinic North Atlantic basin during the late Cenomanian oceanic anoxic event. *Paleoceanography*, 17(4), 1051.

Kuypers, M.M.M., Pancost, R.D., Sinninghe Damsté, J.S., (1999) A large and abrupt fall in atmospheric CO2 concentration during Cretaceous times. *Nature*, 399, 342-345.

Kuypers, M.M.M., van Breugel, Y., Schouten, S., Erba, E., Sinninghe Damsté, J.S., (2004b) N_2-fixing cyanobacteria supplied nutrient N for Cretaceous oceanic anoxic events. *Geology*, 32(10), 853-856.

Leckie, M., Bralower, T.J., Cashmann, R., (2002) Oceanic anoxic events and plankton evolution: Biotic response to tectonic forcing during the mid-Cretaceous. *Paleoceanography*, 17(3), 1041.

Liaaen-Jensen, S., (1978) Chemistry of carotenoid pigments. In: R.K. Clayton, W.R. Sistrom (Eds.), *Photosynthetic Bacteria* (Ed. by R.K. Clayton, W.R. Sistrom), pp. 233-247. Plenum Press, New York.

Marzi, R., Torkelson, B.E., Olson, R.K., (1993) A revised carbon preference index. *Organic Geochemistry*, 20(8), 1303-1306.

Meyers, P.A., (2006) Paleoceanographic and paleoclimatic similarities between Mediterranean sapropels and Cretaceous black shales. *Palaeogeography, Palaeoclimatology, Palaeoecology*, 235(1-3), 305-320.

Mort, H., Jacquat, O., Adatte, T., Steinmann, P., Föllmi, K., Matera, V., Berner, Z., Stuben, D., (2007a) The Cenomanian/Turonian anoxic event at the Bonarelli Level in Italy and Spain: enhanced productivity and/or better preservation? *Cretaceous Research*, 28(4), 597-612.

Mort, H.P., Adatte, T., Föllmi, K.B., Keller, G., Steinmann, P., Matera, V., Berner, Z., Stüben, D., (2007b) Phosphorus and the roles of productivity and nutrient recycling during oceanic anoxic event 2. *Geology*, 483-486.

Ohkouchi, N., Kashiyama, Y., Kuroda, J., Ogawa, N.O., Kitazato, H., (2006) The importance of diazotrophic cyanobacteria as primary producers during Cretaceous Oceanic Anoxic Event 2. *Biogeosciences*, 3(4), 467-478.

Ourisson, G., Rohmer, M., Poralla, K., (1987) Prokaryotic Hopanoids and other Polyterpenoid Sterol Surrogates. *Annual Review of Microbiology*, 41(1), 301-333.

Peters, K.E., Moldowan, J.M., (1991) Effects of source, thermal maturity and biodegradation on the distribution and isomerization of homohopanes in petroleum. *Organic Geochemistry*, 17, 47-61.

Peters, K.E., Walters, C.C., Moldowan, J.M., (2005) *The Biomarker Guide, 2nd edition*. Cambridge University Press, Cambridge.

Petsch, S.T., Berner, R.A., Eglinton, T.I., (2000) A field study of the chemical weathering of ancient sedimentary organic matter. *Organic Geochemistry*, 31(5), 475-487.

Philip, J., Babinot, J.-F., Tronchetti, G., Fourcade, E., Ricou, L.-E., Guiraud, R., Bellion, Y., Herbin, J.-P., Combes, P.-J., Cornee, J.-J., Dercourt, J., (2000) Late Cenomanian, Map 14. In: *Atlas Peri-Tethys palaeogeographical maps* (Ed. by J. Dercourt, M. Gaetani, B. Vrielynck, E. Barrier, B. Biju-Duval, M. Brunet, J. Cadet, S. Crasquin, M. Sandulescu). CCGM/CGMW, Paris.

Rashby, S.E., Sessions, A.L., Summons, R.E., Newman, D.K., (2007) Biosynthesis of 2-methylbacteriohopanepolyols by an anoxygenic phototroph. *Proceedings of the National Academy of Sciences*, 104(38), 15099-15104.

Rohmer, M., Bouvier-Nave, P., Ourisson, G., (1984) Distribution of hopanoid triterpenes in prokaryotes. *Journal of general microbiology*, 130(5), 1137-1150.

Rowland, S.J., (1990) Production of acyclic isoprenoid hydrocarbons by laboratory maturation of methanogenic bacteria. *Organic Geochemistry*, 15, 9-16.

Sakata, S., Hayes, J.M., McTaggart, A.R., Evans, R.A., Leckrone, K.J., Togasaki, R.K., (1997) Carbon isotopic fractionation associated with lipid biosynthesis by a cyanobacterium: Relevance for interpretation of biomarker records. *Geochimica et Cosmochimica Acta*, 61(24), 5379-5389.

Schlanger, S.O., Arthur, M.A., Jenkyns, H.C., Scholle, P.A., (1987) The Cenomanian-Turonian Oceanic Anoxic Event, I. Stratigraphy and distribution of organic carbon-rich beds and the marine $\delta^{13}C$ excursion. *Geological Society, London, Special Publications*, 26(1), 371-399.

Scholle, P.A., Arthur, M.A., (1980) Carbon isotope fluctuations in Cretaceous pelagic limestones; potential stratigraphic and petroleum exploration tool. *AAPG Bulletin*, 64(1), 67-87.

Schouten, S., Hopmans, E.C., Forster, A., van Breugel, Y., Kuypers, M.M.M., Sinninghe Damsté, J.S., (2003) Extremely high sea-surface temperatures at low latitudes during the middle Cretaceous as revealed by archaeal membrane lipids. *Geology*, 1069-1072.

Schulze, F., Kuss, J., Marzouk, A., (2005) Platform configuration, microfacies and cyclicities of the upper Albian to Turonian of west-central Jordan. *Facies*, 50(3), 505-527.

Schulze, F., Lewy, Z., Kuss, J., Gharaibeh, A., (2003) Cenomanian-Turonian carbonate platform deposits in west central Jordan. *International Journal of Earth Sciences*, 92(4), 641-660.

Simons, D.-J.H., Kenig, F., (2001) Molecular fossil constraints on the water column structure of the Cenomanian-Turonian Western Interior Seaway, USA. *Palaeogeography, Palaeoclimatology, Palaeoecology*, 169(1-2), 129-152.

Sinninghe Damsté, J.S., de Leeuw, J.W., (1990) Organically-bound sulphur in the geosphere: state of the art and future research. *Organic Geochemistry*, 16, 1077-1101.

Sinninghe Damsté, J.S., Frewin, N.L., Kenig, F., De Leeuw, J.W., (1995a) Molecular indicators for palaeoenvironmental change in a Messinian evaporitic sequence (Vena del Gesso, Italy). I: Variations in extractable organic matter of ten cyclically deposited marl beds. *Organic Geochemistry*, 23(6), 471-483.

Sinninghe Damsté, J.S., Kenig, F., Koopmans, M.P., Köster, J., Schouten, S., Hayes, J.M., de Leeuw, J.W., (1995b) Evidence for gammacerane as an indicator of water column stratification. *Geochimica et Cosmochimica Acta*, 59(9), 1895-1900.

Sinninghe Damsté, J.S., Köster, J., (1998) A euxinic southern North Atlantic Ocean during the Cenomanian/Turonian oceanic anoxic event. *Earth and Planetary Science Letters*, 158(3-4), 165-173.

Sinninghe Damsté, J.S., Schouten, S., van Duin, A.C.T., (2001) Isorenieratene derivatives in sediments: possible controls on their distribution. *Geochimica et Cosmochimica Acta*, 65(10), 1557-1571.

Summons, R.E., Franzmann, P.D., Nichols, P.D., (1998) Carbon isotopic fractionation associated with methylotrophic methanogenesis. *Organic Geochemistry*, 28(7-8), 465-475.

Summons, R.E., Jahnke, L.L., Hope, J.M., Logan, G.A., (1999) 2-Methylhopanoids as biomarkers for cyanobacterial oxygenic photosynthesis. *Nature*, 400(6744), 554-557.

Summons, R.E., Powell, T.G., (1987) Identification of aryl isoprenoids in source rocks and crude oils: Biological markers for the green sulphur bacteria. *Geochimica et Cosmochimica Acta*, 51(3), 557-566.

Summons, R.E., Volkman, J.K., Boreham, C.J., (1987) Dinosterane and other steroidal hydrocarbons of dinoflagellate origin in sediments and petroleum. *Geochimica et Cosmochimica Acta*, 51(11), 3075-3082.

ten Haven, H.L., de Leeuw, J.W., Rullkötter, J., Sinninghe Damsteé, J.S., (1987) Restricted utility of the pristane/phytane ratio as a paleoenvironmental indicator. *Nature*, 330, 641-643.

ten Haven, H.L., De Leeuw, J.W., Schenck, P.A., (1985) Organic geochemical studies of a Messinian evaporitic basin, northern Apennines (Italy) I: Hydrocarbon biological markers for a hypersaline environment. *Geochimica et Cosmochimica Acta*, 49(10), 2181-2191.

ten Haven, H.L., Rohmer, M., Rullkötter, J., Bisseret, P., (1989) Tetrahymanol, the most likely precursor of gammacerane, occurs ubiquitously in marine sediments. *Geochimica et Cosmochimica Acta*, 53(11), 3073-3079.

Thomas, J.B., Marshall, J., Mann, A.L., Summons, R.E., Maxwell, J.R., (1993) Dinosteranes (4,23,24-trimethylsteranes) and other biological markers in dinoglagellate-rich marine sediments of Rhaetian age. *Organic Geochemistry*, 20(1), 91-104.

Tyrrell, T., (1999) The relative influences of nitrogen and phosphorus on oceanic primary production. *Nature*, 400(6744), 525-531.

van Kaam-Peters, H.M.E., Schouten, S., De Leeuw, J.W., Damste, J.S.S., (1997) A molecular and carbon isotope biogeochemical study of biomarkers and kerogen pyrolysates of the Kimmeridge Clay Facies: palaeoenvironmental implications. *Organic Geochemistry*, 27(7-8), 399-422.

van Kaam-Peters, H.M.E., Sinninghe Damsté, J.S.S., (1997) Characterisation of an extremely organic sulphur-rich, 150 Ma old carbonaceous rock: palaeoenvironmental implications. *Organic Geochemistry*, 27(7-8), 371-397.

Volkman, J.K., Barrett, S.M., Blackburn, S.I., (1999) Eustigmatophyte microalgae are potential sources of C_{29} sterols, C_{22}-C_{28} n-alcohols and C_{28}-C_{32} n-alkyl diols in freshwater environments. *Organic Geochemistry*, 30(5), 307-318.

Volkman, J.K., Barrett, S.M., Blackburn, S.I., Mansour, M.P., Sikes, E.L., Gelin, F., (1998) Microalgal biomarkers: A review of recent research developments. *Organic Geochemistry*, 29(5-7), 1163-1179.

Wendler, J., Lehmann, J., Kuss, J., (in review) Orbital time scale, intra-platform basin correlation, carbon isotope stratigraphy, and sea level history of the Cenomanian/Turonian Eastern Levant platform, Jordan.

Chapter III

Oceanographic and climatic dynamics in the Late Cretaceous Equatorial Atlantic (ODP Site 1259): A compound-specific stable isotope approach into the formation of organic-rich sediments

Julio Sepúlveda[1,2,*], Arne Leider[2], Kai-Uwe Hinrichs[2]

First draft of article in preparation for submission to
Earth and Planetary Science Letters (September 2008)

[1]International Graduate College – Proxies in Earth History (EUROPROX), University of Bremen, Germany

[2]Organic Geochemistry Group, MARUM – Center for Marine Environmental Sciences and Department of Geosciences, Leobener Strasse, University of Bremen, 28359 Bremen, Germany

*Corresponding author: Tel.: +49 421 218 65742; fax: 49 421 218 65715. E-mail address: sepulved@uni-bremen.de (J. Sepúlveda)

Keywords: Late Cretaceous, Coniacian, Oceanic Anoxic Event, Demerara Rise, Ocean Drilling Program, Lipid biomarkers, Stable isotopes.

ABSTRACT

The stable isotopic composition of carbon and hydrogen ($\delta^{13}C$ and δD) of aquatic- and terrestrial-plant-derived *n*-alkanes from a 800-ky-long Coniacian record from the western equatorial Atlantic (Ocean Drilling Program Site 1259, Demerara Rise) was used to assess oceanographic and climatic variations involved in the formation of cyclic carbonate- and organic-rich sediments. Two different aquatic sources of short-chain *n*-alkanes (SCA) were identified based on their $\delta^{13}C$ values, marine algae and cyanobacteria (*n*-C_{17} and *n*-C_{21} with $\delta^{13}C$ values of -34 to -27.2), and heterotrophic bacteria (*n*-C_{16} *n*-C_{18} with $\delta^{13}C$ values of -31.6 to 24.5‰). For most part of the record the $\delta^{13}C$ of long-chain *n*-alkanes (LCA) is consistent with an origin from land plants using C_3 metabolism. Periods of enhanced marine productivity were identified by positive $\delta^{13}C$ excursions in *n*-C_{17}, likely reflecting rapid growth rates of phytoplankton under eutrophic conditions. These periods coincided with the presence of microfossils indicative of enhanced upwelling and were accompanied by ^{13}C enrichments of C_{29} and C_{31} *n*-alkanes thought to reflect changes in continental vegetation, e.g., increasing contribution of C_4 plants, a shift possibly coupled with enhanced marine productivity and organic matter burial and associated changes in ρCO_2. In addition, these periods were marked by δD enrichments in *n*-C_{17} suggestive of changes in δD_{water} due to variations in the hydrological czcle, suggesting a tightly coupled marine-terrestrial system. Our results generally agreed with current depositional models for the formation of eccentricity-driven cyclic sedimentary sequences; however, they revealed a more complex interplay of the climatic and oceanographic regime.

III.1. INTRODUCTION

The massive burial of organic matter over vast areas of the Cretaceous' oceans, known as oceanic anoxic events (OAE; Jenkyns, 1980), has been the focus of intense research due to its implications for global climate and the carbon cycle (e.g., Arthur et al., 1987; Schlanger et al., 1987; Kuypers et al., 1999). Elevated levels of primary production in surface waters and/or preservation of organic matter under oxygen-depleted conditions are the most prominent scenarios to explain the formation of black shales (Sinninghe Damsté and Köster, 1998; Kuypers et al., 2002; Mort et al., 2007). This situation has been suggested to result from the interaction of unusual and extreme environmental conditions such as elevated concentrations of atmospheric CO_2 (Bice et al., 2006), high sea surface temperatures (Schouten et al., 2003; Bice et al., 2006; Forster et al., 2007), rising sea level (e.g., Arthur et al., 1987; Schlanger et al., 1987), massive magmatic episodes (Turgeon and Creaser, 2008), and changes in oceanic circulation (e.g., Erbacher et al., 2001). However, it remains difficult to explain the occurrence of such extraordinary environmental conditions for extended periods of time. The Coniacian-Santonian interval (OAE3) has received less attention than other OAEs, in spite of its duration (~ 2.7 Ma; Meyers et al., 2006) and recent evidence of a complex oceanic-atmospheric interaction associated to the formation of black-shales (Nederbragt et al., 2007; Friedrich et al., 2008).

Ocean Drilling Program (ODP) Leg 207 successfully recovered Late Cretaceous sediments from the Demerara Rise off the coast of Surinam, providing continuous records of extended black shale sequences covering the Albian-Santonian (Erbacher et al., 2004), and offering an extraordinary opportunity for studying paleoceanographic and paleoclimatic processes in the Equatorial Atlantic. These sediments are characterized by the cyclic alternation of organic-rich layers, mostly composed of fecal pellets and lenses of organic matter, and of carbonate-rich layers composed of pelagic carbonate-rich beds or foraminiferal packstones (Nederbragt et al., 2007). The deposition of carbonate-rich layers seem to be affected by increased carbonate production and intervals of winnowing

under vigorous atmospheric and oceanic circulation, and thus to upwelling intensity, whereas organic-rich layers seem to be related to increased carbonate dilution by terrigenous fluxes and less intense upwelling (Nederbragt et al., 2007). The cyclic deposition of these sediments appears to be strongly linked to orbital Milancovitch cycles, mainly in the eccentricity frequency (Flögel et al., 2008b; Friedrich et al., 2008), with a minimum contribution of obliquity (Flögel et al., 2008b). This differs from ODP Site 959 in the tropical African margin, where orbital frequencies with shorter phasing clearly dominate cyclic river discharge and black shale formation (Beckmann et al., 2005). Cyclic changes in the abundance of planktic and benthic foraminifera in Demarara Rise are suggested to reflect changes in the mean latitudinal position of the Intertropical Convergence zone (ITCZ) leading to fluctuations in the precipitation/upwelling regime, and promoting changes in surface water productivity and the presence of a very shallow oxygen minimum zone (OMZ; Friedrich et al., 2008). However, the influence of the ITCZ on upwelling and marine productivity is controversial; model simulations suggest that black-shale formation in the equatorial Atlantic was triggered by climatic variability in mid to southern latitudes rather than by changes in the ITCZ (Flögel and Wagner, 2006). Furthermore, high resolution records of redox variability (März et al., 2008) suggest the alternation of permanent oxygen-depleted waters and euxinia in shorter cycles than as found in studies based on bulk geochemistry (Flögel et al., 2008a; Friedrich et al., 2008). Additionally, the presence of low but variable $\delta^{15}N$ values in Coniacian sediments from Demerara Rise suggests that diazotrophy was the main source of nutrient nitrogen during certain intervals of black-shale formation, implying the presence of upwelled waters with a low inorganic N/P ratio (Junium and Arthur, 2007). Thus, oceanographic processes of higher complexity than usually assumed might have interacted during the Late Cretaceous.

We study the molecular distribution and isotopic composition of marine- and terrestrial-derived *n*-alkanes from a sedimentary sequence spanning the Early Coniacian at Demerara Rise. This record includes two cycles of alternating carbonate- and organic-rich sediments described elsewhere to be driven by orbital eccentricity (Nederbragt et al., 2007; Flögel et al., 2008a; Friedrich et al., 2008). We study the relationship between primary production, upwelling intensity, and continental runoff as main triggers for the

cyclic deposition of these sediments by providing new insights into the coupling of both marine and terrestrial carbon reservoirs.

III.2. MATERIALS AND METHODS

III.2.1. Study area and samples

The Demerara Rise is a ~ 220-km wide submarine plateau located at ~ 5 °N in the western tropical Atlantic, it stretches for ~ 380 km along the coast of Suriname and the French Guyanas (Fig. III.1.), and it was formerly located south of Senegal at ~ 0° N of paleolatitude during Cretaceous times (Erbacher et al., 2004). Rifting and faulting processes separated the Guinea and Demerara Plateaus along an east-west–striking fault system during the Early Cretaceous, rapidly subsiding and reaching water depth of ~ 2000 m by the Late Cenomanian (Arthur and Natland, 1979). Water depths vary from about 700 m on the plateau to more than 4500 m at the abyssal plain and distal Orinoco Fan in the North West area (Erbacher et al., 2004). ODP Site 1259 Hole C (9°18.0240′ N, 54°11.9694′ W) was drilled on the northern slope of the Rise at a water depth of 2354 m (Fig. III.1.). Sediments are characterized by dark-laminated organic-rich claystones, occasionally interrupted by dark-light laminae or coarser greyish carbonate-rich intervals (Erbacher et al., 2004; Nederbragt et al., 2007). Molecular and bulk geochemical analyses indicate the presence of thermally immature marine-derived algal and bacterial organic matter (Erbacher et al., 2004; Meyers et al., 2006).

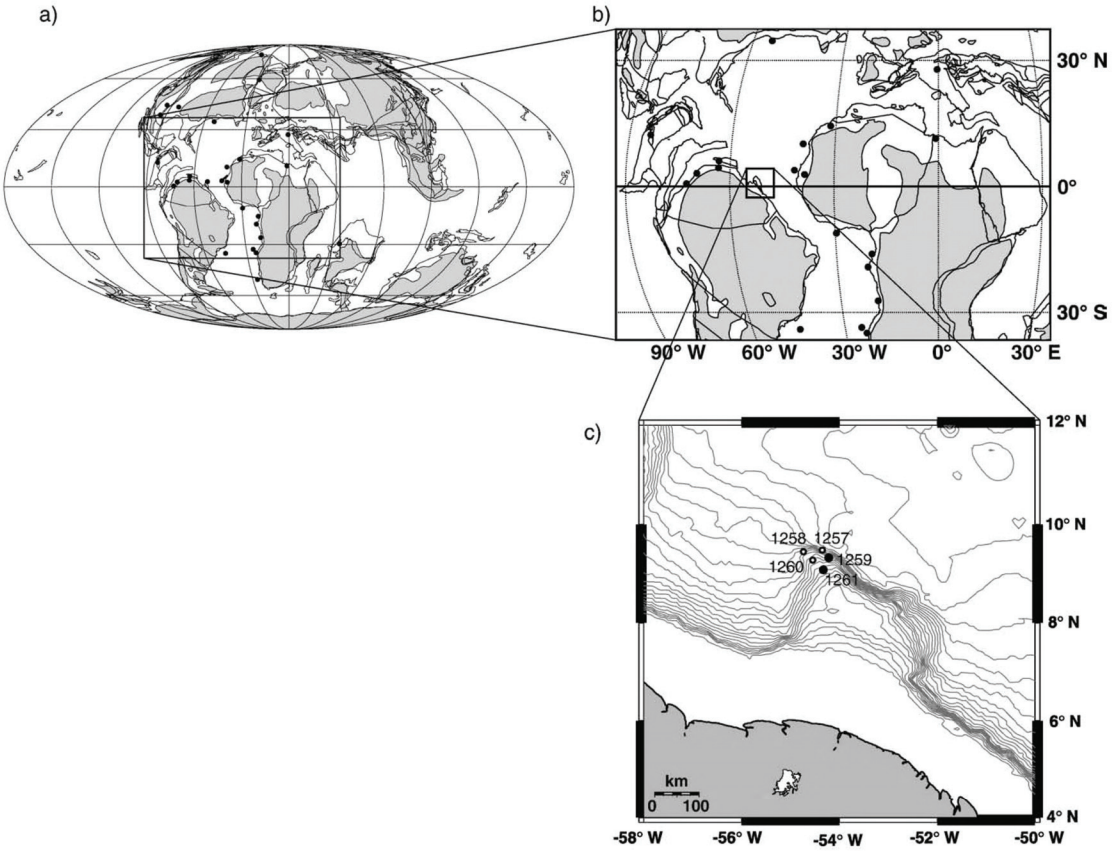

Figure III.1.. (a) Map showing a global plate-tectonic reconstruction for 80 Ma BP. Gray areas represent regions above sea level, white areas represent oceans, black lines depict plate boundaries. Black dots indicate locations of reported Late Cretaceous organic matter-rich deposits (Wagner et al., 2004 and references therein). (b) Close-up of the equatorial Proto-Atlantic, with Demerara Rise enclosed by the rectangle. (c) Present-day bathymetry of Demerara Rise with drill sites including 1259 (from März et al., 2008).

For the present study a total of 71 samples were obtained at a resolution of ~ 3.5 cm from a 3.56-m-long section (depth interval 505.70 - 509.26 mcd; Fig. III.2.), including sections 12R-5, 12R-CC, 13R-1, 13R-2, and 13R-3. These samples correspond to calcareous nannofossil zone CC13 (M. furcatus) and planktonic foraminifera zone KS23 (D. concavata) and are Coniacian in age (Bornemann et al., 2008; Friedrich et al., 2008). Average linear sedimentation rates (LSR) of 5 cm/Ma for Site 1259 during the Coniacian (Erbacher et al., 2004) yield a period of sedimentation of about 712 ky for the studied interval. This section was selected because it contains two intervals of characteristic cyclic alternations of carbonate- and organic-rich sediments (Fig. III.2.), as found along most of the record from ODP Site 1259, and recently described to represent

eccentricity-driven sedimentation (Friedrich et al., 2008). Total organic carbon (TOC) and calcium carbonate ($CaCO_3$) values measured at high resolution (every 1.5 cm) varies between 2 and 22%, and between 41 and 91%, respectively (Fig. III.2.; Bornemann et al., 2008; Friedrich et al., 2008).

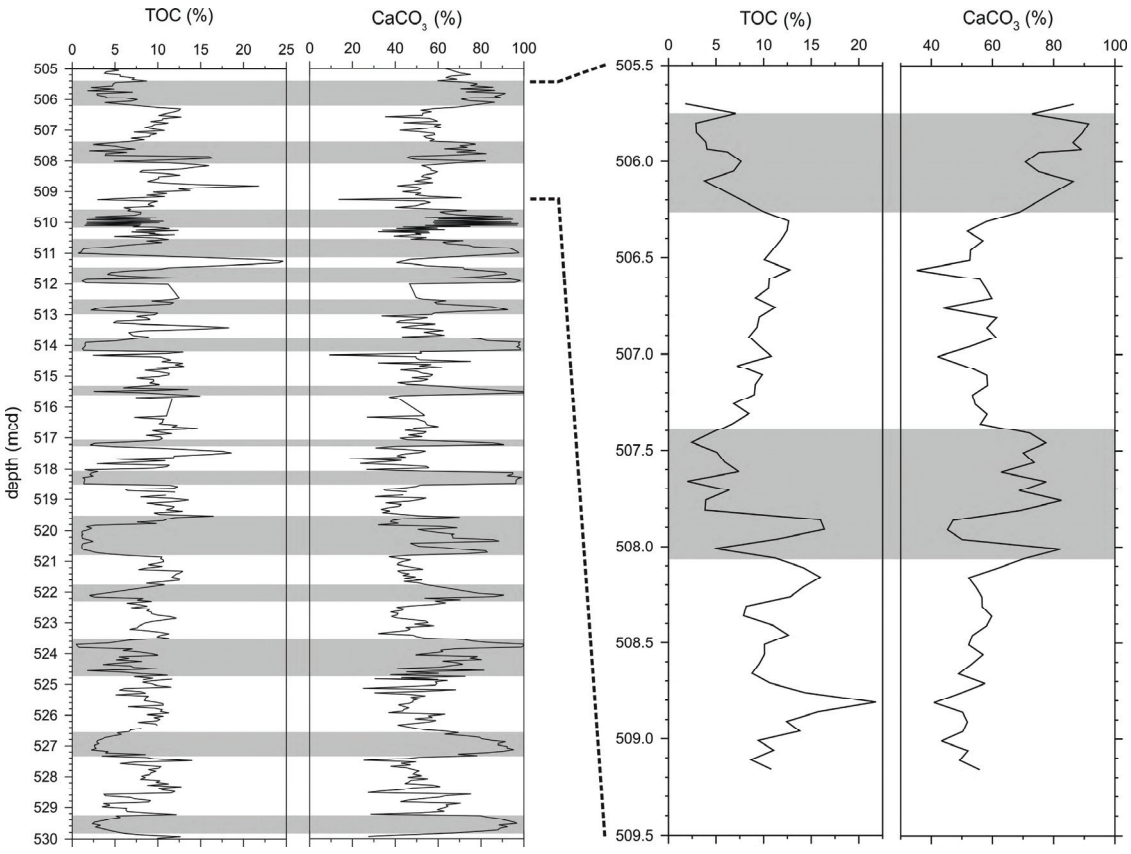

Figure III.2. Total organic carbon (TOC) and carbonate content (CaCO3) against depth in meters of composite depth (mcd) of ODP Site 1259. Left panel shows a 25-m-long sequence of cyclic alternations of carbonate- and organic-rich intervals (gray and white areas, respectively). Right panel shows the interval used in this study.

III.2.2. Lipid analysis, gas chromatography – mass spectrometry (GC-MS)

In order to reduce laboratory contamination, all glassware was combusted at 450°C for eight hours and rinsed with methanol (MeOH), dichloromethane (DCM), and hexane before use. Between 5 and 20 g of sediment were ground to powder in an agate mortar and homogenized. Samples were extracted in a MARS microwave system (CEM Corporation) using a solvent mixture of DCM:MeOH 3:1 (at least 3x, until the solvent extracts became colorless) at 80°C for 20 minutes. Before extraction, 2 μg of hexatriacontane, docosanoic acid, 1-nonadecanol and 2-methyl octadecanoic acid were added as internal standards. Total lipid extracts (TLE) were combined after centrifugation and concentrated under a stream of nitrogen using a Turbovap LV Evaporator. TLEs were then separated into asphaltenes and maltenes using small Pasteur pipettes filled with combusted glass wool and $NaSO_4$, and eluted with hexane and DCM, respectively. Elemental sulfur was removed from the maltenes using acid-activated copper (4 N HCl, rinsed consecutively with Milli-Q, MeOH, DCM, and hexane). Maltenes were fractionated into hydrocarbons, ketones and esters, alcohols, and fatty acids using Supelco DSC-NH_2 solid phase extraction glass columns (6 mL, 500 mg sorbent; Hinrichs et al., 2000). Hydrocarbons were identified by coupled gas chromatography-mass spectrometry (GC-MS) as described elsewhere (Sepúlveda et al., accepted)

After GC-MS analysis, *n*-alkanes were separated from branched and cyclic hydrocarbons by using urea adduction. Samples were concentrated under a N_2 flow, dissolved in 3 ml of hexane/DCM 2:1, mixed with 2 ml of saturated urea solution in MeOH (20 g Urea in 120 ml MeOH), and stored at -25 °C for 20 minutes. Later, solvent was blown down under a N_2 stream and the steps described above were repeated twice. Then, samples were evaporated; urea crystals were washed with 10 ml of hexane and centrifuged at 2000 rpm for 15 seconds. The hexane phase, including branched and cyclic compounds, was pipetted off and collected as non-adduct fraction; this step was repeated three times. Urea crystals were then dissolved with 5 ml of Milli-Q water and mixed with 10 ml of hexane/DCM 4:1. The solvent phase was pipetted off and saved as the adduct fraction including n-alkanes; this step was repeated three times. The adducted fraction was concentrated and transferred to inserts using hexane and analyzed by GC-MS as

described above. The efficiency of the method (yield of about 50-70%) was obtained by comparing the concentration of *n*-alkanes before and after urea adduction, and by using an injection standard (20 µg *n*-C_{22} anteiso alkane).

III.2.3. Isotopic analysis

Compound-specific carbon and hydrogen isotope analyses were performed by gas chromatography-combustion-isotope ratio mass spectrometry (GC-C- irm-MS) consisting of a Thermo Finnigan Trace GC Ultra coupled via a Thermo Finnigan GC Combustion III interface to a Thermo Finnigan Delta Plus XP mass spectrometer. For carbon isotope analyses the GC was equipped with a RTX-5MS fused silica capillary column (30 m; 0.25 mm ID; 0.25 µm film thickness) and the temperature conditions were identical to those described above. Helium was used as carrier gas. The interface was equipped with a combustion oven at 940 °C. Carbon isotope ratios are reported as δ values ($\delta^{13}C$, in ‰) relative to the VPDB standard. Multiple CO_2-pulses of known $\delta^{13}C$ value at the beginning and end of each run were used for calibration. Instrument precision (~ 0.22‰ or better) was regularly checked by injecting a mixture of *n*-alkanes (*n*-C_{15} to *n*-C_{29}) with known isotopic compositions. The isotopic composition of biomarkers was determined relative to an injection standard of know isotopic composition (docosanoic acid).

For hydrogen isotope measurements the GC was equipped with a RTX-5MS fused silica capillary column (60 m; 0.25 mm ID; 0.25 µm film thickness), and the temperature conditions were identical to those described above. A high-temperature pyrolysis reactor at 1440 °C pyrolyzed the sample quantitatively to H_2 gas before introduction into the MS. Pulses of hydrogen with known isotopic composition were used as the primary reference. The H_3 factor (Sessions et al., 2001) was monitored daily by using H_2 gas at different partial pressures. The accuracy of the system (better than 5‰) was evaluated daily by using a certified standard mixture of 15 *n*-alkanes (C_{16}-C_{30}) with known isotopic composition, and a 5-fold range of concentrations (A. Schimmelmann, Biogeochemical Laboratories, Indiana University). δD values were corrected to the VSMOW scale by co-injecting three standards with known isotopic composition (C_{10}, C_{20}, and C_{30} fatty acid

methyl esters) plus naphthalene. Only peak intensities larger than 1500 mV have been considered for δD values.

III.3. RESULTS AND DISCUSSION

III.3.1. Concentrations of selected hydrocarbons and biological sources

n-Alkanes were mainly represented by the C_{15-35} homologues with a general dominance of short-chain *n*-alkanes (SCA) between *n*-C_{15} and *n*-C_{21} (Fig. III.3.). Concentrations of the most abundant homologues (*n*-$C_{16,17,18,21}$) varied between 0.2 and 190 μg gdw^{-1} and paralleled with depth; in general, they exhibited higher concentrations during organic-rich intervals between 506.36 and 507.26 mcd, and between 508.46 and 508.75 mcd (Fig. III.3.). This trend did not change significantly when concentrations were normalized to TOC (data not shown). SCA are mostly derived from aquatic algae and microorganisms including photosynthetic bacteria (Han and Calvin, 1969; Cranwell et al., 1987). Even numbered SCA homologues between C_{12} and C_{22} are generally linked to bacterial sources (Grimalt and Albaigés, 1987), whereas *n*-C_{17} usually derives from photosynthetic algae and cyanobacteria (Han and Calvin, 1969; Cranwell et al., 1987), although it can be also found in purple sulfur bacteria (Jones and Young, 1970). The *n*-C_{21} homologue has been reported as the major *n*-alkane present in the marine diatom *Rhizosolenia setigera* (Blumer et al., 1971) and has been observed as dominant *n*-alkane in selected Pleistocene samples from high productivity areas off Walvis Bay (Hinrichs et al., 1999). The concentration pattern observed for these four homologues suggests coupled production in the water column and/or preservation in sediments.

Long-chain *n*-alkanes (LCA) were characterized by C_{27-35} homologues with an odd-over-even predominance as evidenced by carbon preference index (CPI) values up to 12, characteristic of epicuticular waxes of vascular plants (Fig. III.3.; Eglinton and Hamilton, 1967). Concentrations of *n*-C_{29}, *n*-C_{31}, and *n*-C_{33} paralleled with depth and varied between almost zero and 20 μg gdw^{-1}; the lowest values were found below and above 508 and 506.36 mcd, respectively, whereas maximum values were present between

506.5 and 507.9 mcd (Fig. III.3.). Considering the rather specific source of LCAs, their concentration is commonly used to track changes in the input of terrestrial organic matter into the marine realm (e.g., Meyers, 1997). Concentrations of LCA were generally up to one order of magnitude lower than SCAs, consistent with a largely marine origin of the organic matter (cf., Meyers et al., 2006; Beckmann et al., 2008).

Concentrations of the acyclic isoprenoids phytane (Ph), pristane (Pr), and lycopane (Ly) varied between almost zero and 25 μg gdw, and showed similar downcore profiles as SCA (Fig. III.2.). In aquatic environments, Ph and Pr derive mostly from the degradation of the phytyl side chain of chlorophyll-*a* found in many photosynthetic algae and cyanobacteria, as well as from bacteriochlorophyll-*a* and -*b* derived from purple sulfur bacteria (Brooks et al., 1969). Additional sources of Ph could possibly include lipids from methanogenic and halophilic archaea (Rowland, 1990), as well as tocopherols (antioxidants in plants and algal lipid membranes) for Pr (Goossens et al., 1984). In marine environments they are usually interpreted to derive from photosynthetic primary producers unless their carbon isotopic composition suggests a different source. Ly is abundant in water and sediment samples from both oxic and anoxic environments (Wakeham et al., 1993). Potential biological precursors include methanogenic archaea (Brassell et al., 1981) and phototrophic algae (Wakeham et al., 1993). The similarity of profiles of SCA, Ph, Pr, and Ly suggest that variations of these compounds are linked to changes in primary production in surface waters.

Biomarkers such as Ph can be severely influenced by sulfurization during early diagenesis in euxinic environments (Koopmans et al., 1996), and this process has been reported to occur at Demerara Rise (Beckmann et al., 2008; März et al., 2008). TOC exhibits a good correlation with total S in the studied section (data not shown), whereas biomarkers do not show a clear correlation with TOC (e.g., maximum TOC at 508.81 mcd. parallels a minimum in biomarkers). This suggests a cautious interpretation of productivity variations based on concentrations; thus, we also focus on the compound-specific isotopic composition of biomarkers.

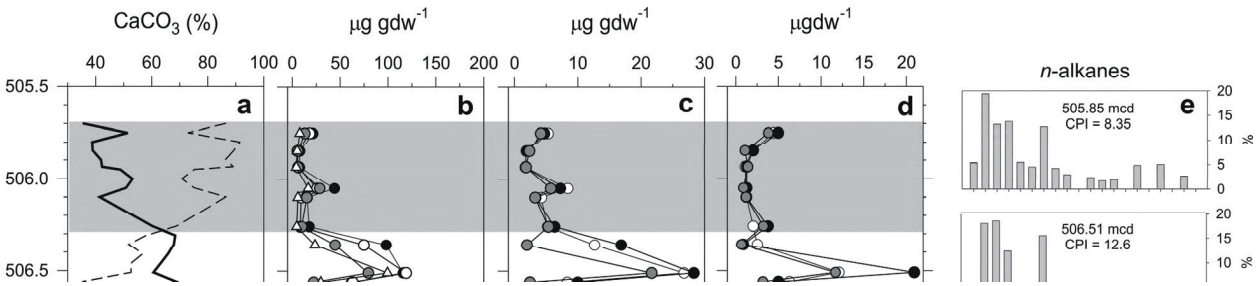
CaCO3 (%)
μg gdw-1
μg gdw-1
μgdw-1
n-alkanes
505.5
506.0
506.5
a
b
c
d
e
505.85 mcd
CPI = 8.35
506.51 mcd
CPI = 12.6
%
%